SLICKENSIDE PETROGRAPHY:
SLIP-SENSE INDICATORS AND CLASSIFICATION

A thesis presented to the Faculty
of the State University of New York
at Albany
in partial fulfillment of the requirements
for the degree of
Master of Sciences

College of Sciences and Mathematics
Department of Geological Sciences

Young-Joon Lee

1991

SLICKENSIDE PETROGRAPHY:
SLIP-SENSE INDICATORS AND CLASSIFICATION

Abstract of

a thesis presented to the Faculty

of the State University of New York

at Albany

in partial fulfillment of the requirements

for the degree of

Master of Sciences

College of Sciences and Mathematics

Department of Geological Sciences

Young-Joon Lee

1991

ABSTRACT

Petrographic study has been carried out on slickenside thin sections, to find out reliable microstructures for determining the slip-sense of faults, and to classify slickensides morphologically. Thin sections are made cut parallel to the striation and perpendicular to the slip plane. Many useful slip-sense indicators are found in thin section even though such indicators may be absent in hand specimens. They are (1) off-set or bending of once-continuous bodies such as veins, layers, grains or twin lamellae, (2) crystal fibers growing nearly parallel to the slip direction, (3) extensional fractures aligned oblique to the slip plane, (4) S-C geometries in ductile materials, and (5) Riedel- and P- shear fractures associated with the main slip surface.

Two distinct layers may exist adjacent to the slickenside surface. One is terming *coating*: a discrete layer of material immediately under the slip surface. The other is termed the *deformed host layer* which is a zone of deformation in the host rock developed parallel to the slickenside. Slickensides are classified into four morphological types depending on the presence or absence of coating and deformed host layers. They are type A (deformed host layer only), type B (coating and deformed host layer), type C (no coating and no deformed host layer), and type D (coating only).

This morphological classification can be a first step toward further genetic interpretation of slickensides, which could eventually be used to infer conditions of faulting. Possible development paths of each slickenside type indicate that present slickenside morphology can be influenced by rock type, slip-rate and depth of faulting during slip and by weathering and precipitation of veins along the pre-existing slip surface after slip. Although this classification is not yet fully

satisfactory, it can perhaps be extended and improved by further systematic slickenside studies.

ACKNOWLEDGEMENTS

Professor Win Means suggested the topic of this thesis. During this work, he was always generous to me though I struggled at first. I really appreciate his assistance, discussing problems during this study, and suggesting many useful ideas. He also gave me a chance to go to the G. S. A. meeting. It was a valuable experience for me to become familiar with current trends in geology. I also thank him for preparing the thin sections from his slickenside collection in advance before I started this work. Some samples used in this work were collected by other people and provided to Win Means. However, I regret that I can not acknowledge individuals here because their identity is unknown to me. Therefore, I thank various unknown geologists.

I would like to thank my committee members, Professors George Putman and Bill Kidd for reading my manuscript and for suggesting many helpful comments. I specially thank Jin-Han Ree and Youngdo Park, who always helped me in all aspects during this work. Other graduate fellows, Rob Alexander, Steve Tice, Rolf Herrmann and Christoph Arz were always beneficial to me for useful discussions and help during this work. I particularly thank Becky Alexander (Rob's wife) who helped me to improve my English and correct my thesis manuscript. I am grateful to Diana Paton for her administrative help during my stay in SUNY at Albany.

I thank my parents in Korea, who always guide their only son's steps in the path of righteousness. I also thank my wife Yun-Mi for her endless encouragement and patience whenever I was confronted by problems.

Finally, my study in the U.S.A was possible with the Korean Government Overseas Scholarship. I thank the advisor of Ministry of Education in the Korean Consulate General at New York for conducting administrative procedures related to the scholarship without any problems.

TABLE OF CONTENTS

LIST OF FIGURES

LIST OF TABLES

CHAPTER 1. INTRODUCTION

1.1 PURPOSE OF STUDY

Slickensides have been widely used by field workers as reliable indicators for the slip direction of faults and in some cases for the slip sense (e.g. Tjia 1964 and 1967, Norris and Barron 1969, Durney and Ramsay 1973). Also some works have made an attempt to relate slickenside structures to seismic activity (e. g. Engelder 1974a) and to the stress state that caused faulting (e. g. Angelier 1979). Recent research on slickensides is focused more on new aspects: first, new mechanisms for slickenside steps (Petit 1987), slickenside striations (Means 1987), and modes of slickenside initiation (Will and Wilson 1989); and second, slickenside development history as related to faulting (Power and Tullis 1989, Spray 1989b).

However there has been little published petrographic detail on slickensides. The aim of this study is to provide systematic descriptive information about slickensided fault rocks, using conventional petrographic microscopy. This may make some contribution to slickenside studies, which can eventually be useful for geologists in the field, or assist in making reliable paleostress estimates based on slickensides.

The thesis is composed of three main chapters. Chapter 2 aims to provide sense-of-slip criteria on slickensides on the microscopic scale. Chapter 3 proposes a morphological classification of slickensides. An attempt is made to link each type of slickenside to particular faulting conditions. Chapter 4 is to show case studies of selected examples. The slip conditions and slip history related to slickenside developments in each example are inferred from microstructural and mineralogical evidence.

1.2 PREVIOUS STUDIES ON SLICKENSIDES

The term slickenside was used in the early nineteenth century for structures in lead ore-bearing veins in England.

> *"The two faces (of a fault in limestone) in contact appear as though they had been polished and are ribbed or somewhat fluted; and the face of each is sometimes covered by a remarkably thin coating of lead ore; these planes, when separated, are the slickensides of the Mineralogist"* (Conybeare and Phillips, 1822, p348, mentioned in a geologic dictionary by Dennis, 1967, p136).

The definition of slickensides has been controversial and more specialized terms have been proposed, such as slickenline and slickenstep, for striation and step structures on the slip surface (Fleuty 1975). Also, in some text books fiber-vein coated surfaces or non-fibrous, fault-cast vein are not considered to be slickensides (e. g. Suppe 1985, p264). In addition, Will and Wilson (1989) have suggested a new definition of slickensides to cover non-frictional slickensides produced by ductile shearing, that is "a strain modified zone of variable thickness at a slip plane, whose surface displays any kind of markings produced during displacement on this surface". These new terms and definitions may be useful in some cases. In this study, however, slickensides are defined simply as "shiny or smooth fault surfaces commonly striated in the slip direction" (e. g. Means 1987).

Slickensides often display step structures, perpendicular to the striations. These step structures have been traditionally interpreted as indicators of the sense-of-slip on the slickensides, with the riser facing the direction of displacement of the opposite block (e. g. Hills 1940, Billings 1954). However, the validity of this interpretation has been questioned by Paterson (1958). Additional field (Tjia 1964) and experimental (Gay 1970, Hobbs *et al.* 1976, p 305) evidence supports the suggestion by Paterson that the risers may face opposite to the direction of

displacement of the opposing block. Norris and Barron (1969) have described two types of steps: accretion steps formed by accretion of material on the slickenside and fracture steps formed by combinations of minor fractures.

Striations on slickensides have been known as reliable indicators for the direction of fault movements. Various types of slickenside striations have been summarized by Means (1987, fig. 1). Durney and Ramsay (1973) suggested that striations on slickensides could be due to the growth of fibrous minerals along the fault plane rather than being structures formed by abrasive asperity ploughing. Engelder (1974a) has noted that carrot-shaped grooves on slickensides which have a small groove length to total slip ratio and only occur during stick slip sliding mode can be possible indicators for seismic slip as well as for sense-of-slip. Besides being used as indicators of slip direction, striated slickensides have now been used by many workers to estimate regional stress orientations. (e. g. Angelier 1979).

A number of papers have recently been written that make new contributions to the study of slickensides. Means (1987) has introduced a new type of slickenside striation. By shearing paraffin wax, he found a slickenside surface characterized by nesting of continuous ridges and grooves in ductile materials, and recognized slickensides with similar morphology in shales. Petit (1987) has described a variety of fracture step mechanisms including some kinds of steps which face opposite to the slip direction. Petit and Laville (1987) have described imperfectly planar slickensides with low luster that formed during shearing of unconsolidated sediments. Laurent (1987) suggested a new technique to decide the slip sense of a fault by using the combined geometries of mechanical *e* twin lamellae in carbonate minerals adjacent to the slip plane. Will and Wilson (1989) have carried out an experiment using pyrophyllitic clays, which behaved plastically, to produce the slickenside surfaces with continuous ridges and grooves as described by Means (1987). They suggested an initiation mechanism of slickensides in which the slip

plane initiated from C and C' planes by localized ductile shearing. Power and Tullis (1989) described a slickenside interpreted as recording cyclic seismic and interseismic slip. Spray (1989b) has reported mass formation on slickensides during a high-slip rate of frictional faulting.

In addition, there have been many indirect slickenside studies, accompanied by frictional experiments or natural fault rock studies, not mentioned above, which have contributed to the study of slickensides by providing information about slip mechanism, slip condition and deformation process related to slickenside development (e. g. Friedman *et al.* 1974, Engelder *et al.* 1975, Elliott 1976, Aydin 1978, Aydin and Johnson 1978, Moore *et al.* 1989).

1.3 SLICKENSIDE COLLECTION AND THIN SECTION PREPARATION

The samples of slickensided rocks used in this study were from a slickenside collection made by Dr. W. D. Means (State University of New York at Albany) mostly from the northeastern United States. One of his slickenside specimens, but not included in this study, has been referred to in a previous publication (Means 1987, fig. 6). Some information on each sample used in this study is summarized in Table 1.1.

As most slickensided rock samples are composed of just one block with the opposite block missing, thin sections were made by a somewhat special method as follows (Fig. 1.1). Two chips of a slickensided rock labeled as A and B in the figure are prepared by cutting parallel to the striation and perpendicular to the slip plane. Chip A is flipped over and glued on chip B with epoxy cement with about 1 mm space between them. After that, thin sections were made from these glued chips in the normal way. This method has the advantages that it places the slickenside

material near the center of the thin section (which guards against loss during grinding) and it gives two views of the slickenside in each thin section.

Table 1.1 Summary of slickensided fault rocks

spec. No.	13	17	18	19A	19B	21	24
rock type	gabbro	granite	granite	mafic ig.	mafic ig.	mudstone	mudstone
location	NJ Highlands	NJ Highlands	NJ Highlands	NJ Highlands	NJ Highlands	Latham NY	Latham NY
slip sense (1) indicator	fiber offset P-shear bending	extension offset R-shear	offset R-shear bending	fiber extension	fiber S-C	-	-
coating (2)	chlorite fiber	epidote vein	epidote vein	tremolite fiber	chlorite fiber	-	quartz vein
mor. type (2)	B	B	B	B	B	A	B

spec. No.	30	36	41	58	59	60	63
rock type	limestone	mudstone	sandstone	gr. gneiss	gr. gneiss	mudstone	quartzite
location	Latham NY	Clarksville NY	Laurel Ck. PA	unknown CT	unknown CT	Schodack Landing,NY	unknown CT
slip sense indicator	-	-	step	step	foliation bending	S-C foliation	-
coating	calcite and opaque veins	-	quartz fiber	quartz vein	gouge	chlorite layer	-
mor. type	B	C	B	B	B	B	C

spec. No.	66	70	71	72	76	78	81
rock type	altered gabbro	sandstone	mudstone	mudstone	gabbro	Bt-Gt schist	marble
location	Klamath Mts. OR	Hartford NY	Latham NY	Schodack Landing, NY	Paradox L. NY	Brant L. NY	Paradox L. NY
slip sense indicator	fiber	fiber	fiber extension	fiber foliation	S-C	offset S-C	-
coating	serpentine fiber	quartz fiber quartz gouge	quartz and calcite fibers	biotite fiber unknown m.	biotite, serpentine and chlorite layers	-	gouge
mor. type	D	D	B	B	B	A	B

Table 1.1 (continued)

spec. No.	83	86	92	99	104	105	108
rock type	mafic ig.	marble	mylonite	slate	breccia	mudstone	mudstone
location	Glens Falls NY	Marriottsville MD	Berkshires MA	Bear Valley Coal Mine, PA	Germantown NY	Glenmont NY	Glenmont NY
slip sense indicator	S-C	kink	S-C	-	S-C step	S-C	-
coating	chlorite layer	chlorite	-	coal	chlorite layer	chlorite layer quartz vein	-
mor. type	B	B	-	B	B	B	C

spec. No.	111	116	117	124
rock type	sandstone	coal slate	breccia	mudstone
location	Poestenkille Falls, NY	Bear Valley Coal Mine, PA	Sterling Hill Mine, NJ	Glenmont NY
slip sense indicator	step S-C	-	-	-
coating	-	coal	gouge?	quartz and opaque vein
mor. type	A	B	B	D

1. Referred to in Chapter 2.
2. Referred to in Chapter 3.

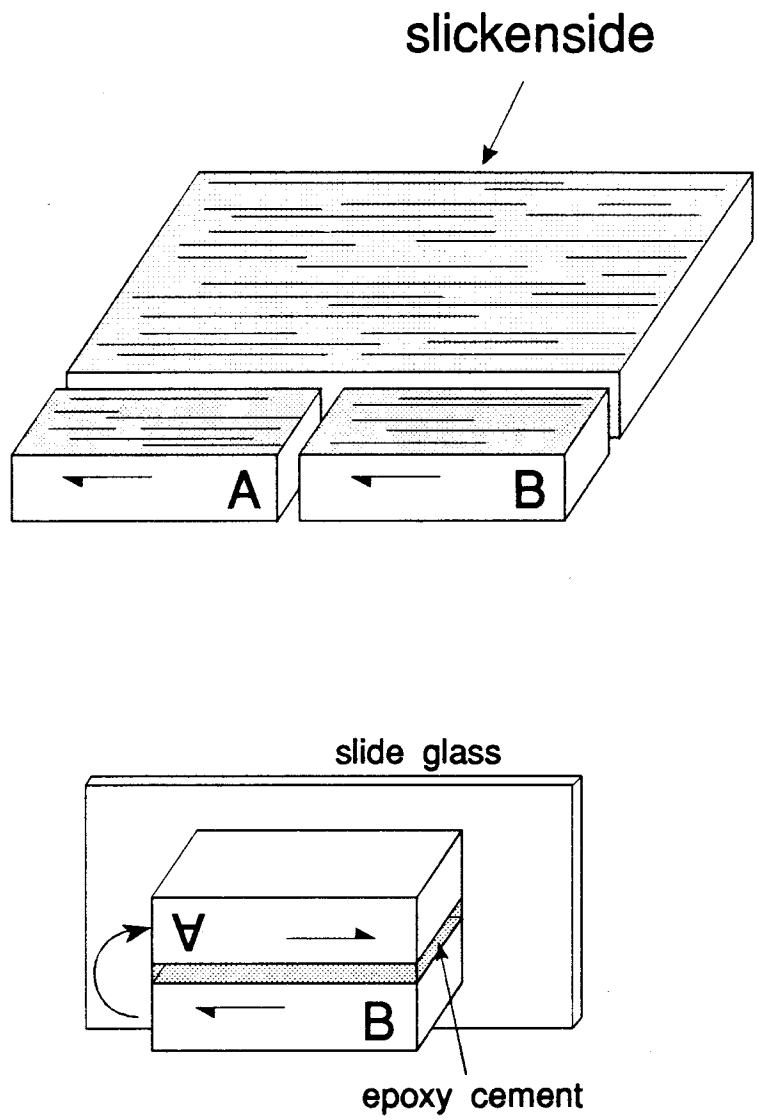

Figure 1.1 A schematic diagram showing how thin sections for this study were made from slickensided fault rocks.

CHAPTER 2. SENSE-OF-SLIP CRITERIA IN THIN SECTIONS OF SLICKENSIDES

2.1 INTRODUCTION

Slickensides have been used for many years to infer the sense-of-slip on faults (Hills 1940, Billings 1954). On the hand specimen-scale, fault steps on slickensides are useful for determining the slip sense as well as slip direction. Systematic research on natural slickensides has helped to define types of step structures on slickensides in terms of minor fracture development and new material formation (Norris and Barron 1969, Durney and Ramsay 1973, Petit 1987). Other slickenside structures such as carrot-shaped grooves occurring as a result of frictional wear during faulting have been described as another reliable sense-of-slip indicator on the hand specimen-scale (Engelder 1974a).

However, these sense-of-slip indicators are sometimes difficult to use, since they may not be observable or ambiguous in hand specimens. Means (1987) has described a slickenside type of which the striations are produced by continuous ridges and grooves, not showing any noticeable sense-of-slip indicator in hand specimens. Also later weathering or another slip event can cause the obliteration of the pre-existing sense-of-slip indicators. Therefore, it becomes desirable to make use of any microscopic indicators present as well. Indeed, a start has been made at finding and describing microscopic indicators on slickensides (Laurent 1987, Power and Tullis 1989).

This chapter is intended to further advance knowledge of microscopic sense-of-slip indicators on slickensides. Detailed microscopic observations were made in slickenside thin sections from various rock types. The reliability of the sense-of-slip

indicators can be checked when more than two different types of indicators are identified. Some of the features described in this chapter have already been used for deciding the slip (or shear) sense in other geologic structures (Simpson and Schmid 1983, Lister and Snoke 1984). All sketches are drawn for dextral slip movement to avoid complications.

2.2 OFFSET AND BENDING

Offset of planar or linear features is the most fundamental criterion for recognizing the relative movement of the displaced blocks along a fault plane. However, slickenside specimens usually preserve just one side of the fault, so that it is impossible to find offset across the plane. Instead, micro-scale offset features are visible around minor shear fractures approximately parallel to the main slickenside surface.

Domino-type offset occurs on the grain-scale (Figs. 2.1b & c). The location of each example is indicated in Figure 2.1a, illustrating the restored position of the thin section in hand specimen. An actinolite band in a small hornblende grain is sinistrally offset by inside fractures with high angle to the slickenside plane (Fig. 2.1b). As this grain is in contact with the main slickenside surface, it is implied that the main slip-movement has directly caused the fractures. Individual parts of the band are rotated in the direction of slip, a feature which sets up a contrary shear motion between the fragments. Therefore the slip sense of the domino-type offset is opposite to that of the main slickenside (Simpson and Schmid 1983). The main dextral slip sense is confirmed by the bending of the cleavage planes in another hornblende grain.

A similar feature is observed along a minor shear fracture in Figure 2.1c. A hornblende grain is displaced across the dextral P-shear fracture which branches

Figure 2.1 Grain-scale domino-type offsets in a slickenside in gabbro (No. 13). (a) Schematic diagram indicating the positions of each microscopic sense-of-slip indicator in the thin section (shaded). Microscopic P-shear fractures are reconstructed by extending to the slickenside surface. (b) Domino-type offset of actinolite band in a small hornblende grain along the main slickenside surface. The hornblende grain is detached from a large grain on the left. The large grain is bent by dextral slip movement. (c) Domino-type offset of actinolite bands in a hornblende grain and chlorite fibers, along a P-shear fracture.

(a)

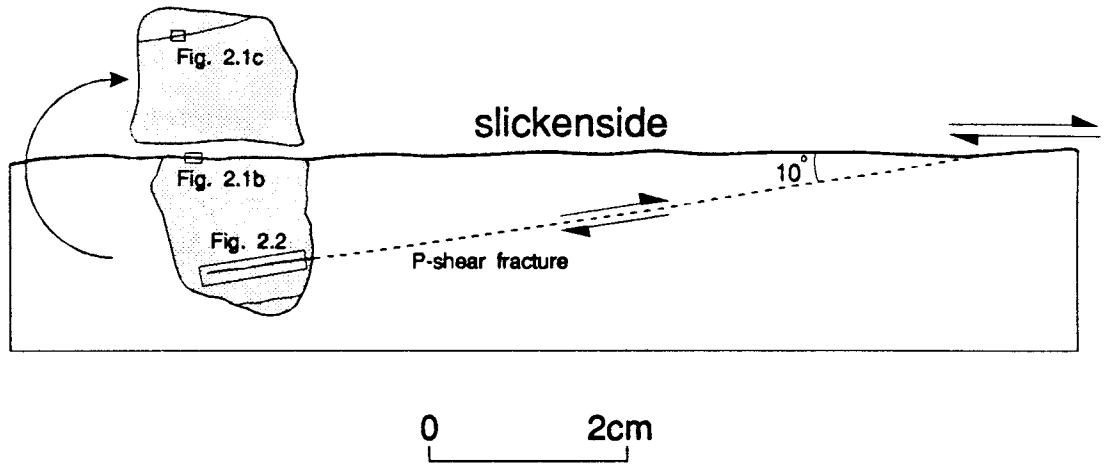
Fig. 2.1c
slickenside
Fig. 2.1b
10°
Fig. 2.2
P-shear fracture
0
2cm

(b)

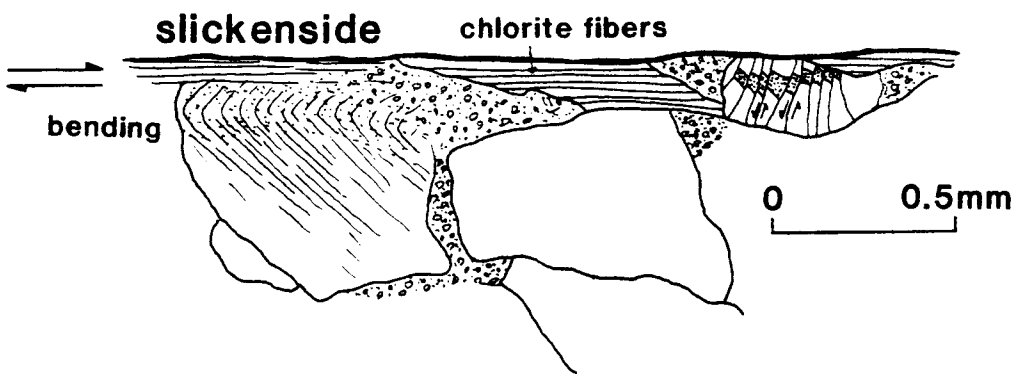
slickenside
chlorite fibers
bending
0
0.5mm

(c)

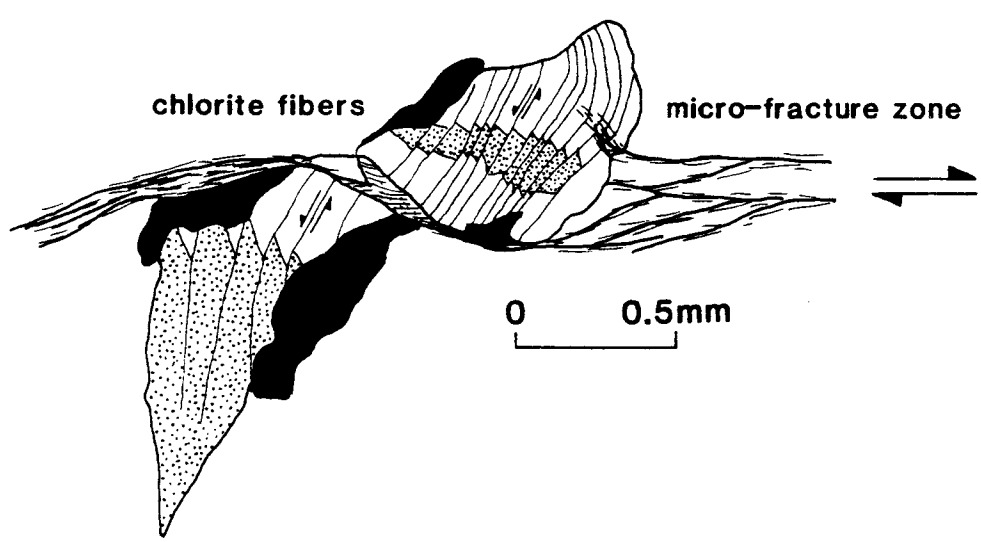
chlorite fibers
micro-fracture zone
0
0.5mm

from the main slip plane. Along the hornblende cleavage, actinolite bands in the grain show the same domino-type displacements as those in Figure 2.1b.

Another useful microscopic slip-sense indicator is offset of grains along minor shear fractures parallel to the slickenside. An example of grain offset is shown in the same slickenside thin section of Figure 2.1. Dextral offset of 26 grains is recognized along a P-shear fracture (Fig. 2.2). As indicated in Figure 2.1a, the angle between the main and minor shear fracture is approximate 10^{o}, so that the slip sense of the minor fracture is taken to be the same as that of the main slip plane from the Riedel fracture geometry (Petit 1987, Moore *et al.* 1989, and Logan *et al.* 1979). In most of the grains, except for grains t and u, the lengths of offset faces are well matched across the fracture. From the terminating point of the fracture, the amount of displacement in each grain increases toward the main slip plane (the right side in the diagram). This can be accommodated by a combination of a difference between internal stretching of two blocks across the slip plane (Means 1989) and a micro-scale fracture duplex structure similar to large-scale thrust duplex geometry (e. g. Boyer and Elliott 1982, fig. 19).

In general, offset difference between two neighboring pairs of material points is expected along stretching faults and the change in offset amount is gradual rather than abrupt (Means 1990). An abrupt change in offset is shown in the enlarged circle in Figure 2.2 and the simple stretching model cannot explain this abrupt change. A possible explanation is shown in Figure 2.3 based on current thin section configuration. In the thin section, two different fractures are observed along the upper and lower boundaries of small fractions of grains l and m, forming the fracture bounded duplex (Fig. 2.3a). Offset amount d_{no} is much larger than offset amount d_{lm}. A prior stage was reconstructed by moving the upper block to the left along the fracture (f2) and slightly modifying some grain boundaries, to remove the offset of grain k (Fig. 2.3b). However, this restored diagram still shows offsets of

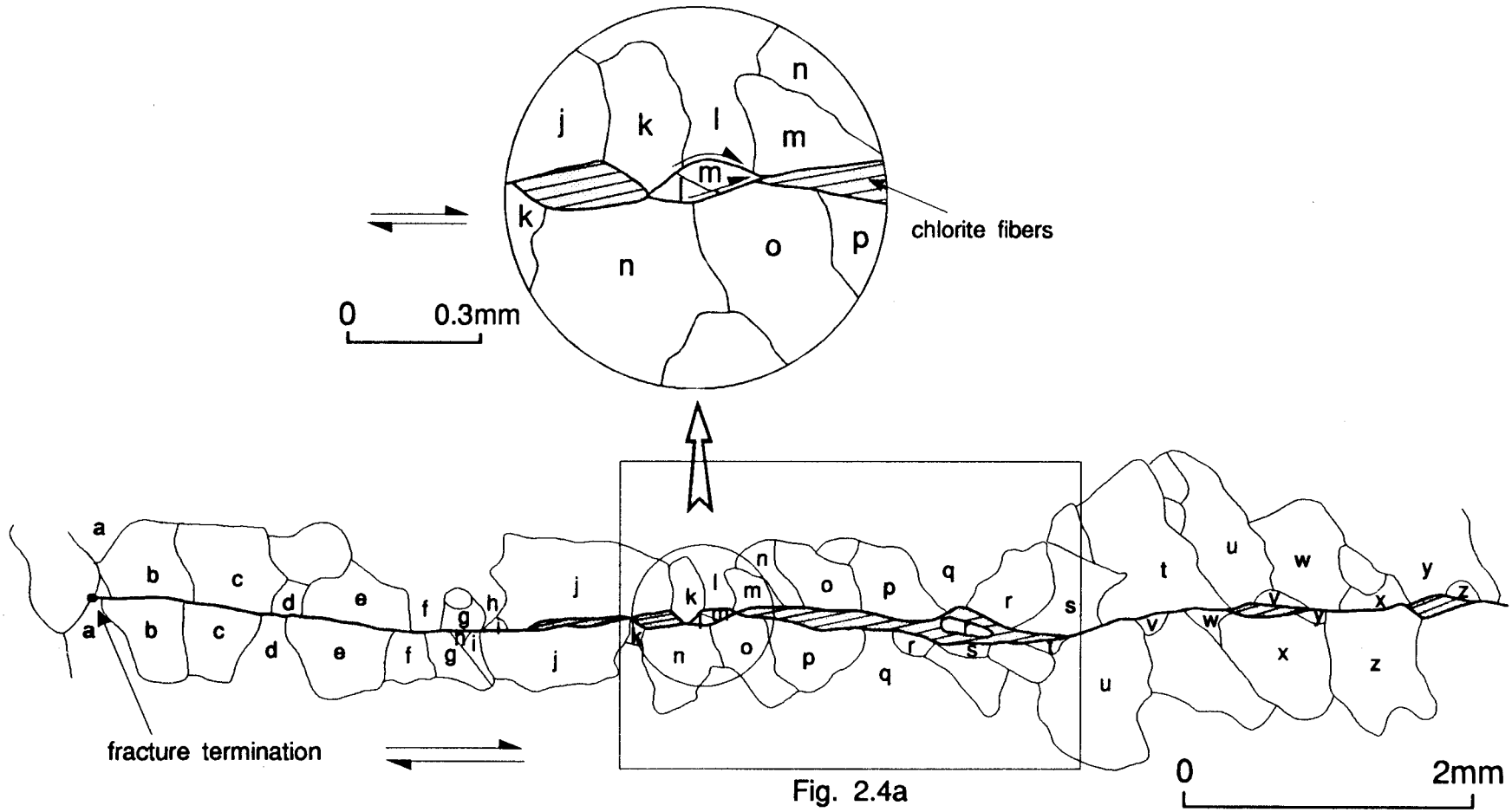

Figure 2.2 Grain offsets along a P-shear fracture. 26 grains whose offsets are identified along the fracture are labeled alphabetically. Enlarged circle indicates a fracture duplex structure contributing to different slip amounts along the fracture (see Fig. 2.1 for its position).

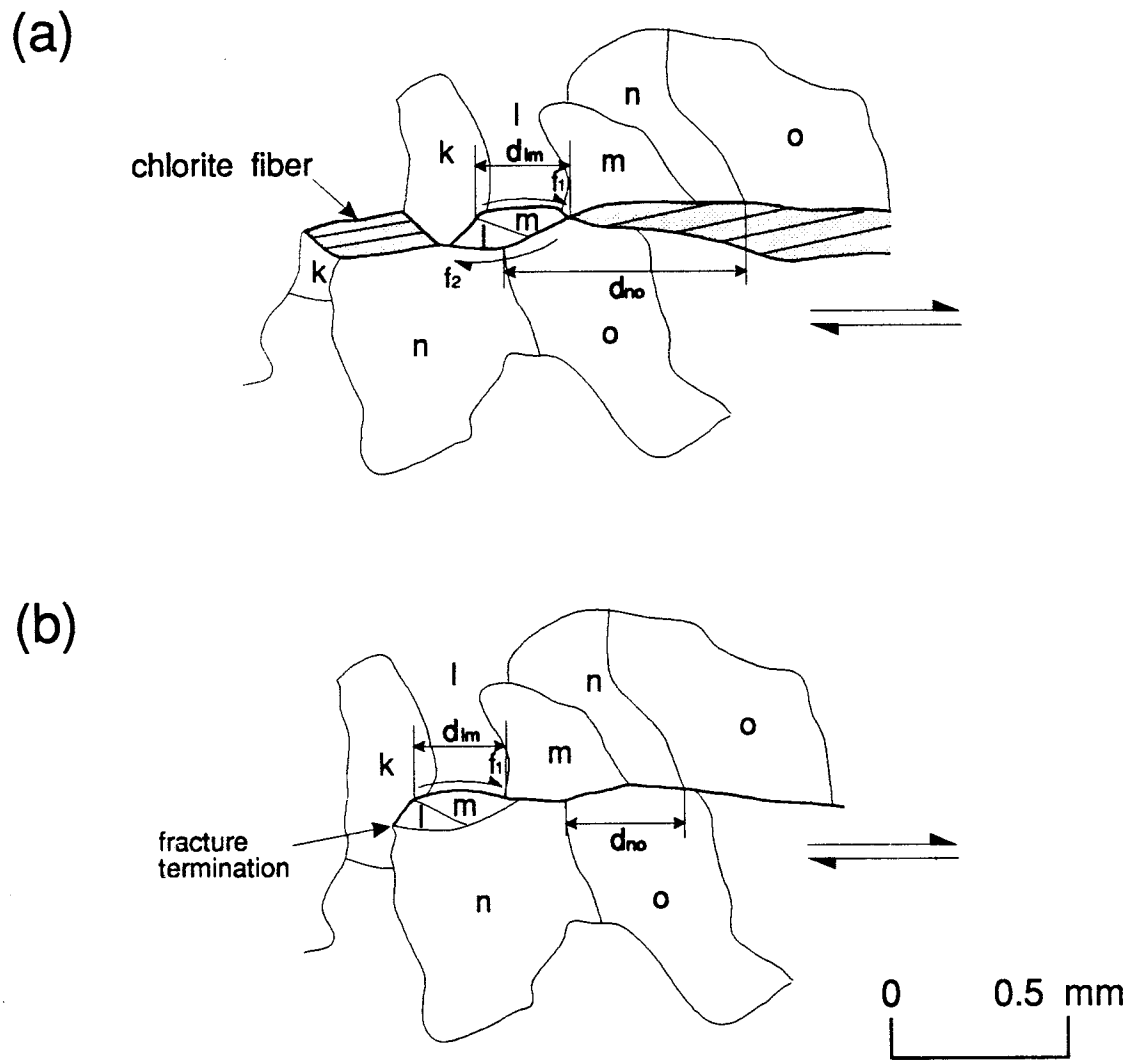

Figure 2.3 Sequential diagrams illustrating why different amounts of offset between neighboring points in Figure 2.2 can occur. (a) Current view in thin section showing a fracture duplex structure (fractures f1 and f2). (b) A reconstructed diagram of (a), by removing the offset of grain k. Offsets of grains l, m, n and o still remain along f1 fracture. d_{lm}: offset of the grain boundary between grains l and m. d_{no}: offset of the grain boundary between grains n and o.

grains (grains l, m, n and o) which are not much different from each other (see offsets of d_{lm} and d_{no}). These grain offsets can be explained by another fracture (f1) which has developed prior to the f2 fracture. Although, from the current thin section geometry, it is impossible to confirm that the two phases of fracturing have occurred sequentially from f1 to f2 or contemporaneously, this fracture duplex structure can explain the abrupt changes in offset amounts between neighboring grains.

Micro-scale bending or dragging is another criterion which can be used for determining the slip sense. Bending of planar features such as mineral cleavage, twin lamellae and micro-scale veins can be caused by local shear strain near the slip surface. In Fig. 2.1b, a large hornblende grain that was crushed and partly altered to actinolite near the slip surface displays a cleavage bending by dextral shearing. The direction of the bending indicates the movement direction of the missing block of the slickenside. The dextral slip sense is also supported by the domino-type offset in the same diagram.

2.3 CRYSTAL FIBERS

Since crystal fiber steps on slickensides were described by Durney and Ramsay in 1973, they have been used as one of the best sense-of-slip criteria for fault movement. As a gap is opened by a combination of fractures (Gamond 1983, 1987) or by the irregularity of the slip plane (Durney and Ramsay 1973), crystal fibers grow with orientations nearly parallel to the slip direction. This is the most common type of fiber growth associated with slickensides. Here, they are referred to as *dilation fibers*.

Many geologists use the term fiber to illustrate this type of crystallization, usually from quartz or calcite in dilated gaps. Strictly speaking, the term fiber is not

suitable for layer silicates such as chlorites and micas, since their geometry is planar not linear. Etymology suggests that fiber be reserved for linear features. However, not only because of a lack of an appropriate term but also to cover all similar crystal growth features, the term fiber is kept in this study in describing the layer silicates.

Figure 2.4a shows typical dilation fibers in dilated gaps along a minor shear fracture. Chlorite fibers are oriented parallel to the slip direction. The direction of the fibers indicates that the upper block has been moved relatively to the right. From the direction and length of the fibers, we can decide the slip sense as well as the amount of fracture displacement.

In this study, another type of crystal fibers that originate by a different mechanism was observed on slickensides: *replacement fibers*. Replacement fibers can result from the replacement of pre-existing coating minerals or of host rock minerals in slickensided rocks. In Figure 2.4b, quartz fibers in a slickensided sandstone crystallize on the lee side of a step with preferred orientations. Slight undulatory extinctions are seen in some grains (dotted lines). A gouge layer develops between the fibers and host rock. In contact with the gouge, these fibers are likely to crystallize partially by the replacement of pre-existing quartz gouge. This replacement is indicated by unclear boundaries between the fibers and gouge, and the existence of fine-grained relict gouge in the fibers.

A fine-grained mudstone slickenside in Figure 2.4c is covered with right-stepping fault steps on the slickenside surface which consist of layer silicate fibers showing preferred orientations. The direction of the fibers is slightly inclined to the left compared to the main slip surface. The slip sense can be inferred to be dextral from the geometry of the step structure (Durney and Ramsay 1973). The boundaries between the fibers and host rock are very irregular and ambiguous.

In the enlarged diagram (Fig. 2.4d), some relicts of the host rock are enclosed in the fibers. The orientation of the fiber minerals (extended dotted lines)

(a)

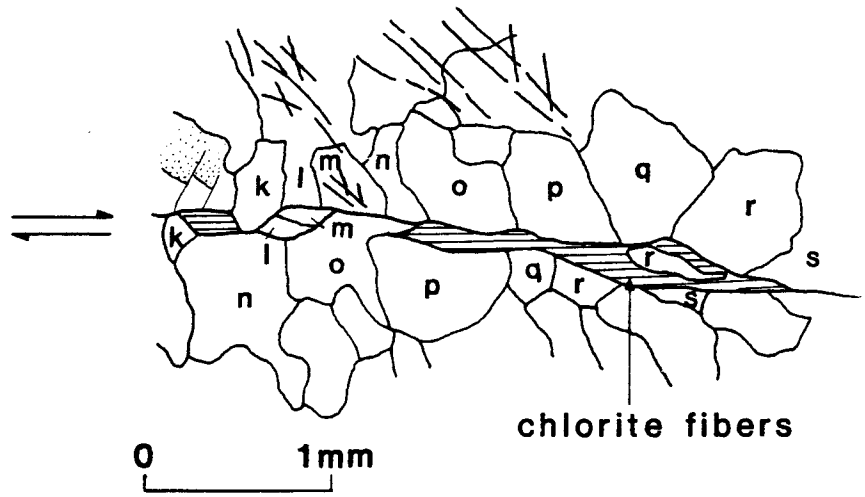

(b)

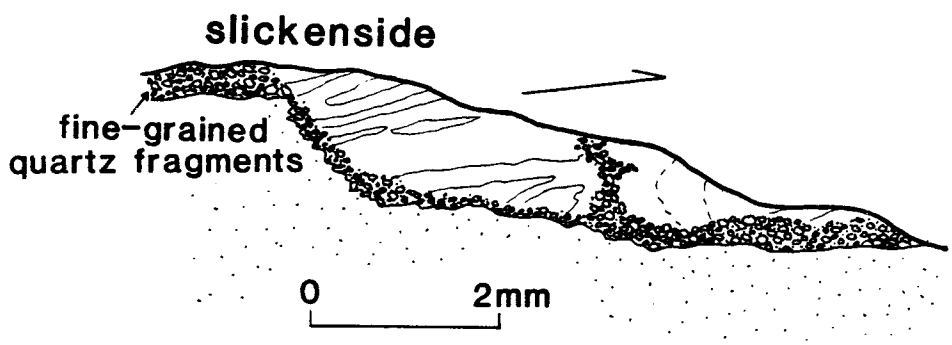

Figure 2.4 Various types of crystal fibers on slickensides. (a) Dilation fiber (from Figure 2.2) along a P-shear fracture. Grain r is separated into three parts with chlorite fiber growth in the gaps. (b) Replacement fiber in a sandstone slickenside (No. 70). (c) Step structure composed of layer silicate fibers in a mudstone slickenside (No. 72). (d) An enlarged part of (c) showing replacement fibers. The fiber directions are traced into the relict host grains (surrounded by dashed lines). The direction of the fibers is different in each domain 1, 2, 3 and 4. Arrows in (b), (c) and (d) indicate the movement direction of the upper block parallel to the fiber direction.

(c)

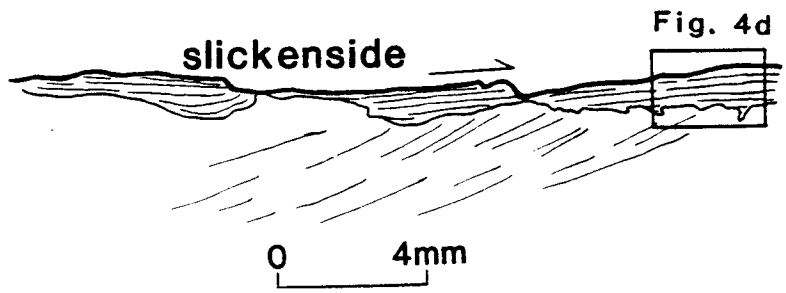

(d)

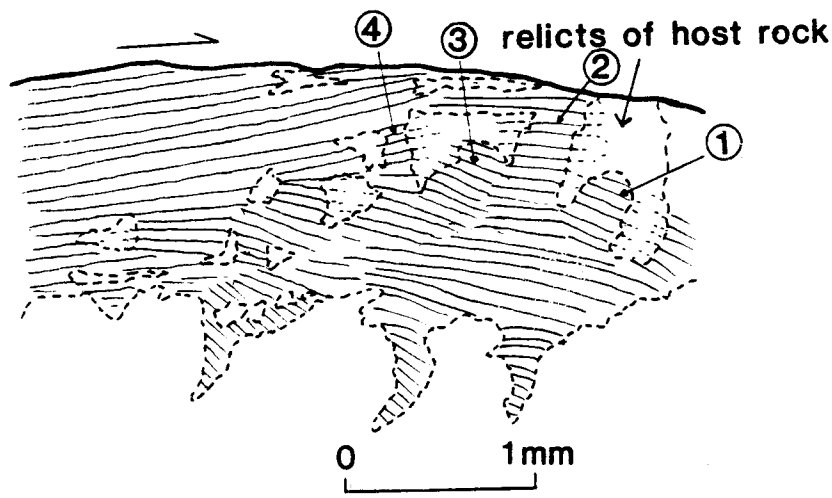

Figure 2.4 continued.

is traced into the relicts, which may reflect partial replacements of the host rock by the fiber minerals. By gradual replacement along fractures, the fibers are extended nearly normal to each fracture wall. This may cause the localized differences in orientations of the fibers (positions 1, 2, 3 and 4 in Fig. 2.4d). There are three evidences of the replacement: the irregular boundary between the fiber and host rock ; the pseudo-fibers in the relicts of the host rock; the local changes in fiber direction. But the overall fiber direction is nearly constant (Fig. 2.4c).

It is difficult to state that all parts of the fibrous minerals shown in the Figures 2.4b and 4d resulted from replacement alone. However, some parts of the fibers are considered to develop by replacement processes according to the evidence above. Although the mechanisms of dilation and replacement fibers are different from each other, the direction of the fibers is parallel to the slip direction. However, unlike simple dilation fibers, if fibers in a dilated gap are developed by a combination of both dilation and replacement processes, the total length of fibers will exceed the real dilation length of the gap (Table 2.1).

2.4 EXTENSIONAL FRACTURES

Extensional fractures, commonly referred to as tensional gashes or cracks, occur especially where brittle deformation is predominant. They are usually arranged perpendicular to the maximum stretching direction during faulting and are filled with vein minerals (see also Suppe 1985, p268).

Micro-scale extensional fractures are developed along the main slip surface (Fig. 2.5a) and along R-shear fracture (Fig. 2.5b) on slickensides in granites. Because of coatings, the slickenside surfaces on the hand specimen-scale do not exhibit any structure indicating the slip sense. The host rock in Figure 2.5a is mainly composed of feldspars and is fractured and fragmented along the slip surface. The

Table 2.1 Comparison between dilation and replacement fibers.

fiber type	dilation	replacement
source of fiber	fluids injected into dilated gap	fluids and components of pre-existing coating mineral or host rock
characteristics	crystallization from fluid	change in grain shape (fibrous) and composition by replacement of pre-existing materials
fiber direction	parallel to slip	parallel to slip
dilation amount vs. fiber length (1)	fiber length = dilation amount	fiber length > dilation amount

(1): In a gap with fibrous minerals.

(a)

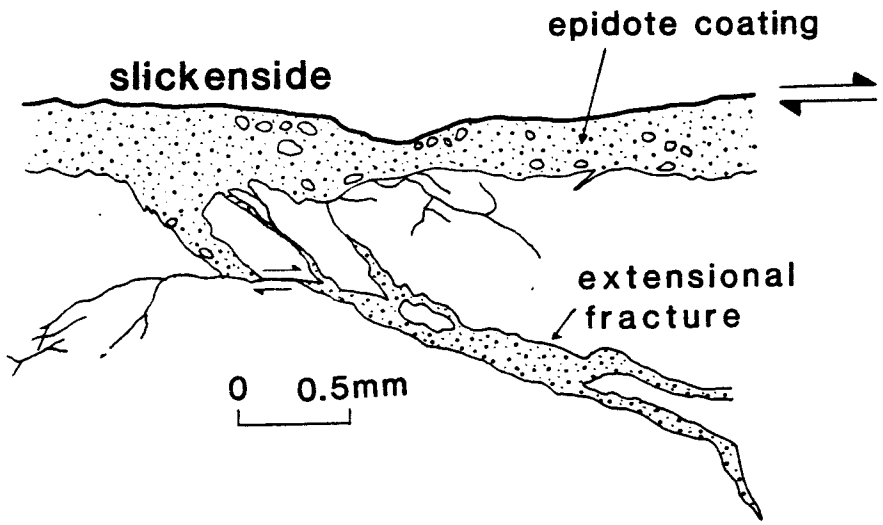

(b)

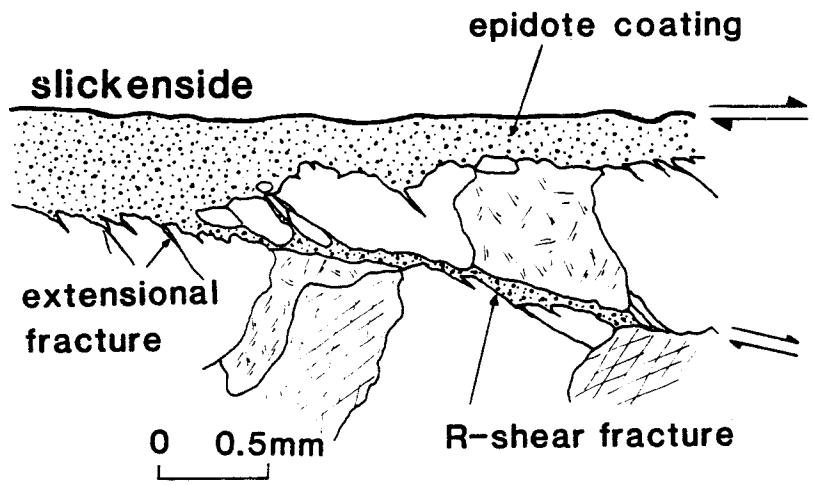

Figure 2.5 Extensional fractures along the main slip plane (a) and minor R-shear fracture (b). (a) The direction of opening is indicated by a pair of small shear-sense arrows (No. 17). (b) Grain offset along the R-shear fracture indicates dextral slip of the fracture (No. 18). Both extensional fractures in (a) and (b) dip in the movement direction of the upper block.

slip surface is coated with a layer of fine-grained massive epidote about 0.2 mm in thickness. A microscopic extensional fracture filled with epidote is inclined to the right. The extensional fracture represents dextral slip movement based on its geometry (Petit 1987, fig. 1). Smaller extensional fractures are developed parallel to the main extensional fracture. These fractures play an important role in fragmentation of the host rock near the slip surface. A few fragments of the host rock are included in the epidote coating.

Another example of an extensional fracture appears along a minor R-shear fracture (Fig. 2.5b). The slip sense of the shear fracture is recognized as dextral by offset of grains. Wedge-shaped small extensional fractures are arranged along the shear fracture as well as the main slip surface.

It is sometimes difficult to distinguish a true extensional fracture from a shear fracture if they both have a similar inclination angle to the slip surface and an opened gap. In the shear fracture, an opened gap can be caused by later intrusion of vein materials. Therefore, to use an extensional fracture as sense-of-slip criterion, lack of displacement along the fracture must be verified. In Fig. 2.5a, the leaning of the fracture against the shear direction of the main slip surface with a shallow angle (about 20°) may suggest that an R-shear fracture had initiated first and was followed by an opening parallel to the slip direction. However, no evident offset along the fracture contradicts to the pre-occurrence of shear fracture in the initial stage.

2.5 S-C GEOMETRY AND OBLIQUE PREFERRED ORIENTATION

The S-C geometry and oblique preferred orientation to the shear surface have usually been described in ductile shear zones and are often used as shear sense indicators (Berthe *et al.* 1979, Lister and Snoke 1984). Some of these features are

also recognized in slickensided rocks. The localized plastic deformation or cataclastic shear flow near the slickenside surface can produce the distinctive planar fabrics, especially in fine-grained mica-rich host rocks or in coating materials on slickensides (Fig. 2.6). Few studies have been done treating these fabric developments on slickensides (Will and Wilson 1989), since most slickensides are considered to be products of brittle deformation in the frictional regime.

Figure 2.6a shows a localized narrow shear band near the slickenside. This narrow shear band is usually observed in fine-grained mudstone or shale slickensides. There are two distinctive planar fabrics corresponding to S and C surfaces. Strongly concentrated fine-grained layer silicates define the C surface parallel to the main slip plane. Within the shear band, weakly elongated quartz grains and layer silicates constitute the S surface of sigmoidal shape. The deformation of the host rock is localized only in the shear band. No other deformation feature is prominent in the adjacent host rock.

This S-C relationship is also found in the coating materials of some slickensides. Newly formed chlorite coatings on a slickenside show two composite preferred orientations of sigmoidal shape equivalent to the S and C planes (Fig. 2.6b). A shear band is produced by the rearrangement of pre-existing foliations parallel to the slip plane, indicating dextral slip movement. The development of these S-C geometries in the host rock or coatings indicates a localized shear strain along the slip surface.

The preferred orientations of layer silicates developed oblique to the slip surface can be used as a good indicator of the slip sense of a fault. When they are simultaneously formed with faulting, the cleavages of the layer silicates are approximately oriented to the maximum stretching direction which is oblique to the slip surface (Fig. 2.6c). A quartz vein intruded into the chlorite layers shows undulatory extinction boundaries parallel to the main slip (horizontal dotted lines),

Figure 2.6 Deformation fabrics developed in slickensided mudstones (a and b) and a mafic igneous rock (c). (a) S-C geometry in a localized shear band. S and C surfaces are defined by preferred orientations of layer silicates. Late synthetic shear planes (C') are weakly developed (No. 60). (b) S-C alignments of newly formed chlorites along the slip surface. Foliations in the host rock are rearranged obliquely in a shear band near the slip surface (No. 105). (c) Oblique preferred orientations of chlorites. The inclination of chlorites indicates the dextral slip sense of the slickenside. A quartz vein shows trails of opaque minerals. The inclination of the trails is opposite to that of the chlorite layers (No. 19B).

(a)

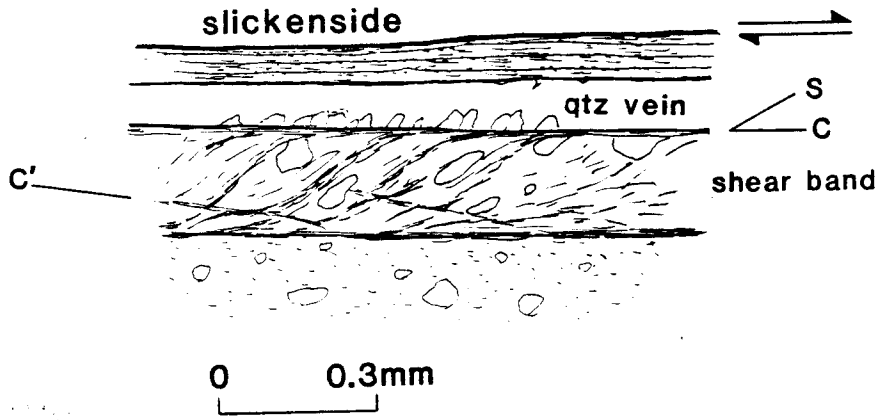
slickenside
qtz vein
S
C
C'
shear band
0
0.3mm

(b)

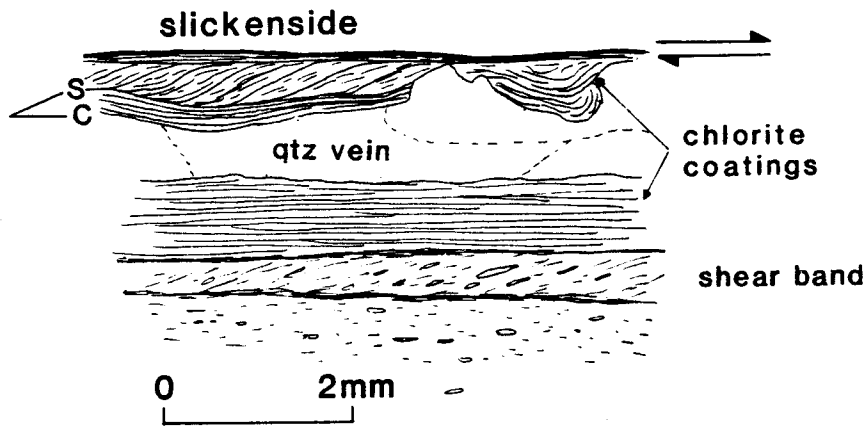
slickenside
S
C
qtz vein
chlorite
coatings
shear band
0
2mm

(c)

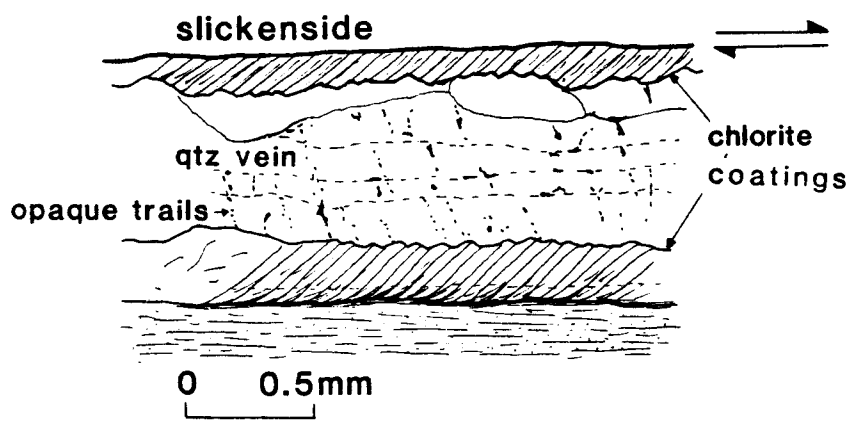
slickenside
qtz vein
chlorite
coatings
opaque trails
0
0.5mm

but it is not clear if this is directly related to slip events. Opaque trails are arranged at high angle to the slip plane. Cox (1987) has suggested that such inclusion trails within antitaxial quartz fibers may depict the true growth direction of the quartz related to the stress regime. If the inclined opaque trails in Figure 2.6c are developed by this mechanism, they may indicate a weak sinistral slip movement which has occurred during crystallization of the quartz vein.

2.6 RIEDEL-TYPE SHEAR FRACTURES

Riedel-type minor shear fractures associated with the formation of slickensides are also valuable in determining the slip sense. They have already been applied in several fault rock studies (Petit 1987, Power and Tullis 1989, Moore *et al.* 1989). Figure 2.7 shows a schematic pattern of the minor fractures associated with a dextral slip movement from the labelling scheme of Logan *et al.* (1979). Only two synthetic shear fractures, P and R are described in this section, since antithetic shear fractures R' and X and extensional fracture T are equivalent to the domino-type offset and extensional fracture, respectively.

In Figure 2.8, a shallow-angle shear fracture branching from the main slickenside surface displaces perthite lamellae in feldspar grains dextrally. This minor fracture has an R orientation, inferred from the slip sense and orientation of the inclined fracture with respect to the main slip (Fig. 2.7). Another example of the R-shear fracture is shown in Figure 2.5b which is identified by the grain offset and small extensional fractures along the fracture.

P-shear fractures slightly inclined to the main slip plane are recognized in Figure 2.1a. Although their contact points with the main slip plane are not visible in the thin section, the slip sense and geometry of the fractures are recognized from other sense-of-slip indicators and the restored diagram. Like the R-shear fracture,

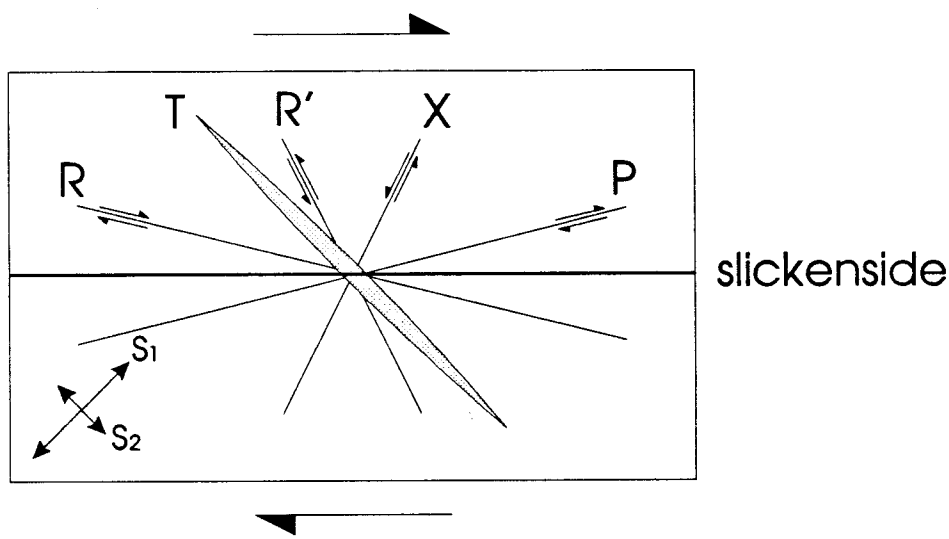

Figure 2.7 Schematic diagram representing the Riedel-type geometry on slickensides relative to the principal directions (S1 and S2) in dextral slip movement. Synthetic shear fractures, R and P, antithetic shear fractures, R ' and X and an extensional fracture T are arranged with the particular direction and angle relationship to the main slip plane. Fracture arrays and lettering scheme were combined from Logan *et al.* (1979) and Moor *et al.* (1989).

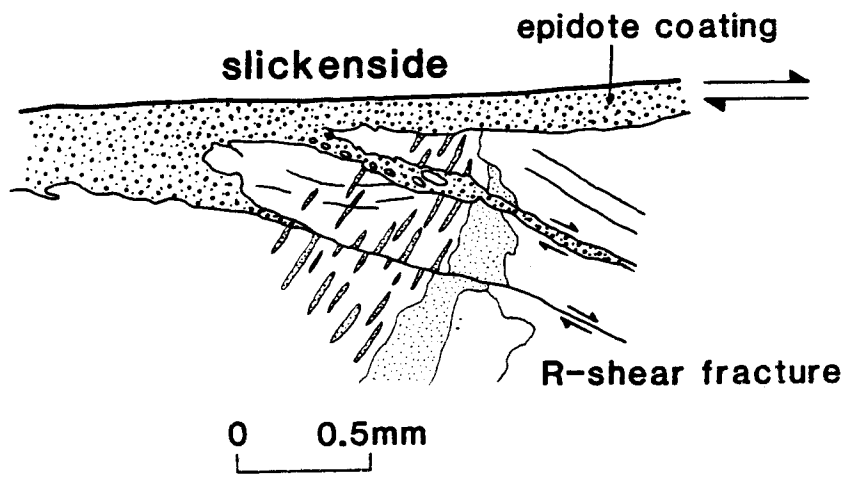

Figure 2.8 R-shear fractures indicated by offset of perthite lamellae in a granite slickenside (No. 17). The slip sense of the shear fracture is the same as that of the main slickenside. A massive epidote vein covers the original fracture plane in the granite.

the slip sense of the P-shear fracture is identical with that of the main slip surface. The only difference between the two fractures is that the leanings of R- and P-fractures are against and toward the shear direction of the main slip surface, respectively. Therefore, if based on the inclination geometry of minor shear fractures alone, it is impossible to recognize the slip sense of the fault. It is required that the slip sense of the minor shear fracture is decided first.

2.7 SUMMARY

The most useful microscopic criteria for determining the slip sense on slickensides are: *offset* and *bending* of once-continuous bodies; *crystal fibers* growing parallel to the slip direction; *extensional fractures* arranged oblique to and at a high angle to the slip plane; *S-C geometries* and *oblique preferred orientations* by development of syn-slip planar fabrics; and *micro-Riedel fractures* whose slip sense conforms to the main slip sense (Fig. 2.9). Approximately two thirds of the slickenside thin sections used in this study display microscopic sense-of-slip indicators, even though in many cases the slip sense cannot be determined from hand specimens.

Sometimes, more than one type of sense-of-slip indicator is found in a thin section, so that it is possible to use a combination of indicators to make a more confident interpretation of slip sense (e.g. the slickensided gabbro in Fig. 2.1). Most of the sense-of-slip criteria described here also commonly appear in other geologic structures. Field workers, therefore, can easily employ these indicators in those common situations where hand specimen-scale structures do not unambiguously indicate a sense-of-slip.

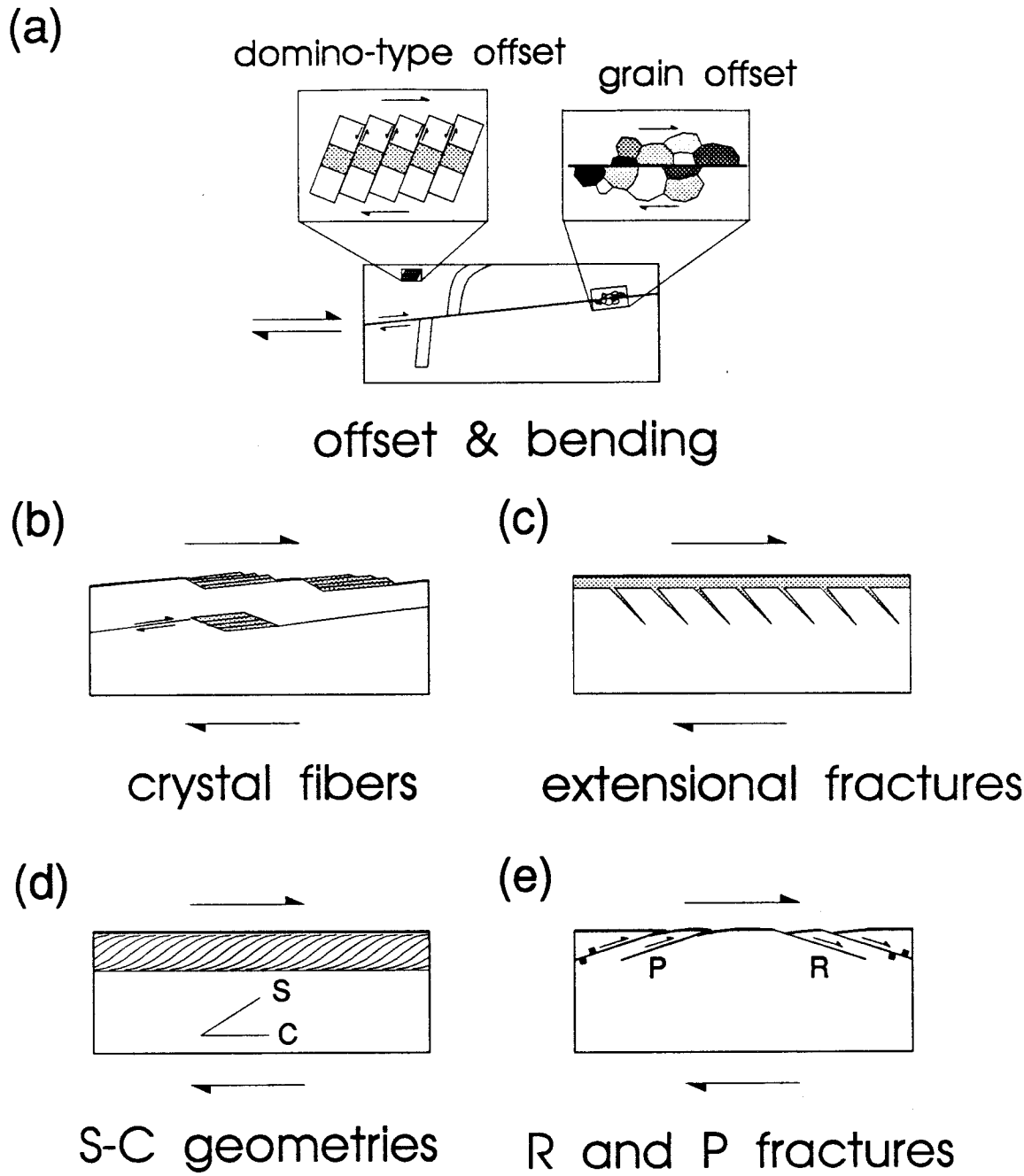

Figure 2.9 Various types of microscopic sense-of-slip criteria on slickensides. (a) Domino-type offset, grain offset and bending. (b) Crystal fibers subparallel to the slip direction on slip plane or in dilated gap. (c) Extensional fractures arranged perpendicular to the maximum stretching direction. (d) S-C arrangements. (e) Micro-Riedel and P shear fractures. All diagrams are drawn with dextral slip sense on major fault plane.

CHAPTER 3. PETROGRAPHIC CLASSIFICATION OF SLICKENSIDES

3.1 INTRODUCTION

Certain types of slickensides have been indicators not only for the slip sense of faulting but also for the physical conditions under which faulting occurred. Some researches have been carried out on the mechanism of slickenside formation and faulting conditions, particularly related to the seismic activity. (Engelder 1974a, Petit and Laville 1987, Power and Tullis 1989, Spray 1989b).

Faulting conditions such as slip-rate, strain-rate, depth, and slip-amount of faulting have been interpreted from the structures developed on slickensides or related features. High slip-rate (the seismic phase) has been suggested by such structures as carrot-shaped grooves (Engelder 1974a), pseudotachylytes and other frictional melts (Sibson 1975, Friedman *et al.* 1974, Spray 1989b). On the other hand, fibrous minerals on the slickenside have been said to indicate a low slip-rate during the aseismic phase (Durney and Ramsay 1973, Elliott 1976). It has been claimed that the crystallographic preferred orientations in slickenside surface material develops at relatively low strain-rates, while cataclasis occurs at higher strain-rates, and that mineral assemblages and microstructures in the host rock can be used to constrain the depth of faulting (Power and Tullis 1989). For the slip-amount, the thickness of gouge layer which often occurs with slickensides has been said to increase with total slip amount in frictional experiment (Engelder 1974b) or in natural fault zone (Scholz 1987, Hull 1988).

Despite the above individual slickenside studies, there is no synthetic article on slickensides in the literature that enables a geologist to use slickensides as a reference and for comparison in fault studies. This chapter aims to provide such a

work. The first part of the chapter proposes a petrographic classification of slickensides based on their morphology in thin section. Detailed information of each slickenside sample is summarized in Table 1.1. The latter part of the chapter examines what information can be extracted from the preserved slickenside structures and how each slickenside type is developed. Rocks of different compositions play an important role in the development of slickensides. Some morphological types of slickensides indicate faulting conditions, especially depth and slip-rate of faulting. This is important in understanding the paths along which slickensides develop and the final slickenside morphologies.

3.2 MORPHOLOGICAL CLASSIFICATION

A morphological classification of slickensided fault rock is proposed here to facilitate the description of various slickenside structures. Two descriptive terms are necessary, firstly to name the distinctive layers developed both on the slickenside surface and in the host rock immediately underlying the slickenside, and secondly to classify the types of slickensides. *Coating* and *deformed host layer* will be used to refer to these two layers (Fig 3.1). Because the two terms are such an integral part of the classification, they are defined first.

3.2.1 Coating and deformed host layer

Coating is a discrete layer of material immediately under the slip surface, with a composition or texture different from that of the host rock. Coatings which have definite upper (at the slickenside) and lower (against host or deformed host) boundaries may develop before, during, or after slip on slickensides. Fibrous mineral growth (Durney and Ramsay 1973), gouge layers (Engelder 1974a), and surface melting layers (Spray 1989b) are examples of coatings.

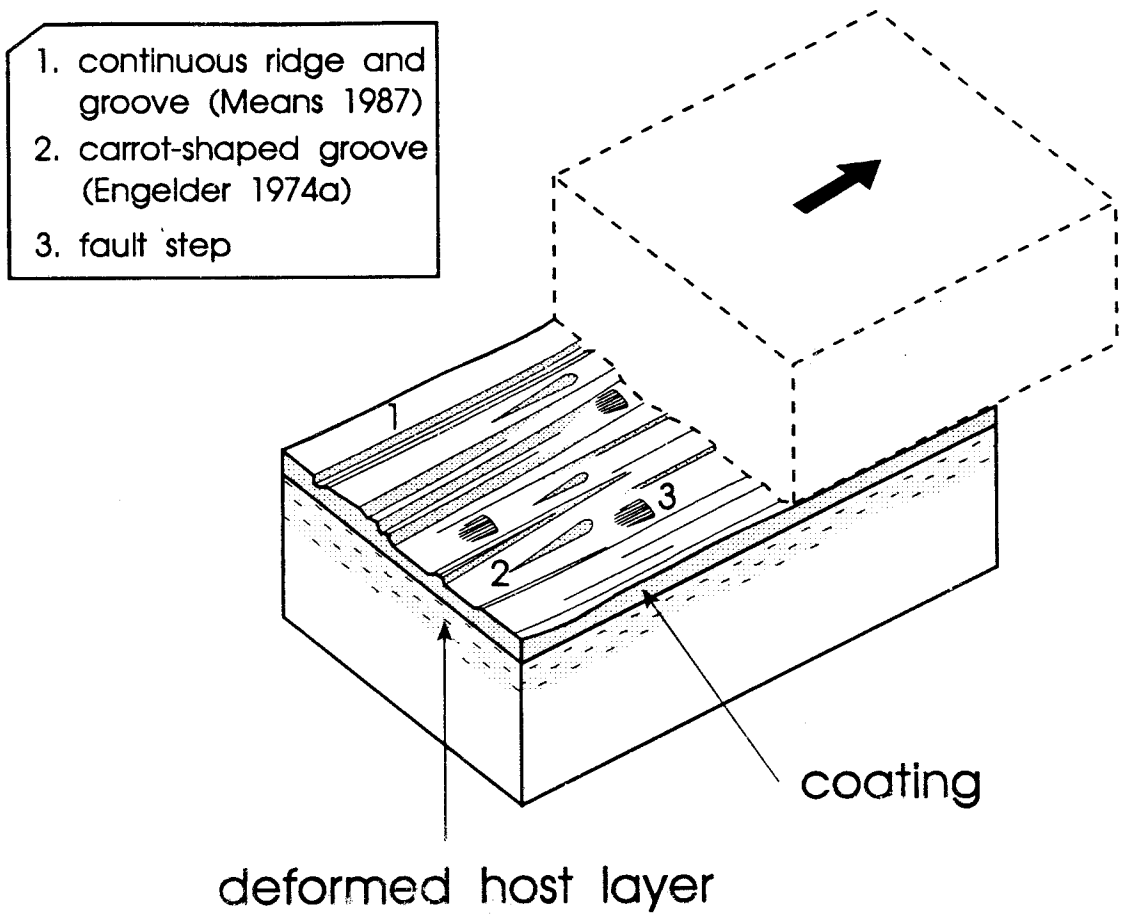

Figure 3.1. Schematic diagram of the interaction between two rock blocks leading to slickenside generation and the formation of related structures. Coating and deformed host layer are developed near the slip surface. Three types of slickenside surface structures labeled are as follows: 1. ridge and groove, a continuous lineation produced by nesting of two intact blocks; 2. carrot-shaped groove, indicating seismic phase of faulting; 3. fault step.

Deformed host layer is a zone of deformed host rock developed parallel to the slickenside. Like coating, It may develop by deformation before, during, or after slip on slickensides. The types of structural change in this zone may involve fracturing, cataclasis or plastic deformation (Aydin and Johnson 1978, Petit and Laville 1987). The boundary between deformed and undeformed host rock is commonly gradational.

Even though slickensides are usually known as a product of brittle deformation, the deformation of the host rock may or may not be brittle, depending on the strain-rate and scale of observation. The thickness of the coating and deformed host layer ranges from microscopic to outcrop scale. In this study, coatings and deformed host layers on a microscopic scale are discussed. A weakness of the present classification is that a given slickenside can be classified differently depending on the scale of the observation.

3.2.2 Four types of slickensides

The classification scheme is based on the existence of microscopic coatings and deformed host layers, and slickensides have been divided into four types (Fig. 3.2). These four types are: type A (deformed host layer only), type B (coating and deformed host layer), type C (no coating and no deformed host layer), and type D (coating only).

The thickness of coating and deformed host layers of 32 thin sections was measured using a micrometer under the microscope. Since the thickness varies from place to place in thin section, a median thickness over the whole thin section was recorded. In many cases, boundaries of the deformed host layer are uncertain because the intensity of deformation gradually decreases towards the undeformed host rock. Therefore, the measurement of deformed host layer may be somewhat arbitrary.

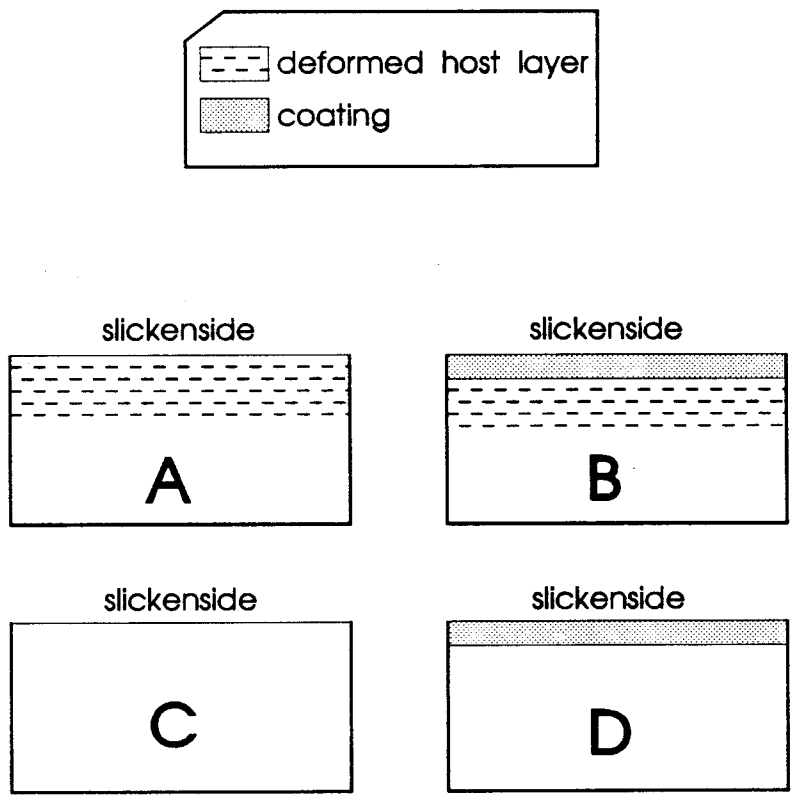

Figure 3.2. Four morphological types of slickensides based on the existence of two distinctive layers, coating and/or deformed host layer. Type A, deformed host layer only; type B, both coating and deformed host layer present; type C, neither coating nor deformed host layer present; type D, coating only.

Table 3.1 illustrates the thickness of coating and deformed host layer measured to a hundredth of a millimeter. Based on the existence of coating and deformed host layer, each slickenside has been classified into the four types. In hand specimen, however, it is sometimes hard to recognize the coating and deformed host layer, even though they are easily identified under the microscope. Therefore, the thin section data of coating and deformed host layer are used to classify the slickensides.

Figure 3.3 shows a graphic representation of slickenside types by plotting the thickness of coating versus deformed host layer for the slickenside thin sections. The host rock types of each thin section are variable in composition, texture, and origin (see Table 1.1). In addition, a micro-scale ductile shear zone rock was plotted. The host rock from this shear zone is fully deformed over the entire thin section area. Due to the limitations of thin section size, the maximum thickness of the shear zone is considered to be 10 mm.

3.2.2.1 Type A

Type A slickensides have deformation structures in the host rock concentrated immediately under the slip surface, with no coating material. The slip surface is thus positioned directly on the deformed host rock. Three thin sections are grouped into the type A (Nos. 21, 78 and 111) and plotted along the vertical axis in Figure 3.3.

Figure 3.4 shows an example of the type A slickenside. The host rock is a coarsely layered mica schist. Along the slip surface, it has a well developed cataclastic or semi-ductile deformation layer defined by crushed, dragged and ground out grains. The original schistosity oblique to the slip surface is overprinted and eventually obliterated by the discrete shear bands of the cataclastic

Table 3.1 Thickness of coating and deformed host layer

Sample No.	thin section (mm)		hand specimen		
	coating	def. host	coating	def. host	mor. type
21	0.00	3.00	X	X	A
78	0.00	1.50	X	O	A
111	0.00	0.70	X	O	A
92*	0.00	>10.00	X	O	-
13	0.13	0.30	X	O	B
17	0.50	1.10	O	X	B
18	0.40	1.40	O	X	B
19A	2.00	0.50	O	X	B
19B	1.50	2.00	O	O	B
24	0.20	0.50	X	X	B
30	0.70	0.10	O	X	B
41	0.02	0.05	O	O	B
58	0.70	0.20	X	X	B
59	0.08	1.10	O	X	B
60	0.30	0.30	O	X	B
71	0.50	3.00	X	X	B
72	0.80	1.70	O	X	B
76	0.50	0.08	O	O	B
81	1.00	1.50	O	X	B
83	0.10	1.20	X	X	B
86	0.05	0.80	O	X	B
99	0.08	1.20	X	X	B
104	0.15	4.00	X	O	B
105	1.00	1.00	O	X	B
116	0.03	3.00	O	X	B
117	2.00	2.00	O	O	B
36	0.00	0.00	X	X	C
63	0.00	0.00	X	X	C
108	0.00	0.00	X	X	C
66	0.20	0.00	O	X	D
70	0.30	0.00	O	X	D
124	0.40	0.00	X	X	D

O: recognizable
X: unrecognizable
*: ductile mylonite in shear zone

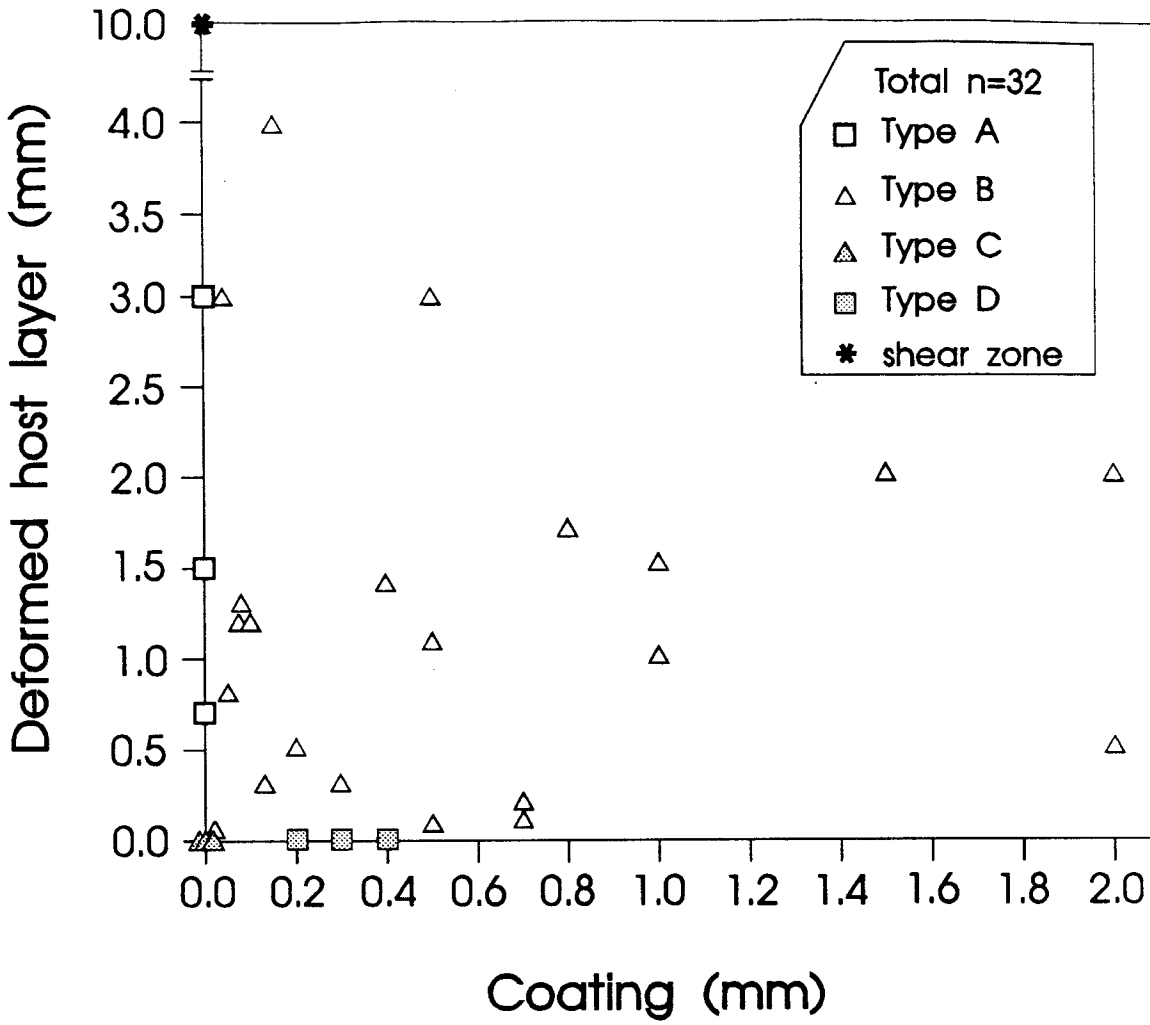

Figure 3.3. Plot of the thickness of coating versus thickness of deformed host layer for samples of this study. The four morphological types of slickensides are shown with different symbols. See Figure 3.9 for rock types.

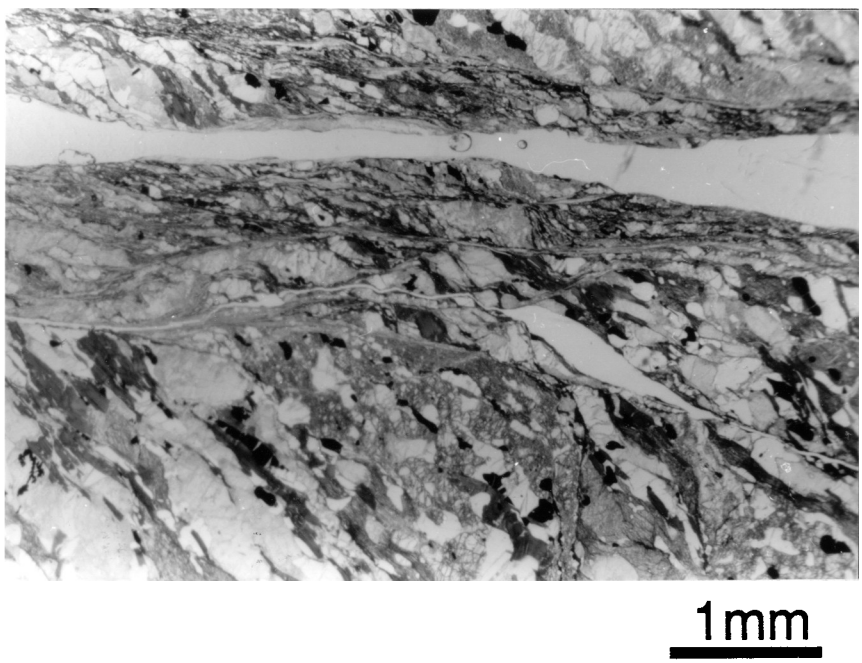

Figure 3.4. Photomicrograph of a type A slickenside (No. 78) illustrating the development of a strong deformed host layer in a mica schist. No coating is found on the slip surface. The deformed host layer shows a S-C geometry defined by discrete C planes parallel to the slickenside and alignments of mica-rich and quartz-rich domains oblique to the slip plane (S). The S-C geometry represents sinistral slip-sense. Plane-polarized light.

deformation. Within the deformed host layer, C and S planes are distinguished and the grain size is reduced.

In two other examples of the type A slickensides, the deformation features of the host rock are similar to that of the above mica schist. Cataclastic or sometimes semi-ductile deformation dominates the deformation of the host rock in this type of slickenside: development of foliation, redistribution of minerals, grain size reduction, and rarely plastic deformation.

3.2.2.2 Type B

Both coating and deformed host layer occur in this type. Out of 32 slickenside thin sections, 23 thin sections (about 72%) are type B slickensides. This may imply that most slickensided rocks are usually associated with both coatings and deformed host layers or can be a sampling bias. The coating is composed of different materials from that of the deformed host layer. A sharp boundary separates the coating and deformed host layer.

An example of a type B slickenside is shown in Figure 3.5. A slickensided granite is fractured and fragmented along the slip surface, and covered with an epidote vein. Fractures are developed within about 1.4 mm from the slip surface. The fracture zone in the host rock and the overlying small rock fragments and epidote vein correspond to the deformed host layer and coating, respectively.

3.2.2.3 Type C

In this type, neither coating nor deformed host layer is developed. This type of slickenside is uncommon because usually rocks in contact with a fault slip surface are likely to be influenced by slip movement and modified to form some deformation features.

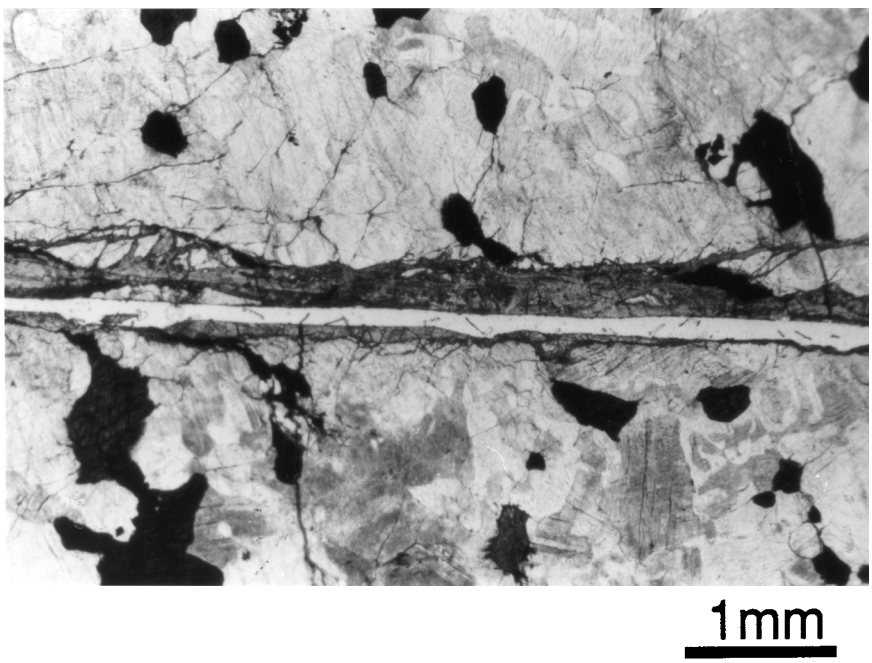

Figure 3.5. Photomicrograph of a type B slickenside (No. 18). A slickensided granite is coated with a massive epidote vein. Immediately under the epidote coating, fractures and small rock fragments concentrated along the slip plane indicate brittle deformation (deformed host layer). Sinistral slip-sense is indicated by extensional fracture and R-shear fracture (see Fig. 2.5b in chapter 2). Plane-polarized light.

Three samples meet the type C requirements: two mudstones (Nos. 36 and 108) and one quartzite (No. 63). Figure 3.6a represents an example of the slickensided mudstones in which neither deformation in the host rock nor coating is identified even under the microscope. The slickenside surface developed on the fine-grained host rock is very smooth. A remarkable feature of the mudstones in this type is that unlike normal slickenside surfaces, no distinctive striation on the slip surface is recognized in hand specimen. Instead, a flat and very shiny slip surface is observed (Fig. 3.6b).

The quartzite slickenside grouped as a type C shows a different slip surface feature from the mudstones. Under the microscope, the slip surface is very uneven and a few relicts of tiny mica flakes are identified sporadically along the uneven surface (Fig. 3.7). However, the present morphology of this slickenside is classified in that of type C slickenside because it does not have either an observable coating or a deformed host layer. The presence of a small amount of mica flakes may indicate that this slickenside originally had a coating material including the mica, but if so the coating must have been removed tectonically or by weathering.

3.2.2.4 Type D

Only the coating is recognized on the slickenside surface in this type. Three samples were identified as a type D slickenside: one mudstone (No. 124), one mafic igneous rock (No. 66) and one quartzite (No. 70).

Figure 3.8 shows an example of the type D slickenside whose host rock is a black mudstone. A quartz-opaque vein which covers the fine-grained host rock is developed immediately under the very smooth slip surface. The host rock does not indicate any noticeable deformation. The boundary between the coating and host rock is sharp and flat, which may be interpreted as a previous slip surface. Later this surface was covered by the quartz-opaque vein. Except for the vein coating, this

(a)

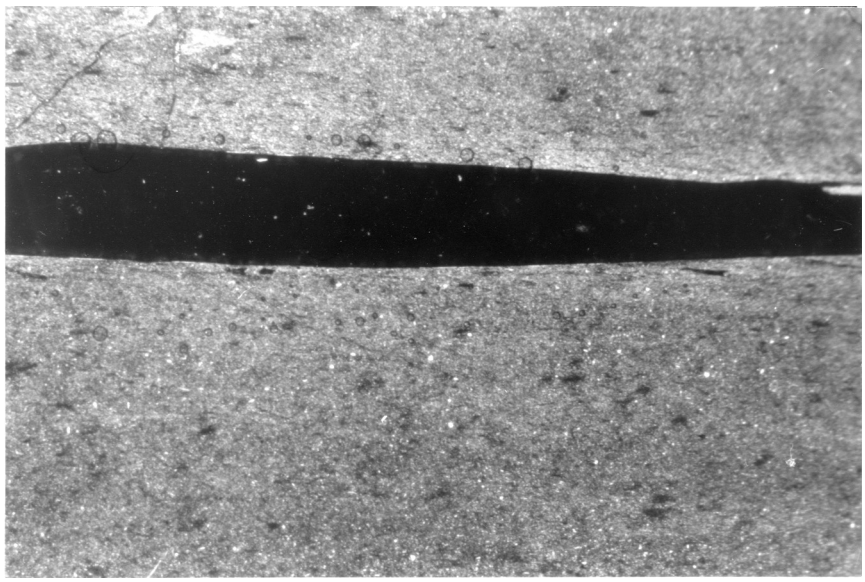

(b)

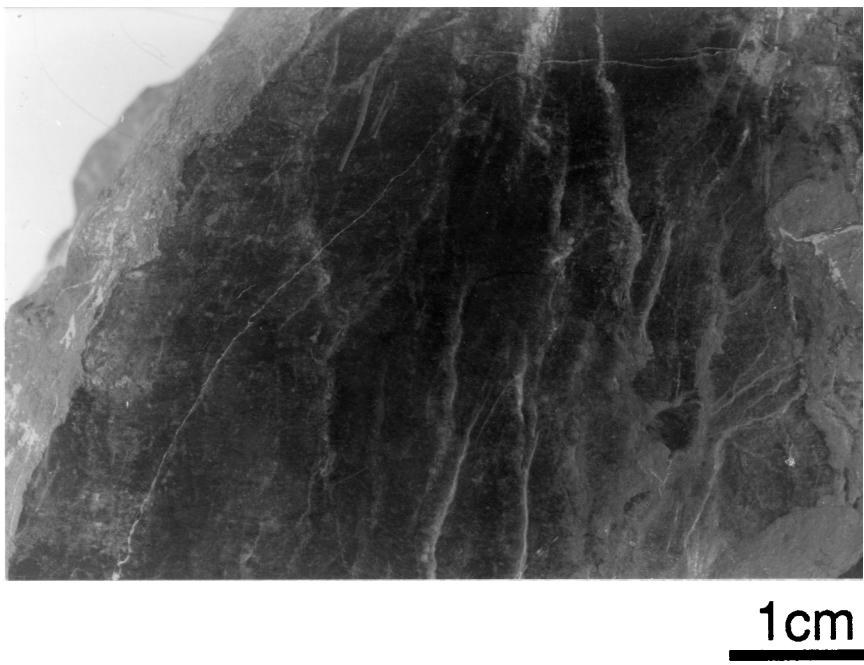

Figure 3.6. (a) Photomicrograph of a type C slickenside (No 108). A mudstone slickenside shows a smooth slip surface which is developed directly on the host rock. No deformation of host rock is recognized. Cross-polarized light. (b) Hand specimen of a type C slickenside in a mudstone (No. 36). No striation is recognized.

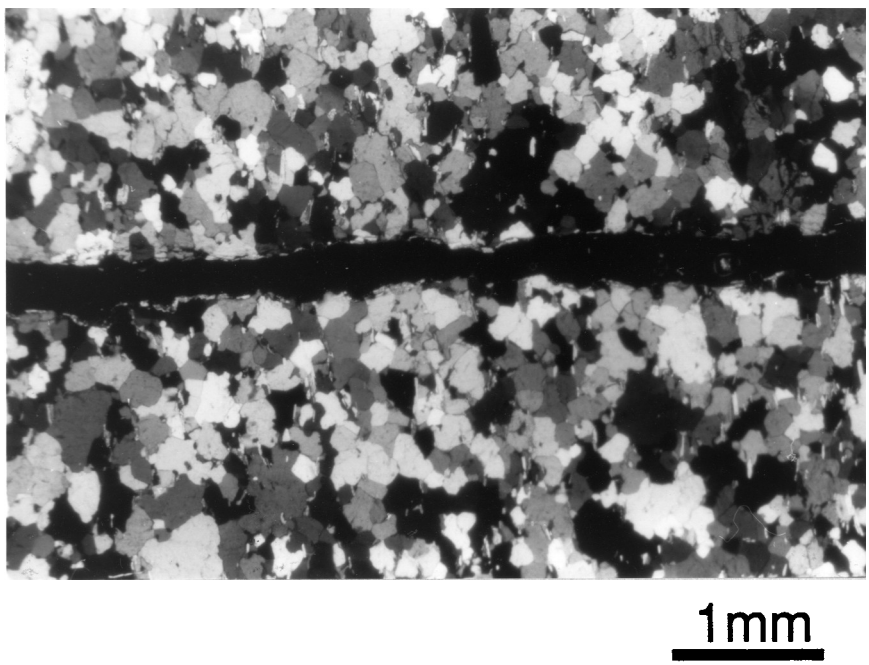

Figure 3.7. Photomicrograph of a type C slickenside by removal of a coating from a pre-existing type D slickenside in quartzite (No. 63). The slickenside has no coating or deformed host layer. The slip surface is rough. A few relicts of mica flakes are seen along the slip surface, indicating that a coating has possibly been removed. Cross-polarized light.

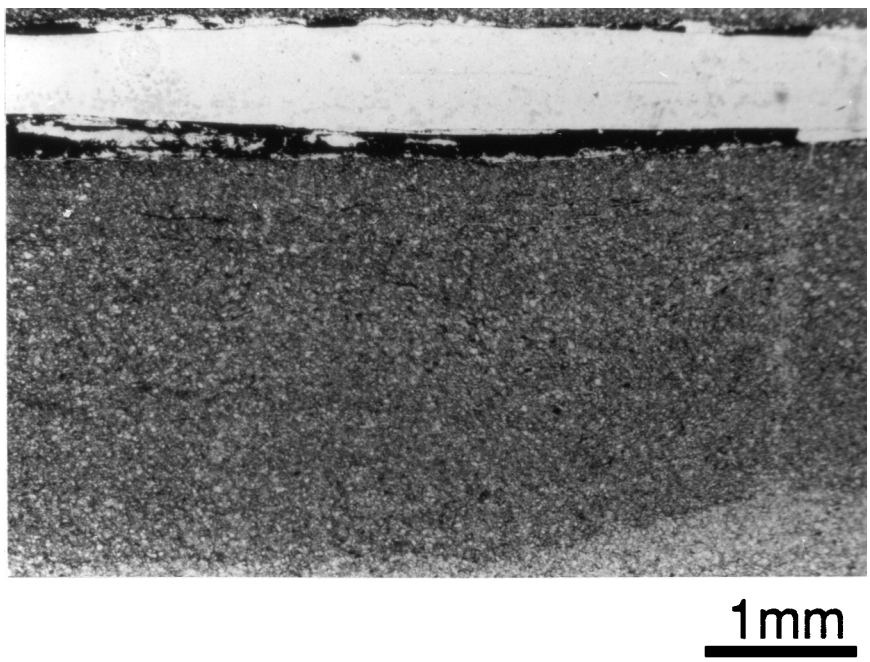

Figure 3.8. Photomicrograph of a type D slickenside (No. 124). A mudstone slickenside is coated with a massive quartz (white) and opaque (black) vein. No deformation of host rock is apparent. Plane-polarized light.

slickenside sample would be the same as the slickensided mudstones of the type C. Thus, the addition of a coating can create a type D slickenside from a pre-existing type C slickenside.

3.3 ROCK TYPES OF SLICKENSIDES

Figure 3.9 shows a distribution of rock types related to the four morphological slickenside types. The slickensided rocks except for a mylonite (No. 92) and two breccias (Nos. 104 and 117) were divided into six different groups, mainly based on their composition and grain size. Quartzite and sandstone, shale and mudstone, and granite and quartzo-feldspathic gneiss were grouped together because of their similarities in composition and grain size. Two distinctive fault rocks, the mylonite from a ductile shear zone and the breccias, were separated from other slickensided rocks because their original rock structures were too strongly modified to assign a normal rock name.

Some rock types may influence either slickenside morphology or development of deformation structures. Slickensided mudstone and shale which are mainly composed of fine-grained, mica, clay and quartz are the most abundant in this slickenside collection. As described previously, the type C slickensides with a smooth slip surface but no evident deformation in the host rock occur only in this rock group (open triangles in the origin of the diagram in Fig. 3.9). A type D slickenside in mudstone (No. 124) is very similar to the type C slickensides, except for the existence of coatings. The host rock of the type D slickenside shows the same feature as those of the type C slickensides.

Six slickensided rock samples are composed of mafic igneous rocks. The most obvious feature that appears in this rock group is the development of crystalline fibrous minerals such as chlorite, actinolite-tremolite, serpentine, etc

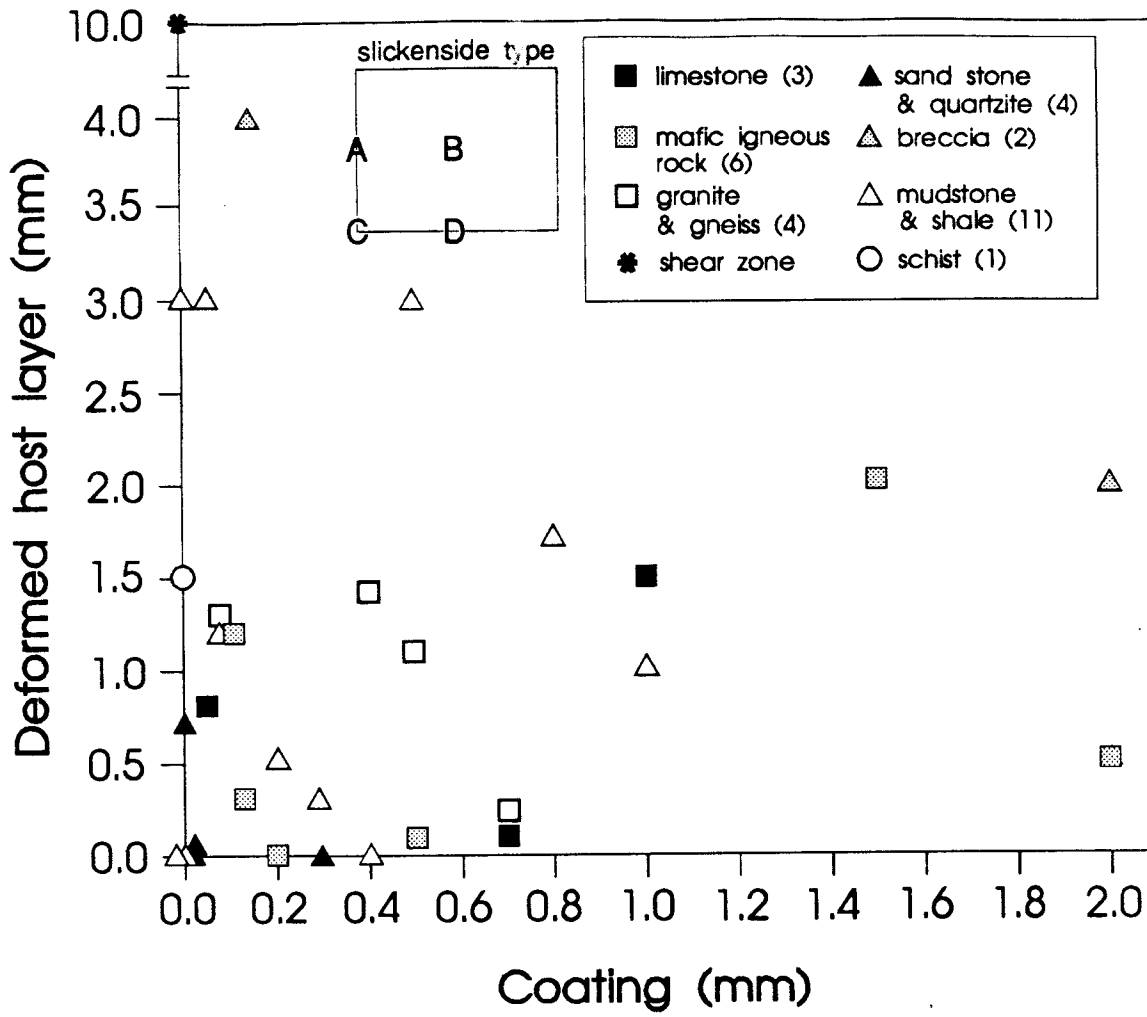

Figure 3.9. The same plot as in Figure 3.3 except that data are symbolized depending on their rock types. Positions of each slickenside type are labeled in the small inset diagram.

(Table 3.2). They show a strong preferred orientation relative to the slip surface. Alteration of mafic minerals such as olivine, pyroxene and amphibole by fluids perhaps led to the development of these layer silicates.

Quartz-rich rocks including sandstone and granitic rock groups show various structures relative to the development of slickensides. Brittle deformation usually prevails in these two rock groups, since slickensides are likely to take place above the depth where quartz and feldspar behave ductilely (e.g. granite in Fig. 3.5). In this case, well-developed gouges as coating, and fractures in the host rock, are characteristic. However, a type A quartzite slickenside shows a strong ductile deformation feature along the slip plane, which is evidenced by plastically deformed, elongated quartz grains (Fig. 3.10). The deformation of the host rocks seems to be dependent upon the physical conditions of faulting rather than the rock composition.

As shown in Figure 3.4, the mica schist slickenside represents a strong semi-ductile flow. The plastic deformation of coarse quartz grains indicates that external conditions play a more important role to create the deformation features than rock compositions. However, it is hard to state the general characteristics of the slickensides in schists from only one sample.

3.4 POSSIBLE PATHS FOR THE FOUR SLICKENSIDE TYPES

In Figure 3.11, possible ways in which the four morphological types of slickensides can develop are drawn from observations of slickensides in thin section. Although this simplified model does not necessarily apply to all slickenside examples, it may suggest some common trends for the development of slickensides.

The development process of slickensides can be divided into *primary* and *secondary* processes. Slickenside morphology developed during slip, whether seismic

Table 3.2 Types of coatings in mafic igneous rocks

spec. No.	13	19A	19B	66	76	83
rock type	altered gabbro	mafic igneous	mafic igneous	alterd gabbro	gabbro	mafic igneous
coating (fibrous layer silicate)	chlorite	tremolite	actinolite chlorite	serpentine	biotite serpentine chlorite	chlorite
mor. type	B	B	B	D	B	B

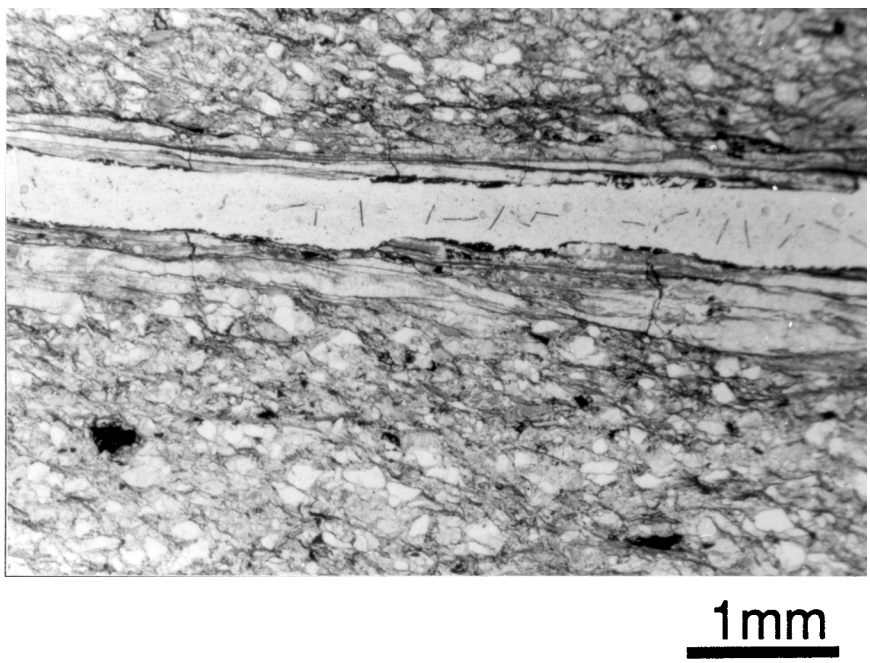

Figure 3.10. Photomicrograph of a type A slickenside developed in a deformed sandstone (No. 111). A strong, localized plastic deformation along the slickenside surface is indicated by elongated quartz grains. Plane-polarized light.

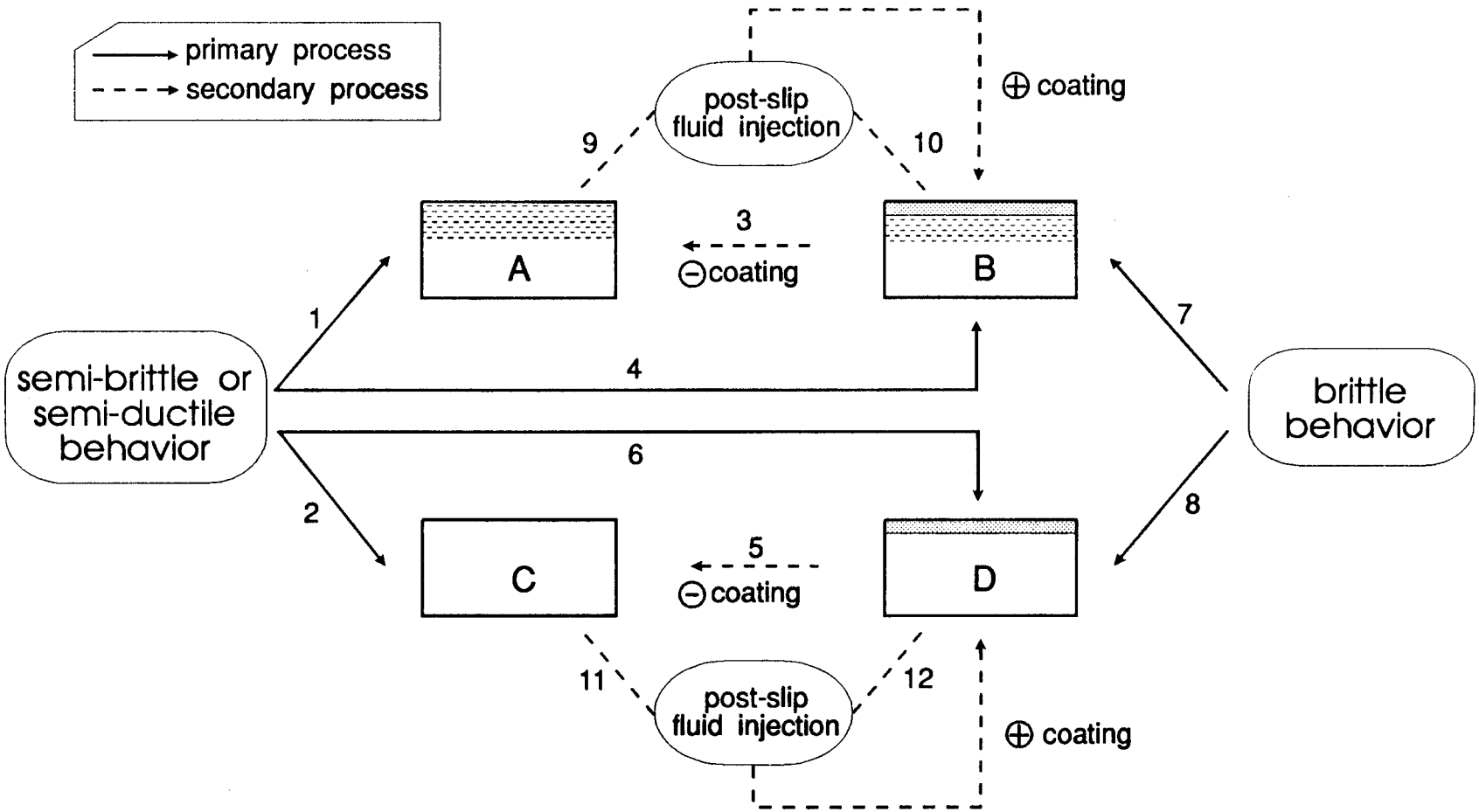

Figure 3.11. Possible paths for the development of the four morphological slickenside types. For type A, paths 1 and 3; for type B, paths 4, 7, 9 and 10; for type C, paths 2 and 5; for type D, paths 6, 8, 11 and 12. See text for a detailed explanation. Paths from secondary processes represent later removal (paths 3 and 5) or addition (paths 9, 10, 11 and 12) of coatings.

or aseismic faulting, is referred to as formed by a primary process. A secondary process, on the other hand, refers in this study to a process by which the slickenside morphology developed by primary processes is changed after slip. In the model of Figure 3.11, it is assumed that only one event of slickenside development occurs along each primary path. In multi-slip events, it will be much more difficult to use such a diagram. Additionally, only coating-addition and coating-removal are considered as secondary processes because the deformed host layers are formed by primary processes. In the following sections, development paths for slickenside types are discussed based on the two processes.

3.4.1 Type A

Two paths (paths 1 & 3) are possible for the development of type A slickensides. A semi-brittle or semi-ductile behavior leads to the deformed host layer in development of slickensides (path 1). The other possible case is that after the formation of a primary type B slickenside, coating can be later removed by weathering to leave a type A slickenside (path 3).

Examples of path 1 are the mica schist in Figure 3.4 and the quartzite in Figure 3.10. In this path, it is difficult for coating to occur because of the close spacing between the semi-ductilely displaced rocks. In addition, the deformation takes place at a depth where coatings (e.g. gouge) by brittle deformation are difficult to form. Although examples of path 3 slickenside are not found among the samples used in this study, path 3 is included as a possibility for type A slickensides since removal of coating is observed in another type of slickenside (e.g. path 5 for type C).

3.4.2 Type B

Four possible cases are present. Two primary type B slickensides can be formed by both semi-brittle (or semi-ductile) and brittle behavior, corresponding to paths 4 and 7, respectively. A possible case of path 4 is that slickensides in the semi-brittle (or semi-ductile) and relatively low slip-rate faulting can be accompanied by a crystalline growth of mineral as coating. Examples of path 4 are found in some mudstone and mafic igneous rocks which contain layer silicate coatings showing a strong preferred orientation and semi-ductilely behaved host layers (Fig. 3.12a). In the brittle regime at shallow depth, a frictional slip is usually accompanied by fragmentation or granulation by fracturing along the slip plane. This process produces gouge or breccia with large angular grains as coating and a fracture zone in the host rock (path 7). An example of this path is in Figure 3.12b.

Another two type B slickensides along paths 9 and 10 can be derived from an addition of coating onto pre-existing primary type A and type B slickensides, respectively. For both paths, coating is produced by veins injected into a pre-existing slip surface. The granite slickenside in Figure 3.5, under which a massive epidote vein is developed, is an example of the path 10.

Coating types reflect the history for the type B slickensides. Three different types of coatings can be discerned. One is a gouge or rock fragment (path 7), another is a crystalline growth with preferred orientations (path 4), and the last is a post-slip injected vein (paths 9 and 10).

3.4.3 Type C

As described previously, two different paths for type C slickenside formation are suggested. A primary type is found in the fine-grained mudstone shown in Figure 3.6a (path 2). Fine-grained, somewhat ductile materials in the rock can develop such a type C slickenside with no evident deformation texture in the host

(a)

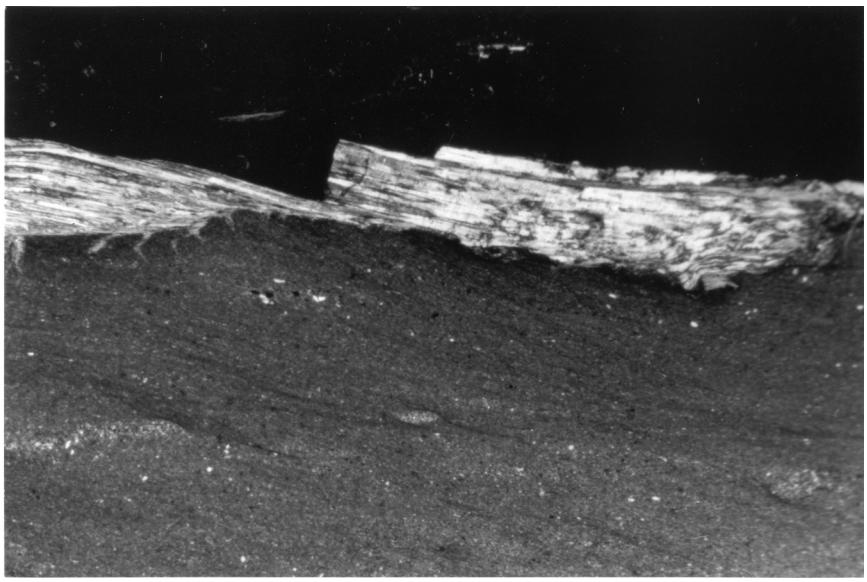

(b)

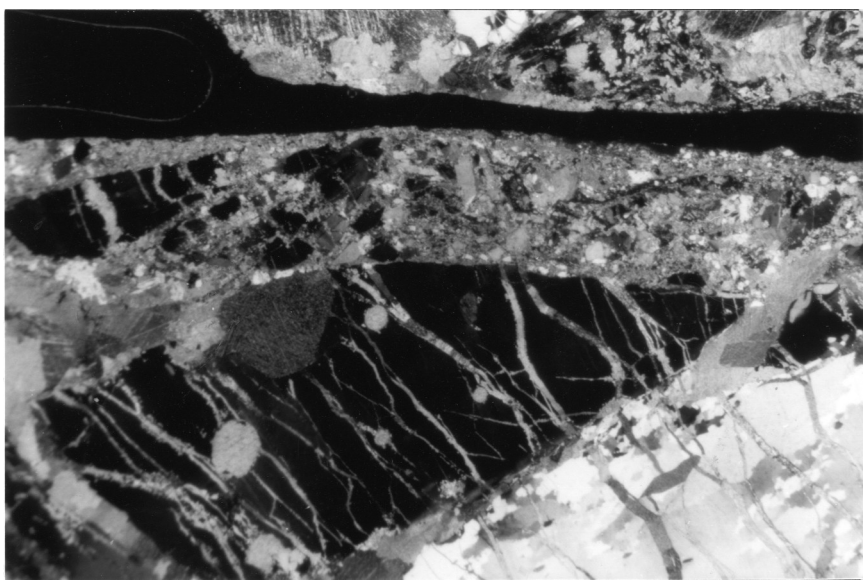

Figure 3.12. Photomicrographs of type B slickensides with different types of coatings (a) A crystalline layer silicate coating (No. 72). Rooted crystalline layer silicates in a mudstone form fault step structures. Cross-polarized light. (b) A gouge coating (No. 81) developed on a slickenside surface. Gouge layers and fractures on a limestone (or marble?) slickenside developed by brittle deformation. Calcite cements the gouge and fills the fractures. Cross-polarized light.

rock. The mechanism of this slickenside type will be discussed in the later part of the chapter. The other path can be caused by late removal of the coating through weathering or a second slip episode from a pre-existing primary type D slickenside, which may be illustrated by the quartzite in Figure 3.7 (path 5).

3.4.4 Type D

Like type B slickensides, the type D slickenside formation can also follow four different paths (paths 6, 8, 11 and 12). The only difference is that type D slickensides do not exhibit any deformation of the host rock. One mechanism for type D slickenside formation is gouge development as coating on the slip surface during brittle deformation occurring at shallow depth of faulting. If the influenced host rock is changed to gouge or rock fragments during faulting without fractures in the host rock, the resulting slickenside will represent a type D morphology (path 8). This procedure is similar to path 7.

Paths 11 and 12 illustrate the processes in which coating can be formed by the injection of fluid (e.g. vein) onto a pre-existing primary type C and type D slickensides, respectively. The mudstone slickenside shown in Figure 3.8 is an example of the path 11 in which the post-slip injected quartz-opaque vein creates a coating. No example for the path 12 appears in this study.

Slickensides following the primary path 6 may rarely occur. As a slip occurs in the ductile host rocks which can develop type C slickensides along path 2, there seems to be very little space between slip surfaces to produce coatings. As shown in the above cases, there can be several mechanisms to produce type D slickensides depending on the type of coating and host rock. Individual examples representing each path will be described in more detail in chapter 4.

Similar to type B slickensides, the difference between primary (path 8) and secondary (paths 11 and 12) for type D slickensides is that coating is made up of

gouge or other brittle deformation products in the path 8 . On the other hand, in the paths 11 and 12 fluids are injected after slickenside formation so that they form coatings of massive vein.

3.5 SLICKENSIDES: POSSIBLE INDICATORS FOR THE SLIP-RATE AND DEPTH OF FAULTING

How are the morphological slickenside types related to faulting conditions? It is difficult to match the slickenside types with faulting conditions as there can be more than two paths for the development of each slickenside type. Therefore, the morphology of slickensides itself does not indicate a particular set of faulting conditions. However the types of coatings and deformed host layers related to each development path can be useful to infer the faulting conditions.

Figure 3.13 illustrates fault slip-rate and depth conditions inferred for slickenside formation and the development of coating and deformed host layer. The diagram delineates the rheological condition for quartz-rick rocks where the temperature for brittle/ductile (Tullis and Yund 1977) or elastic frictional/quasi-plastic (Sibson 1983) transition is approximately 300 °C. For mafic rocks which are rich in feldspar, olivine, and amphibole, the transition is approximately 200 °C higher ($\cong$ 500 °C) than for quartz-rich rocks (Tullis and Yund 1977, 1980, Harper 1985). Therefore, the boundaries in the diagram may be shifted to higher temperature with some extent, for such rocks.

3.5.1 Low slip-rate regime

In a low slip-rate regime of faulting, steady, aseismic shearing of less than about 10cm/year is predominant (Sibson 1977 and 1983). A strong evidence for the low slip-rate is fibrous crystal growth with preferred orientation which commonly

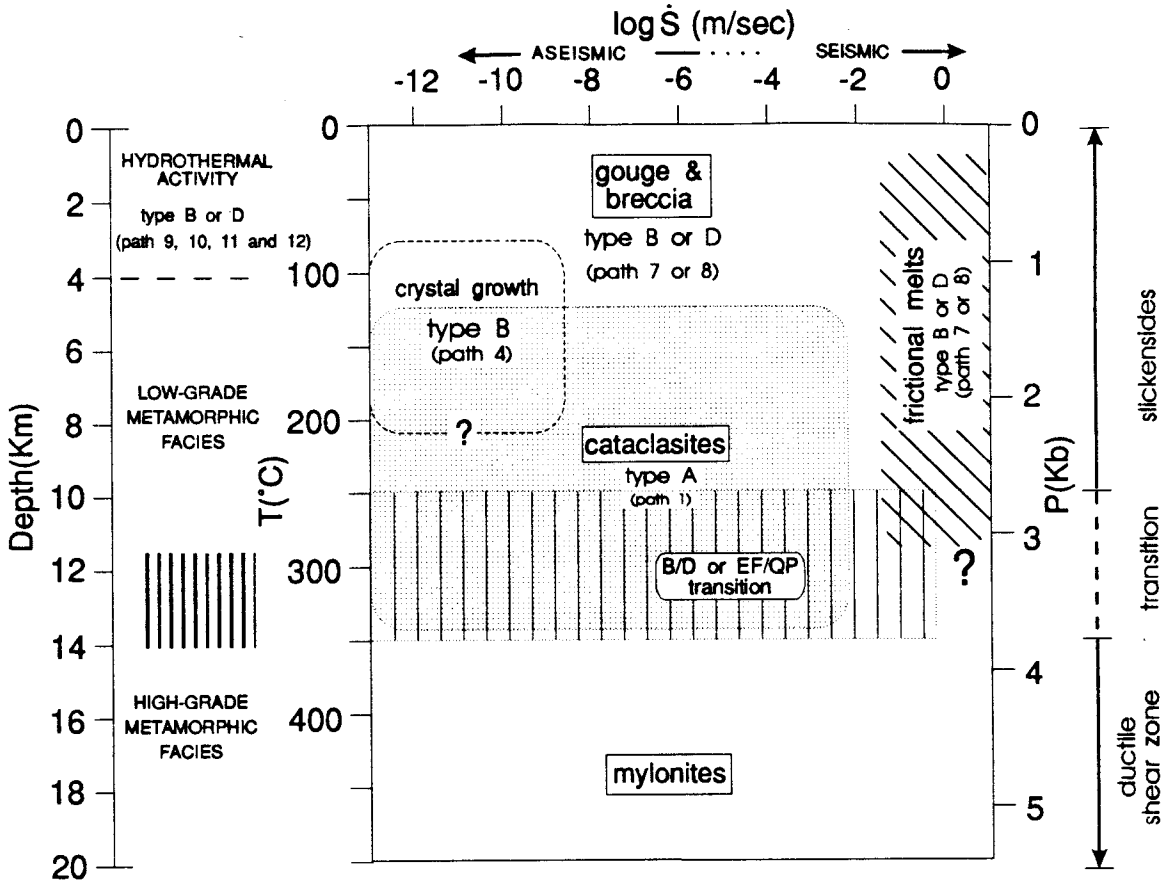

Figure 3.13. Slip-rate versus depth diagram showing associated fault rocks and metamorphic grades in continental crust of quartz-rich rocks. Slickenside types are located in specific faulting conditions related to slip-rate and depth of faulting. Geothermal gradient (ΔT), 25 °C/km (Sibson 1983); Geobarometric gradient (ΔP), 0.27 kbars/km from $P/h = \rho g$, where mean density of crust (ρ) is 2750 kg/m^3 (Turcotte and Schubert 1982, p75), g is the gravity constant (9.8 m/sec^2) and h is depth (km). B/D: brittle/ductile transition. EF/QP: elastic frictional/quasi-plastic transition. (Combined from Sibson 1977, 1983).

constitute coatings on slickenside surfaces (Durney and Ramsay 1973). Quartz, calcite, mica, chlorite, and serpentine showing preferred orientations correspond to this type as mentioned in chapter 2 (Fig 3.12a). These minerals crystallize by pressure solution slip during a slow, aseismic period of faulting (Elliott 1976). In many cases, these coatings originate either from external fluids, particularly hydrothermal fluids, or by reaction of the host minerals with the fluids. In Figure 3.13, the type B slickensides following the path 4 can be developed in this condition.

Spray (1989a) has suggested gouges and cataclasites as products of low slip-rate of faulting where brittle and semi-brittle (or semi-ductile) deformations are the dominant processes respectively, and frictional heating is negligible. As fine-grain size and weak strength of the gouges reduce the frictional energy between the two fault blocks, aseismic slip usually occurs. In this study, gouges are classified as a type of coating whereas cataclasites are a part of the deformed host layer based on their morphological characteristics. In the former case, the type B (path 7) or type D (path 8) (if no deformed host layer) slickensides can be produced with gouge coatings (Fig. 3.12b). In the latter case, slickensides with cataclastic deformed host layers will form at greater depth than those with gouges according to Sibson's fault rock classification (1977). Therefore, the type A slickensides through path 1 can develop in this condition where semi-brittle, partly ductile deformations prevail. The formation of this slickenside with cataclastic deformation may extend through the brittle/ductile transition.

3.5.2 High slip-rate regime

Frictional melts such as glass and pseudotachylyte are believed to occur at a high slip-rate of faulting, of more than 0.1 m/sec (Sibson 1975, Friedman *et al.* 1974, Spray 1989b). They can be generated at either shallow depth or greater depth because their development is dependent primarily upon the slip-rate rather than

depth. Slickensides formed in this regime can develop the type B or type D (if no deformed host layer) morphology in which the frictional melts create coatings on the slickenside surface. Unfortunately there is no example of frictional melting on slickensides found in the slickenside collection of this study.

3.5.3 Depth of faulting

The proportional increase in pressure and temperature with increasing depth in the crust can be represented as geobarometric and geothermal gradients, respectively. According to the classification of Sibson (1977), the development of fault rock changes from gouge to cataclasite to mylonite in that order, as depth (also pressure and temperature) increases and the deformation regime changes from brittle to semi-brittle (or semi-ductile) to ductile, respectively. It implies that in the development of slickensides the gouge coating may give way to a cataclastic deformed host layer with increasing depth.

In the deformed host layer of slickensides, fractures predominate in the brittle field whereas foliated cataclastic flows prevail in the semi-brittle or semi-ductile field including the brittle-ductile transition. The development of a strong foliation by plastically deformed grains dominates in the ductile regime of greater depth. In slickensided fault rock, the microstructures implying plastic deformations, such as kink bands, undulatory extinction and subgrain boundaries may point to local ductile deformation.

Massive veins (e. g. Nos. 18 and 124 in Figs. 3.4 and 3.8, respectively) developed on slickensides with non-preferred orientation may originate from hydrothermal fluids at shallow depth (see Fig. 3.13) or other sources such as fluids produced by dehydration during metamorphism at greater depth. Minerals such as quartz, opaque and epidote precipitate along pre-existing fault planes, which corresponds to paths 9, 10, 11 and 12 in Figure 3.11. This type of coating is

distinguished from the syn-slip (aseismic) fibrous crystal growth (path 4) in terms of the timing of its formation and texture. However, it is difficult to obtain information of the original faulting conditions because of the difference in timing.

Mineral assemblages in the host rock related to slickenside formation may also give information on the depth of faulting. Syn-tectonic mineral phases related to the development of slickensides under specific pressure and temperature conditions may indicate the approximate depth where they formed. An example (No. 13) will be described in chapter 4.

3.6 DISCUSSION

There are three aspects of this chapter which need further discussion. First there is the origin of type A and type C slickensides which do not have any coating. From the morphology and structure exhibited, it can be inferred that these two types require particular conditions for their occurrence. Second, there is the effect of rock type, how the morphology of the slickensides is influenced by the rock type during slickenside development. Third, there is the question to explain how much slickensides can be justified for indicating the faulting conditions.

3.6.1 Type A and type C slickensides

Type A: The deformation features of type A slickensides, particularly in the quartz-rich rock in Figures 3.4 and 3.10, are very similar to those of a ductile shear zone rock (No. 92) (Fig. 3.14). Localized ductile deformation, such as plastically elongated, dragged quartz grains and developments of S-C geometry, is common in the type A slickensides. The shear zone and type A slickenside are plotted together on the vertical axis in Figure 3.3, which means that no coating is present on either rock type. On the other hand, there are two distinctions between them.

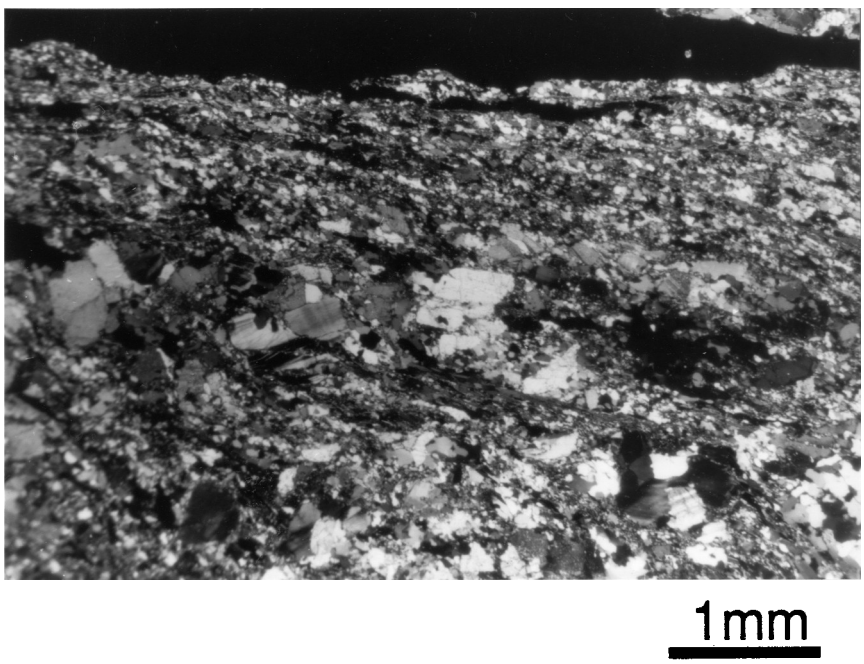

Figure 3.14. Photomicrograph of a quartz mylonite in a ductile shear zone (No. 92). Grain size decreases through recrystallization of quartz grains towards the center of the shear zone. This indicates plastic deformation during shear zone evolution. Cross-polarized light.

Morphologically, the deformation zone of the slickensided rocks is narrow and concentrated immediately underlying the slip surface, whereas in the shear zone sample, the deformation zone is wide and deformation appears to weaken gradually from center to wall. Structurally, slickensides occur in pairs, whereas the central part of shear zone is singular. A continuous offset occurs along the central part of the shear zone (Fig. 3.15). Therefore, the type A slickenside in quartz-rich rock may indicate a transitional environment between brittle faults and ductile shear zones.

Type C: The type C slickenside in Figure 3.6 which has neither coating nor deformed host layer has probably not been described in previous studies of slickensides. Two features of this slickenside are questioned. The first is the absence of coating and deformed host layer (Fig. 3.6a), and the second is the shiny slip surface not showing any observable slickenside striations (Fig. 3.6b). Some possible mechanisms are discussed here for the development of these features. The shine on the slip surface in type C slickenside may be produced by *true polishing,* made by decreasing the roughness of the slip surface directly on the host rock, not by coating of other materials. Two possible mechanisms for the true polishing are suggested. One possibility for the true polishing is a decrease in roughness by grinding of a slip surface during frictional slip (here called abrasive grinding mechanism). However, abrasive grinding is an unlikely explanation for the development of type C slickenside because no evidence is found for frictional grinding in the mudstone slickensides of type C. If this mechanism accounts for the smoothness of the mudstone slickensides, some relicts of ground materials such as gouge and other small fragments, and grooves produced by asperity ploughing might be expected on the slip surface.

The other possibility is a decrease in roughness by steady-state material flow. This mechanism is particularly common in fine grained ductile materials (here called ductile material flow mechanism). Will and Wilson (1989) have suggested a

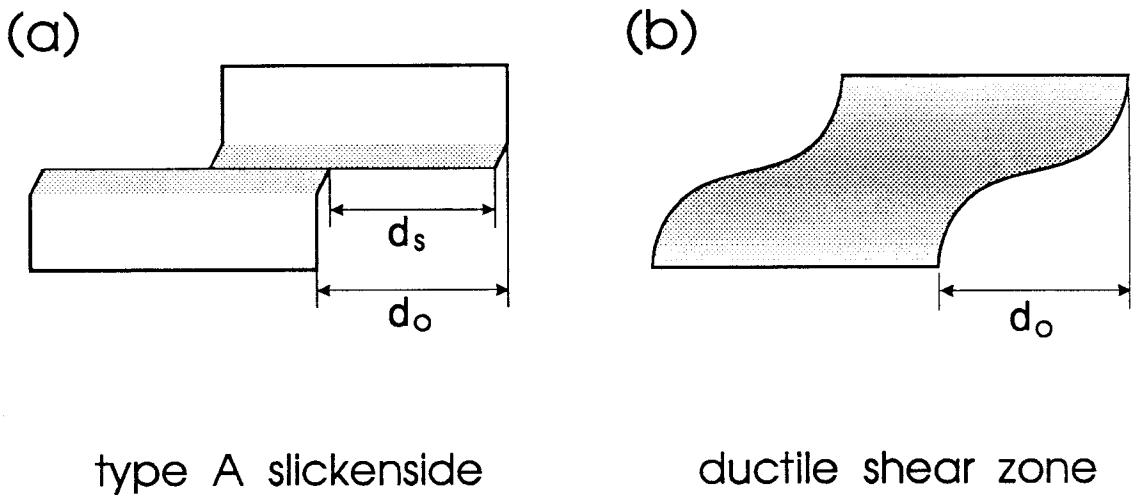

Figure 3.15. Comparison between (a) type A slickenside (path 1) and (b) ductile shear zone (b). In the type A slickenside, offset is caused mainly by slip. The deformation of the host rock is localized only along the slip plane. On the other hand, the same offset results in a gradual attenuation of shearing in a ductile shear zone. ds: slip amount, do: offset amount.

ductile material flow mechanism for shiny slickenside development not showing coating in fine-grained and easy-deformable materials (pyrophyllitic clay) from their experiments. However, unfortunately, the resulting slickensides from the experiment are inconsistent with type C slickenside because they show a deformed host layer from ductile shearing as well as ridge and groove-type striations (Means 1987) on the slip surface. Conclusively, I can not argue for either mechanism for the development of the type C slickenside. Neither mechanism is exactly suitable for the type C slickenside. However, a mechanism associated with ductile material flow seems more likely because of the ductile, fine-grained property of the slickensided mudstones in this study (this property may be variable with degree of cementing, competence, cohesion, or lithification) and no frictional evidence on the slip surface, although it can not explain the absence of striation and deformed host layer in slickenside development.

3.6.2 Effects of rock types

It is important to consider the effect of rock type in the study of frictional sliding behavior. Many sliding experiments have been conducted to simulate natural faulting conditions and to find out sliding characteristics of rocks under different pressure and temperature conditions (e. g. Byerlee and Brace 1968, Engelder 1975). Stesky *et al.* (1974) have shown a change in sliding behavior from stick slip to stable sliding depending on rock type, even under the same external conditions of pressure and temperature. They suggested that a stable sliding mode occurs easily in rock types including such minerals as mica or serpentine, even at low temperature where frictional stick slip sliding is predominant. Therefore, it is emphasized that mica- and other layer silicate mineral-rich rocks may easily deform by stable sliding, even under conditions that are in the stick slip regime for quartz-rich rocks.

For example, slickensides in mafic igneous rocks in this study are usually accompanied by layer silicate coatings showing a preferred orientation. Similar to the fibrous minerals such as quartz and calcite, these coatings imply a low slip-rate of faulting (Durney and Ramsay 1973). Moreover, the rock strength in the mafic igneous rock can be weakened by the alteration of the mafic minerals such as olivine, pyroxene and hornblende to layer silicates or of feldspar to sericite. Additionally, the layer silicate coating on the slip surface may play a role of lubricator to reduce the frictional strength. A relatively low slip-rate of faulting is, therefore, suggested for slickensides in such mafic igneous rocks. This fact may indicate that rock types, as well as external conditions, play an important role in producing a particular slickenside type.

3.6.3. Reliability of the classification of the slickensides

Coatings and deformed host layers of slickensides are easily identified under the microscope even if they are not visible in hand specimen. A slickenside can be classified differently depending upon the scale of observation. For instance, color and composition differences are more noticeable than textural difference to the unaided eye, which usually makes coating easy to identify while the deformed host layers are frequently difficult to recognize in hand specimen. Therefore, microscopic examination is necessary to describe and classify them.

Coatings are usually associated with fault slip event, but not always. For example, some coatings from surface melting and fibrous crystal growth have been known to form during seismic and aseismic periods of faulting, respectively (Spray 1989b, Durney and Ramsay 1973). On the other hand, a vein intruded into a pre-existing slip surface (slickenside) has no direct relation to the fault slip event. In the former case when coatings are formed related to slip, they may be useful in indicating the faulting condition.

Examples of paths in section 3.4 were based on observation of limited thin sections in this study. Other paths not described here are possible. For example, slickensides containing coatings on the slip surface representing former melt may develop along some paths. As mentioned earlier, frictional melts and pseudotachylytes can occur in the brittle regime at variable depths so long as the slip rate is high (Sibson 1975). Therefore, the frictional melts are expected along paths which represent the brittle regime (paths 7 and 8) in Figure 3.11.

3.7 SUMMARY

A classification of slickensides is proposed based on morphology on the microscopic scale. The observations in this study demonstrate the wide variety of slickenside types that could appear in natural fault rocks. Many of these types would probably not be readily recognized in hand specimen.

Some slickenside types can be related to certain faulting conditions and rock type using the principles in Figures 3.11 and 3.13. The classification is divided into two fundamental groups based on the timing of the formation of the slickenside morphology: primary and secondary types. Slickenside types following paths 1, 2, 4, 7 and 8 occur related to fault slip movement whether seismic or aseismic.

Paths 1, 4, 7 and 8 are associated with particular conditions of slip-rate and/or depth of faulting. The type A slickenside following path 1 represents a transition environment between brittle faulting and ductile shear zone. The type B slickenside with crystalline growth (path 4) implies a low slip-rate of faulting during slickenside formation. Brittle deformation at shallow depths dominates the development of type B and type D slickensides following paths 7 and 8.

There are six secondary types in which the present slickenside morphologies develop by changing of primary slickenside types. The slickenside types of paths 3

and 5 are created by the removal of coatings, whereas the slickenside types of paths 9, 10, 11 and 12 are caused by the addition of coatings.

The development of type C slickensides in fine-grained mudstones (path 2) is more dependent on rock composition than faulting conditions.

CHAPTER 4. PETROGRAPHIC DESCRIPTION OF THIN SECTIONS OF SLICKENSIDES

4.1 INTRODUCTION

This chapter aims to apply the framework in chapter 3 (see Figs. 3.11 and 3.13) to six slickenside samples selected on the basis of rock type and/or morphological type. The samples have already been mentioned in the previous two chapters as examples of slip-sense indicators and of slickenside types, but petrographically not described in detail. In some samples, the development of microstructure and mineralization provide informations on variations in slip-rate and effects of fluids. They may be closely related to the cyclic behavior of faulting (Stel 1986, Power and Tullis 1989).

The six thin sections selected are: type A, No. 78 (path 1); type B, Nos. 13 (path 4) and 18 (path 10); type C, No. 108 (path 2); type D, Nos. 70 (path 8) and 124 (path 11). Four samples (Nos. 13, 70, 78 and 108) are believed to have developed their structural and compositional changes during present slickenside formation by a primary process as defined in chapter 3. On the other hand, the other two samples (Nos. 18 and 124) which have a coating of massive vein on a pre-existing slip surface are thought to have developed by a secondary process.

4.2 TYPE A SLICKENSIDE

4.2.1 No. 78

As an example of type A slickenside, a slickenside in a garnet-biotite schist will be described. This rock is coarse grained (averaging 1 mm) with a well defined

schistosity. The slip surface is moderately rough (Fig. 4.1). No coating on the host rock is present whereas intense cataclastic flow deformation has occurred over a thickness of 0.5-1.5 mm immediately under the slip surface.

Undisturbed host rock: The host rock is composed of quartz, feldspar partially altered to sericite, biotite, fractured garnet and a minor opaque mineral. Original schistosities are well preserved with alternating bands of biotite and quartz-feldspar (Fig. 4.2a). Quartz grains show gentle undulatory extinction and subgrain boundaries, which may record some crystal plasticity. Kink bands are prominent in biotites which are oriented along the schistosity. These microstructures are widespread throughout the thin section (Fig. 4.2b). Feldspars are partly altered to sericite and show little sign of internal deformation. Garnets whose grain size is reduced by dilatant cracks cutting across the larger relict grains (~2.5 mm) are surrounded or partly replaced by chlorite and calcite.

Discrete shear planes: Widely-spaced (~0.8 mm), but rarely occurring discrete shear planes are recognized in the undisturbed host rock between about 1 to 4 mm from the slip surface (Fig. 4.2c). Opaque minerals are concentrated along the shear plane. Some quartz, feldspar and biotite grains are partly sheared and fractured across the shear plane. However, the grain size and composition in the part of the host rock where the shear planes develop are the same as those of the undisturbed host rock because the shear planes are discontinuous (2-3 mm) and are only sporadically developed (see sketch in Fig. 4.1).

Cataclastic deformation zone: This zone occurs at the contact with the slickenside surface and is commonly 1 to 1.5 mm thick. It is defined by intense cataclastic and ductile deformation textures (Fig. 4.2d). The change from the undisturbed host rock to the cataclastic deformation zone is a noticeable textural transition. The most marked textural changes are the development of closely spaced foliations and grain size reduction. The anastomosing foliations of 0.2-0.4

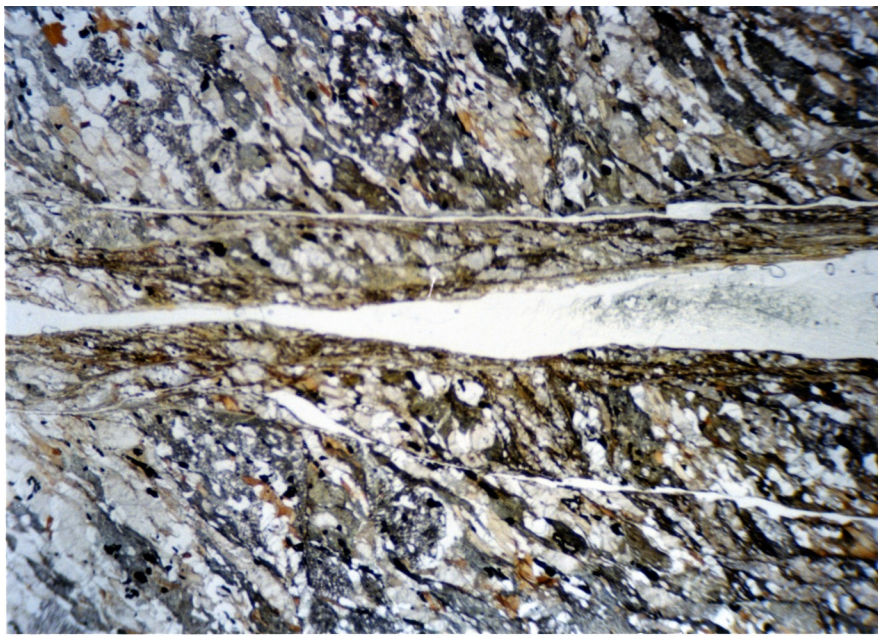

3 mm

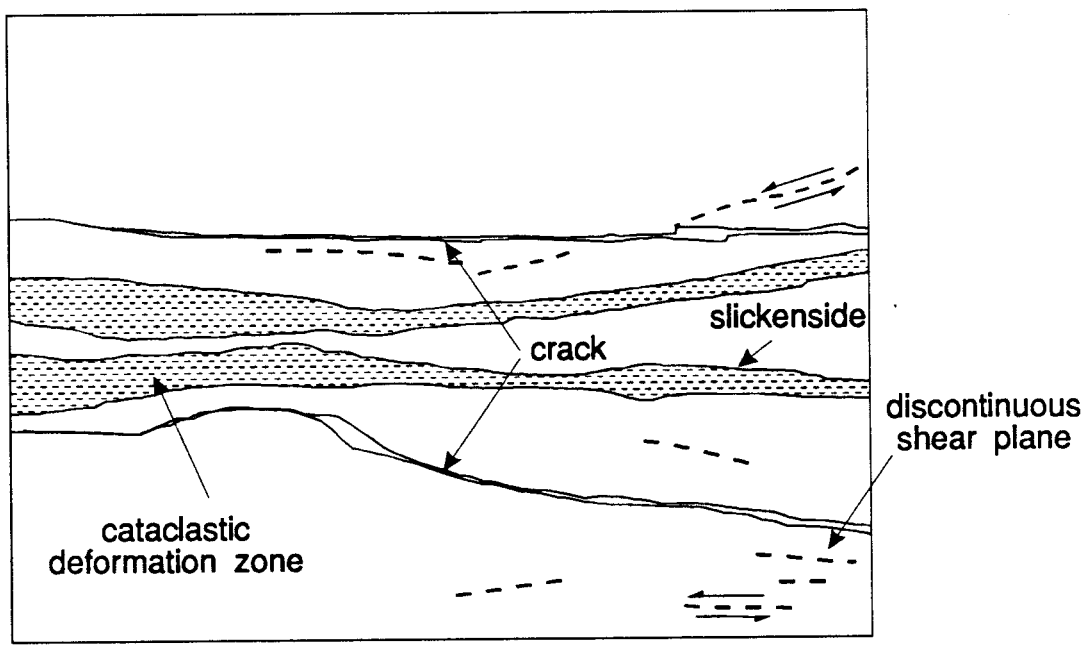

Figure 4.1 Photomicrograph and sketch of slickensided mica schist (No. 78). Dashed lines indicate the position of discrete shear planes. Cataclastic deformation zone (shaded) is characterized by grain size reduction and foliated cataclasite. Plane-polarized light.

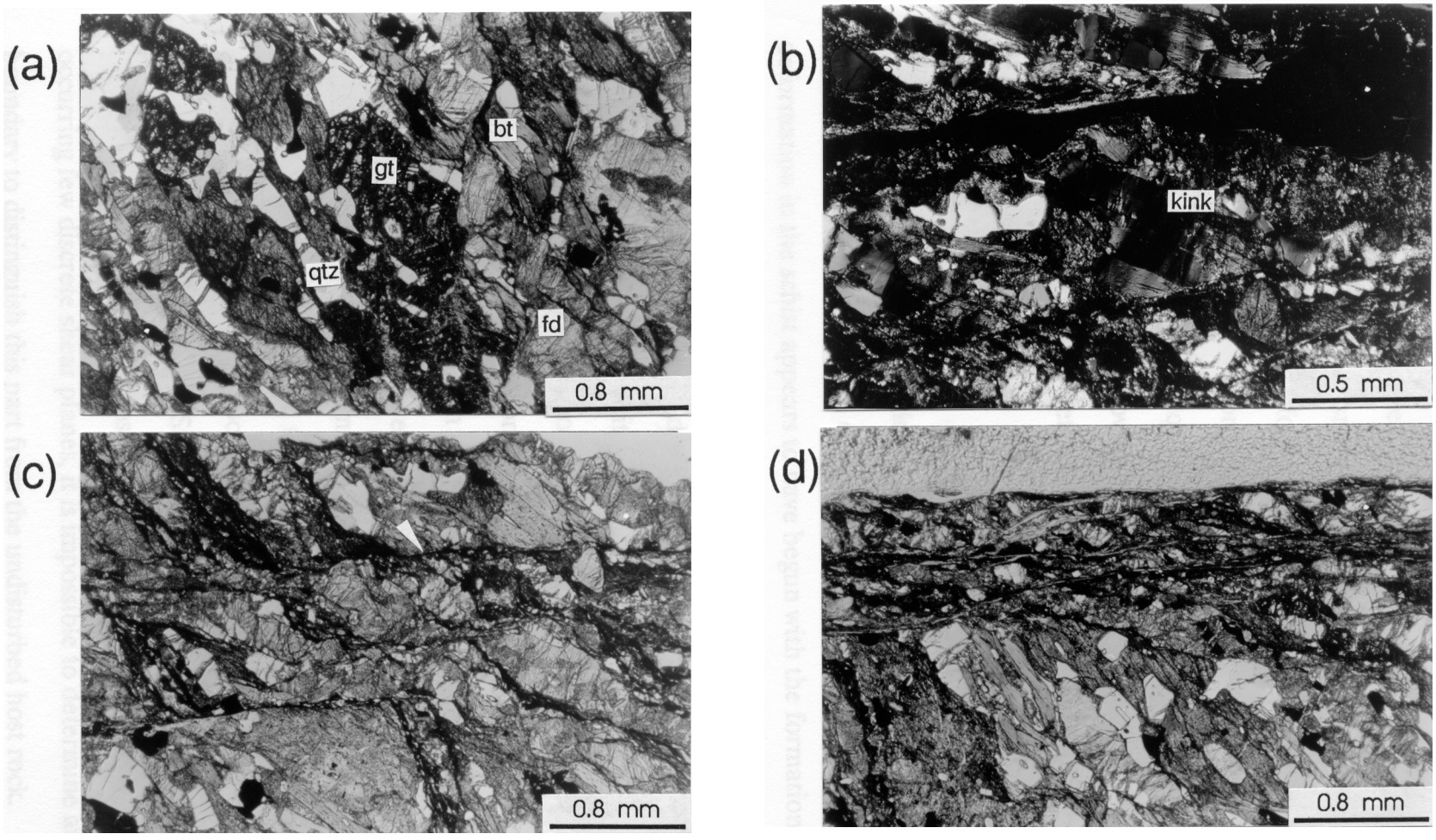

Figure 4.2 Photomicrographs showing textural features of sample 78. (a) Schistosity in undisturbed host rock. (b) Crystal plastic microstructures in quartz (undulatory extinction) and biotite (kink band). (c) Discrete shear planes (arrow). (d) Cataclastic deformation zone. Note increase in deformation from (a) to (c) to (d). (a), (c) and (d): plane-polarized light. (b): cross-polarized light. bt: biotite, gt: garnet, qtz: quartz, fd: feldspar.

mm spacing are defined by concentrations of chlorite films nearly parallel to the slip plane and obliterate the pre-existing schistosity. The grain size decreases to 0.1 mm or less, due to the cataclastic deformation, and distinguishes this zone from the undisturbed host rock. Small porphyroclasts of feldspar and quartz are surrounded by fine-grained matrix (crushed quartz, feldspar, biotite, and garnet) and the anastomosing chlorite films. However, no detectable compositional difference was found between the cataclastic deformed zone and the undisturbed host rock.

4.2.2 Interpretation

There are two different deformation modes in this example: first, weak plastic deformation and second, cataclastic shear flow. The sequence of deformation in the schist appears to have begun with the formation of crystal plastic deformation textures widespread throughout the thin section of rock prior to slickenside formation. The following main cataclastic deformation related to the occurrence of the slickenside reduced the grain size to that of cataclasite and developed the foliation of chlorites. In this stage, a few discrete shear planes also developed in the inside of the host rock.

The slickenside corresponds to the type A slickenside following path 1 according to the classification in chapter 3. No coating is found on the slickenside surface. The deformed host layer is defined by the cataclastic deformed zone where cataclastic, partly ductile deformation facilitates further strain by permitting slip on the zone with chlorite films and fine-grained matrix concentrated near the slip surface. The part of the host rock showing the discrete shear plane was excluded from the deformed host layer. Since it does not represent any difference from the undisturbed host rock in composition and texture except for the localized, rarely occurring few discrete shear planes, it is impossible to determine any reasonable boundary to distinguish this part from the undisturbed host rock.

Cataclastic flow textures with minor plastic deformation developed near the slip surface may indicate that this slickenside formed at lower depths where semi-ductile deformation is dominant at conditions of the brittle/ductile transition zone (Sibson 1977 and 1983).

4.3 TYPE B SLICKENSIDE

Type B slickensides showing both coating and deformed host layer are the most common type in this slickensided rock collection. Two different examples of type B slickensides are described in this section based on the timing of present slickenside development relative to the host rock deformation: the primary process (No. 13) and secondary process (No. 18).

4.3.1 No. 13

The first example of the type B slickensides is a type developed by a primary process in which the slickenside formation was contemporaneous with deformation of the immediately underlying host rock. The host rock is a coarse-grained, altered hornblende gabbro. Low angle minor P-shear fractures extend into the host rock (see Fig.2.1a for the position of the fractures in the thin section). Chlorite fibers appear along both the main slip surface (coating) (Fig. 4.3) and in dilated gaps along the P-shear fractures (see Figs. 2.1c and 2.2 for the chlorite fibers along P-shear fracture). The slip surface is smooth.

Undisturbed host rock: The rock is mainly composed of pyroxene, plagioclase and hornblende, with minor chlorite, calcite and opaque mineral. Alteration is widespread in most minerals of the rock. Most feldspars (plagioclase) are altered to phyllosilicates such as sericite and chlorite along transgranular fractures. Pyroxenes

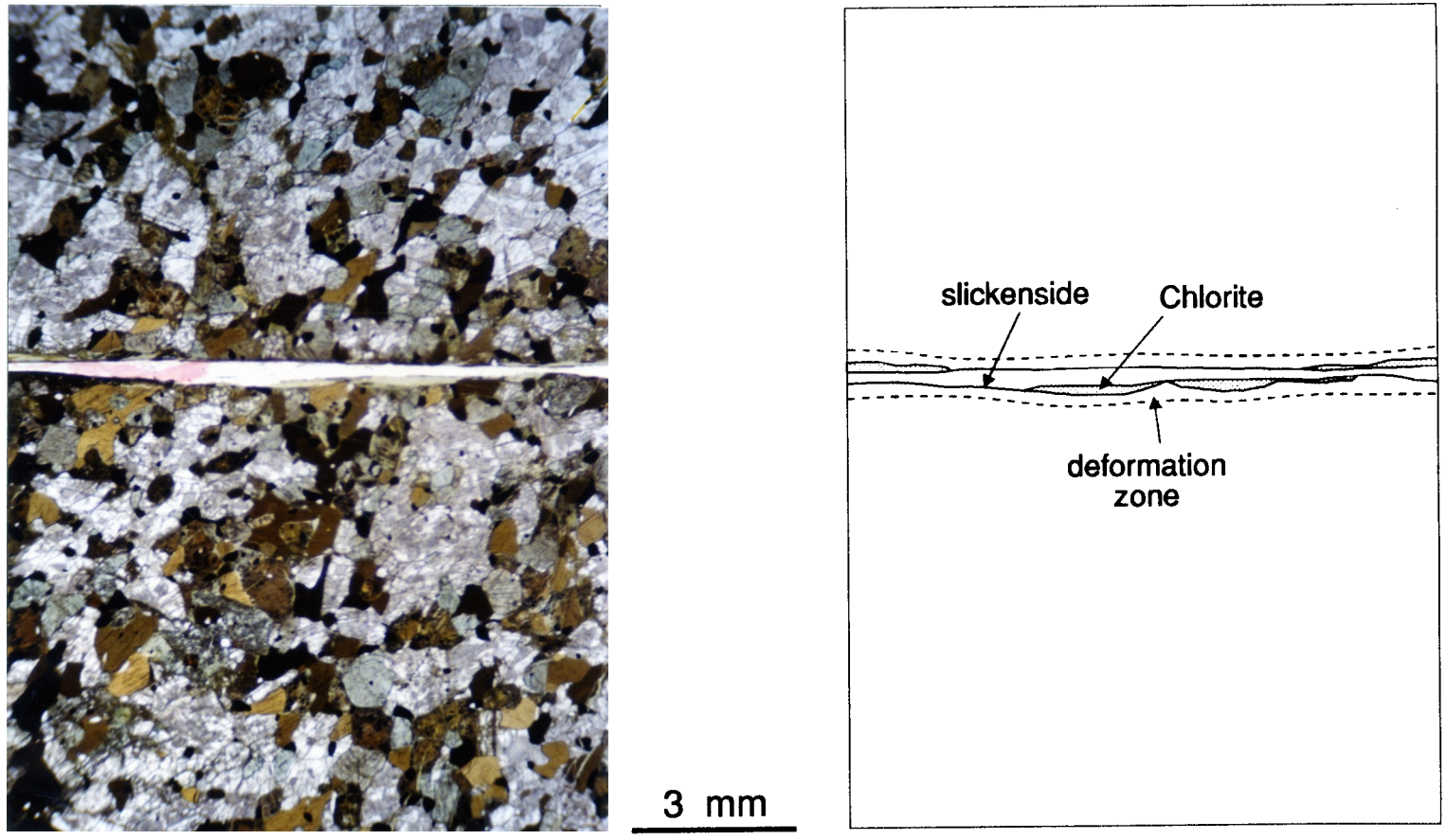

Figure 4.3 Photomicrograph and sketch of slickensided hornblende gabbro (No. 13). Chlorite coating and deformed host layer are developed along the slip plane. Plane polarized light.

are replaced by chlorite and magnetite (Fig. 4.4a). Alteration is more intense along minor shear fractures.

Deformed host layer: This zone is marked by bending and dragging in host-rock minerals and their alteration products, close to the slip surface. Near the slip surface, hornblende grains tend to be partly altered to actinolite showing pseudomorphs of the original hornblende grain shapes (Fig. 4.4b). This alteration of hornblende to actinolite also occurs along minor P-shear fractures. The response of grains to slip is somewhat different according to mineral type. In Figure 4.4b, actinolite formed by alteration of the end of a hornblende grain is bent without breaking. On the other hand, a hornblende grain in Figure 4.4c is broken and displaced rather than bent by the slip. These microstructures are only observed within < 0.5 mm from the slip plane.

Chlorite coating: Averaging 0.1 mm, the chlorite coating is discontinuously developed along the slip surface. It has a strong preferred orientation of chlorite cleavage subparallel to the slip plane (Fig. 4.4d). The boundary between chlorite and host mineral grains is not clear, which may indicate alteration of host minerals to chlorite. Slightly oblique preferred orientations of chlorites indicate the slip sense of the slickenside.

4.3.2 Interpretation

This slickenside corresponds to type B slickenside following path 4. In this case, the host rock deformation and coating type are controlled by the faulting conditions when the slickensides develop. Alteration prevails in the host rock. Feldspar alteration to sericite requires water to drive the alteration reaction. It has been reported that alteration of hornblende to actinolite occurs at temperatures near 500 ℃ within the upper greenschist to lower amphibolite facies (Winkler 1979, Liou *et al.* 1974, 1985). This temperature may correspond approximately to the

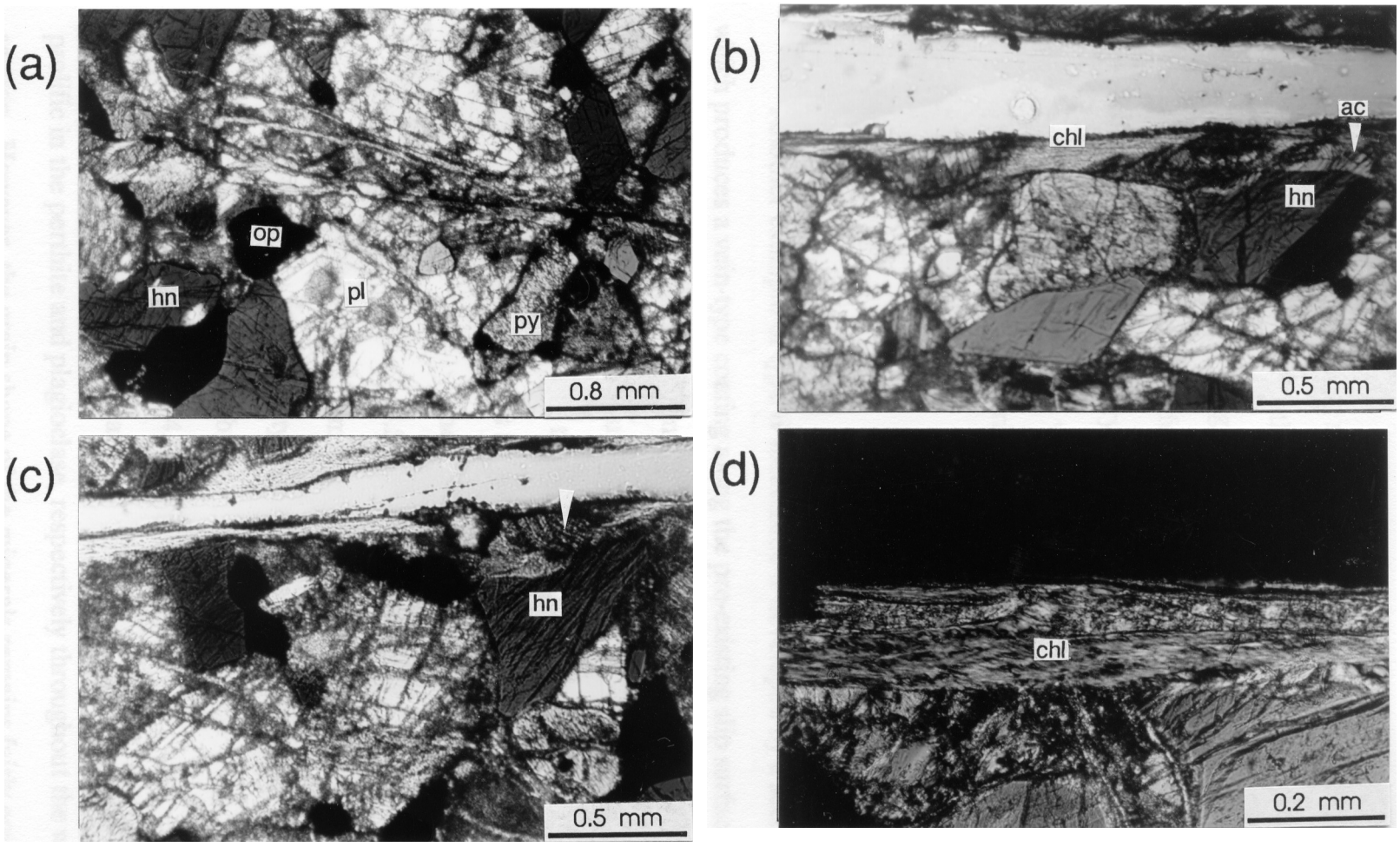

Figure 4.4 Photomicrographs showing textural features of sample 13. (a) Undisturbed host rock showing hydrothermal alterations of minerals. (b) Alteration of hornblende to actinolite (arrow) near slickenside surface. Chlorite fibers grow in dilated gap. (c) Broken hornblende grain (arrow). (d) Chlorite coating showing strong preferred orientations. (a), (b) and (c): plane-polarized light. (d): cross-polarized light. op: opaque, hn: hornblende, pl: plagioclase, py: pyroxene, ac: actinolite, chl: chlorite.

brittle/ductile transition of mafic rocks (Harper 1985). Also such alterations may reduce the rock strength, so that the rock can deform partially in a ductile manner, which is evidenced by the bending of actinolite in Fig. 4.4b (Rutter 1974, 1986).

Also chlorites seem to be formed by alteration of the above main silicates or re-alteration of the actinolite. Crystalline growth of the chlorites on the slip plane may indicate that this slickenside was developed during low slip-rate faulting in order to produce the preferred orientation of the chlorite (Durney and Ramsay 1973, McCaig 1987).

4.3.3 No. 18

Another example of type B slickenside is developed by a secondary process which produces a vein-type coating along the pre-existing slip surface. The host rock is a coarse-grained hornblende granite showing a typical granoblastic texture (averaging 1-2 mm). Under plane polarized light, two distinct surface-subparallel zones could be observed based on composition and/or texture: (1) an epidote vein covering the host granite; (2) an underlying fracture zone in the granite. The fracture zone tends to be limited to the region close to the slip surface. Occasionally, however, it extends far into the host rock. The slickenside surface on the epidote coating is smooth, whereas the contact between the host rock and epidote vein is very rough (Fig. 4.5). Detailed description of each zone is as follows.

Host rock: The rock is composed of quartz, feldspar and hornblende with minor oxide opaque mineral. A typical granitic texture is well developed throughout the thin section. Feldspars are abundant in the host rock which is mainly composed of plagioclase and perthite (Fig. 4.6a). Crystal plastic deformation microstructures are seen especially in feldspar grains. Undulatory extinction and kink bands are prolific in the perthite and plagioclase, respectively throughout the whole thin section. However, the grain shape of the minerals remains fairly equant.

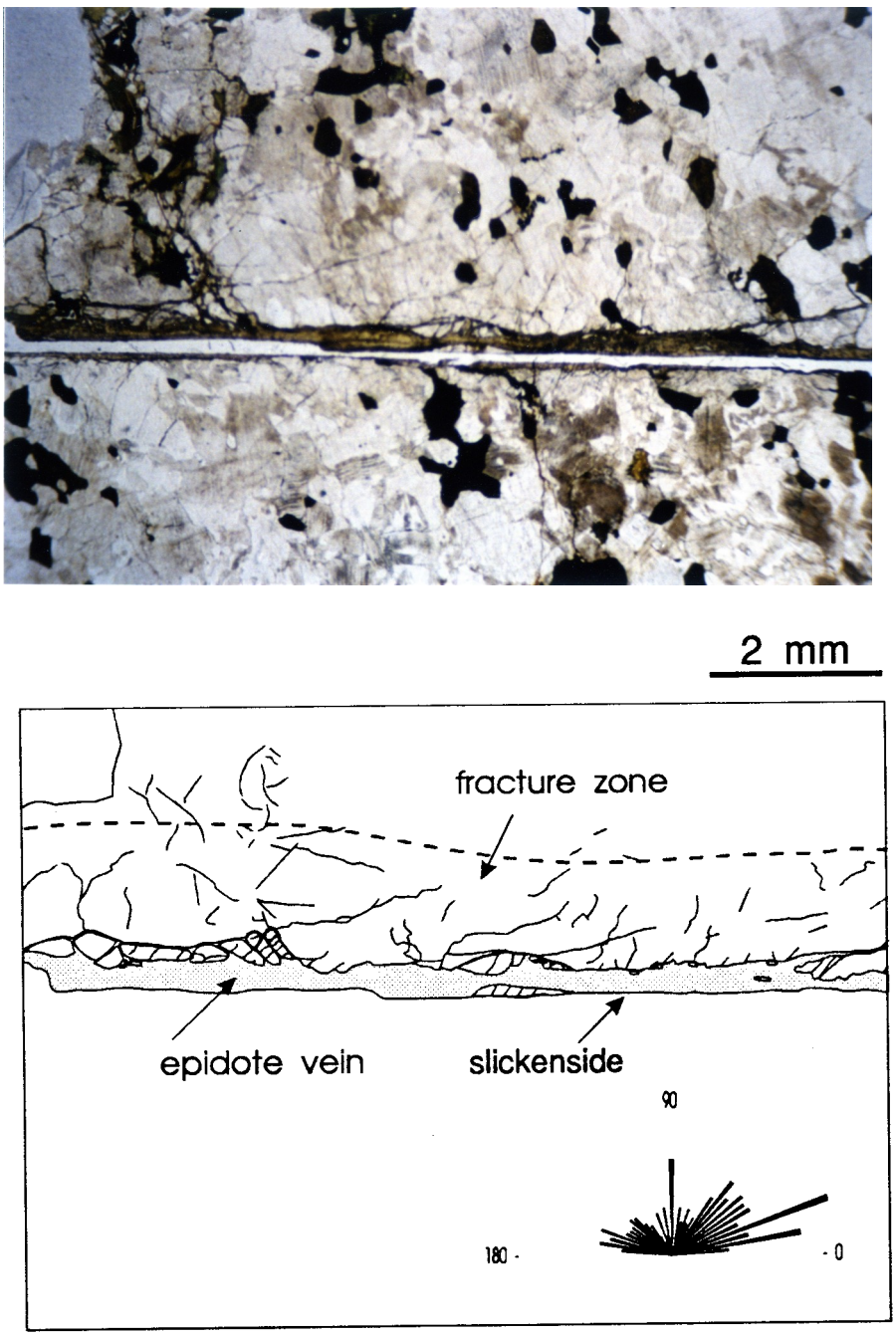

Figure 4.5 Photomicrograph and sketch of slickensided granite (No. 18) showing well developed fracture zone, rock fragments and epidote coating. Rose diagram indicates the trend of fractures. Plane-polarized light.

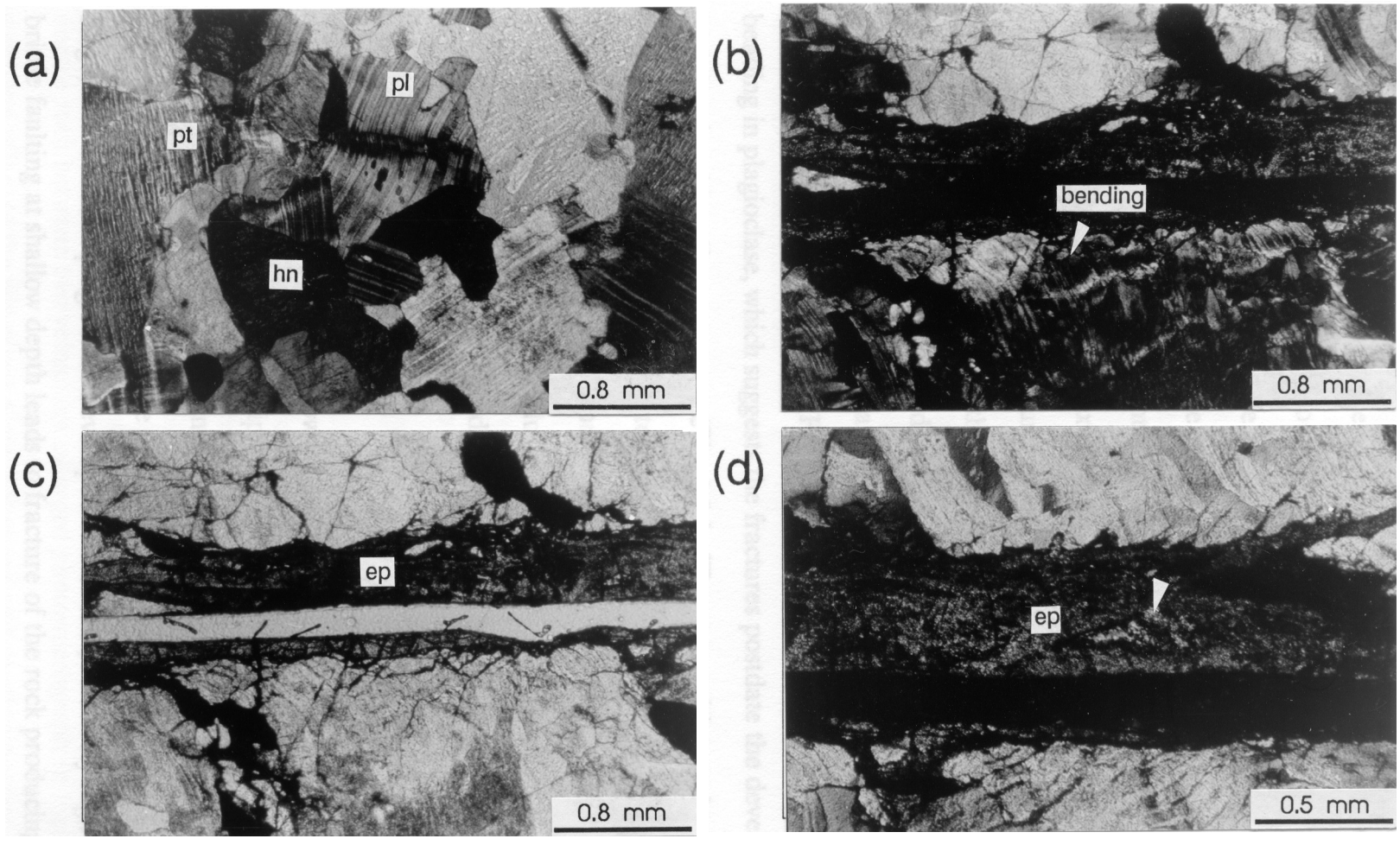

Figure 4.6 Photomicrographs showing textural features of sample 18. (a) Host rock. (b) Bending of plagioclase twins showing sinistral slip sense. (c) Fracture zone developed near the slip surface and epidote coating. (d) Smooth slip surface on the massive epidote vein. Broken rock fragments are included in the epidote vein (arrow). (a), (b) and (d): cross-polarized light. (c): plane-polarized light. pl: plagioclase, pt: perthite, hn: hornblende, ep: epidote.

Fracture zone: The deformed host layer is a narrow fracture zone which is developed within about 1.4 mm from the contact with the epidote vein. The frequency of the fractures decreases away from the slip surface and finally they disappear (Sketch in Fig. 4.5). The rose diagram in Figure 4.5 indicates that the fractures trend mostly 20 to 70^{o} anticlockwise from the slip surface. These dominant fractures are probably extensional fractures (high angle) or R-shear fractures (low angle) developed during a faulting in the granite (see sections 2.4 and 2.6 in chapter 2). In contact with the epidote vein, minor fractures result in an irregular surface of the contact and develop fragments of the host rock corresponding to a pre-existing coating. Weak bending of plagioclase twins is seen near the epidote vein (Fig. 4.6b). Fractures cut through both kink bands and bending in plagioclase, which suggests the fractures postdate the development of kink band and bending structures (Fig. 4.6c). The composition and texture are the same as those in the undisturbed host rock, except for the development of fractures.

Epidote vein: An epidote vein averaging 0.4 mm thick covers the rough surface of the fractured host granite and some epidote also infiltrates the fractures. However, the slickenside surface on the epidote vein is very smooth. The epidote is too fine-grained to identify individual grain shape, which may indicate fast precipitation (Fig. 4.6d). Preferred orientation is not seen.

4.3.4 Interpretation

This slickenside type follows path 10 by a secondary process which develops a massive vein on a pre-existing slip surface. Two different stages of deformation mode are recognized in this slickensided rock. First, minor plastic deformation was widespread in the host rock before the present slickenside formation. During this stage, kink bands in plagioclase developed. After that, relatively high slip-rate brittle faulting at shallow depth leads to fracture of the rock producing the fracture

zone (deformed host layer) and rock fragments on the fault plane (coating). As pore space increases in the fracture zone, fluids injected along the fault surface result in precipitation of the epidote vein along the slip surface and fractures. The fine grain size of the epidote vein may indicate relatively fast precipitation at low temperature and shallow depth. The final slickenside was developed on this fine-grained epidote.

The present slickenside surface with striations is considered to form by another slip event at a later time, different from the event that caused the fractures. Multiple slip events are discussed in the later part of the chapter.

4.4 TYPE C SLICKENSIDE

4.4.1 No. 108

As discussed in chapter 3, Type C slickenside following path 2 is developed especially in fine-grained ductile rock. An example of this type described here is a slickenside in mudstone. The slip surface is very smooth and no coating appears. No host rock deformation is identified, except for a few minor discrete cleavages parallel to the slip surface. Open veins nearly perpendicular to the slip plane are filled with quartz and calcite. Near the slip surface, the veins enclose broken rock fragments produced by fracturing (Fig. 4.7).

The grain size in the rock is too fine-grained to detect individual mineral grains. Few microstructural features related to the slip are recognized even under the microscope. Minor discrete pressure-induced (pressure solution) cleavages which appear dark are locally developed along the slip plane. Relatively large-scale cleavages sketched in Figure 4.7 seem to be formed by vertical collapse of the ductile rock between two veins. An enlarged photomicrograph in Figure 4.8a shows a vertical offset of the slip plane along a fracture and development of slightly

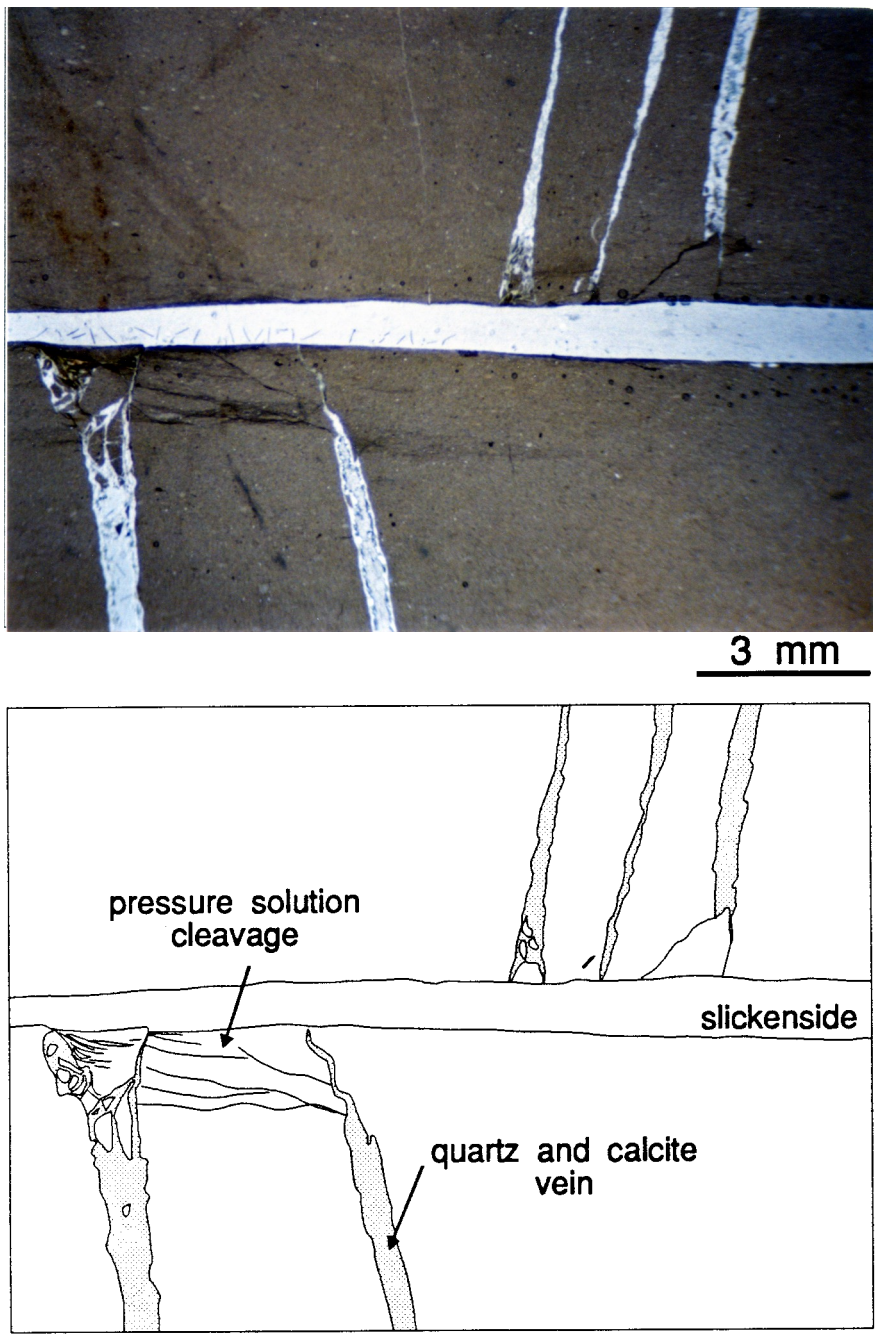

Figure 4.7 Photomicrograph and sketch of slickensided mudstone (No. 108) showing a very smooth slip surface. No deformation is recognized in this scale. Quartz-calcite veins are developed perpendicular to the slip plane. Plane-polarized light.

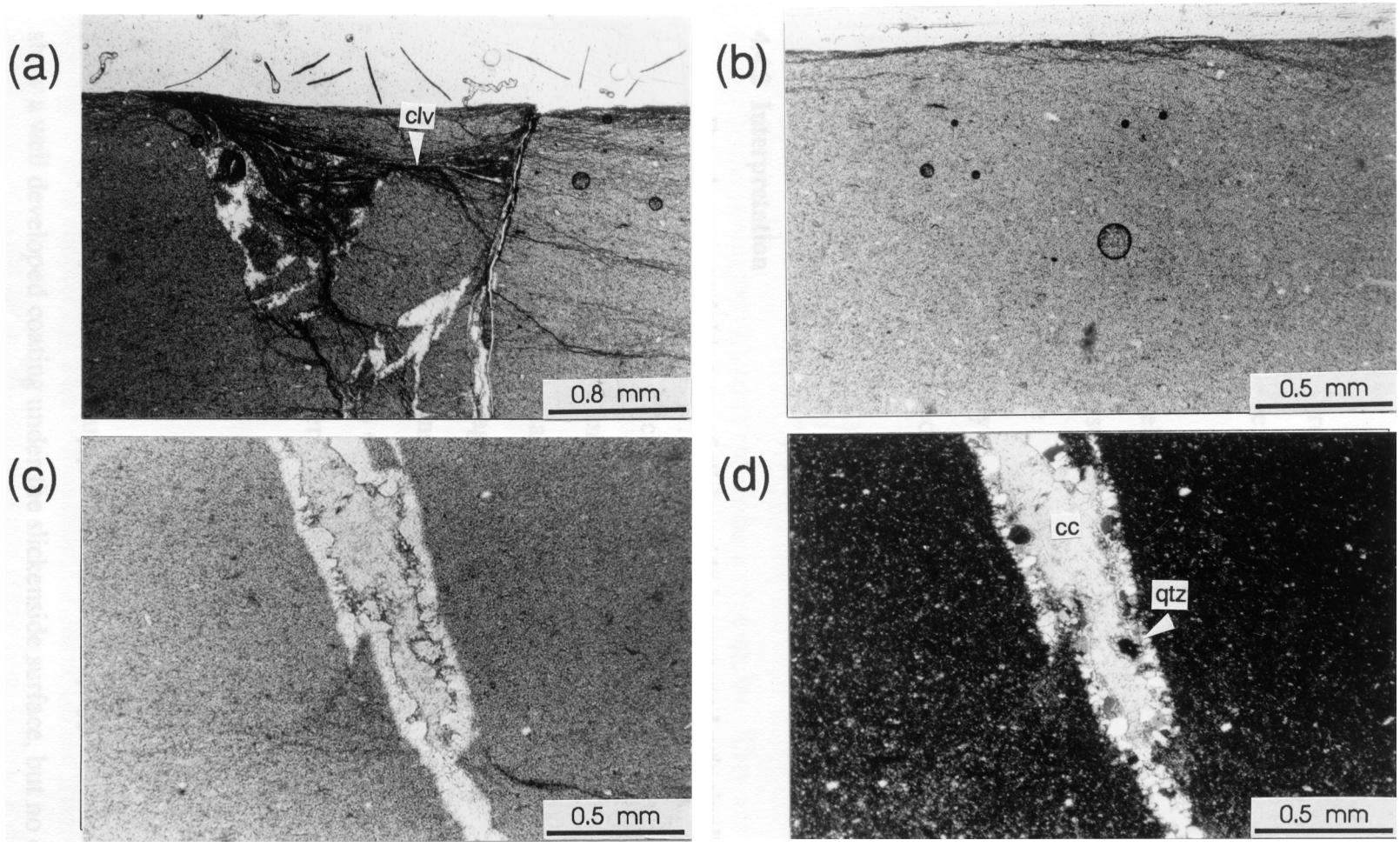

Figure 4.8 Photomicrographs showing textural features of sample 108. (a) Pressure solution cleavages formed by collapse between two fractures. (b) Smooth slip surface with weak cleavage development. (c) and (d) Quartz-calcite vein. Quartz crystalizes from the vein wall. (a), (b) and (c): plane-polarized light. (d): cross-polarized light. clv: cleavage, cc: calcite, qtz: quartz.

depressed cleavages with some broken fragments of the host rock. Figure 4.8b shows how the slickenside surface is very smooth. Negligible minor cleavages are indicated along it.

Extensional veins are developed perpendicular to the slip plane with fillings of quartz and calcite. Quartz crystallized on the vein wall with equant grain shape with massive, fine-grained calcite along the central part of the vein (Figs. 4.8c & d). The tips of the veins point usually toward the slip surface, which may indicate that the vein propagated and branched toward the slip surface and terminated at the slip surface.

4.4.2 Interpretation

Development of this type of slickenside is governed principally by mineralogy and grain size. As already discussed in chapter 3, ductile material flow can be enhanced in fine-grained, hydrated rock (Will and Wilson 1989).

Slickensides in mica- and clay-rich rocks can occur where the material behaves partially in a ductile manner to produce the smooth slip surface. A relatively low slip-rate faulting may be responsible for the ductile behavior resulting in the occurrence of minor cleavages very close to the slip surface and the absense of coating. Later extensional veins may have been formed during stress release. The existence of minor cleavages close to the slip surface is not considered as constituting a deformed host layer, because it is only very locally developed.

4.5 TYPE D SLICKENSIDE

Both primary and secondary process can develop type D slickensides. They show a well developed coating under the slickenside surface, but no deformation of the host rock. Two different examples of type D slickensides are represented based

on the types of coatings formed by a primary process (No. 70) and a secondary process (No. 124).

4.5.1 No. 70

Along the slickenside surface in a sandstone, there is a discontinuous layer of quartz gouge (Fig. 4.9). Fibrous quartz developed from the gouge grows on the lee side of a step on the slickenside. The slip surface is moderately rough. Opaque minerals are concentrated near the slip surface and produce a distinct dark layer between the quartz gouge and the host rock in the figure.

Host rock: The host rock is mainly composed of medium-grained quartz and calcite grains with a matrix of fine-grained clay and opaque minerals. Detrital quartz grains (averaging 0.1 mm) are moderately angular. They are cemented by calcite and silica. Clay and opaque minerals occur between the detrital grains. Some quartz grains show weak undulatory extinction, but it is not possible to identify this microstructure with faulting. Many detrital quartz grains which originated from deformed rocks still include such microstructures. The boundary with gouge is fairly rough (Figs. 4.10a & b).

Quartz gouge: A layer of the quartz gouge about 0.5 mm in thickness is developed on the host rock. The gouge is fine-grained (less than 0.1 mm) and partially welded, so that most quartz grains in the gouge do not show the grain shapes clearly. Opaque minerals are aligned along the boundary between the gouge and host rock.

Quartz fibers: The quartz fibers grow oblique to the slip plane, which indicates the movement sense of the fault. In chapter 2, a partial mechanism for the quartz fiber growth was suggested as replacement of the gouge (replacement fiber, see Fig. 2.3b in chapter 2). The fibrous quartz is distinguished from quartz in the gouge layer by larger grain size and elongate shape (Fig. 4.10c). It appears only at

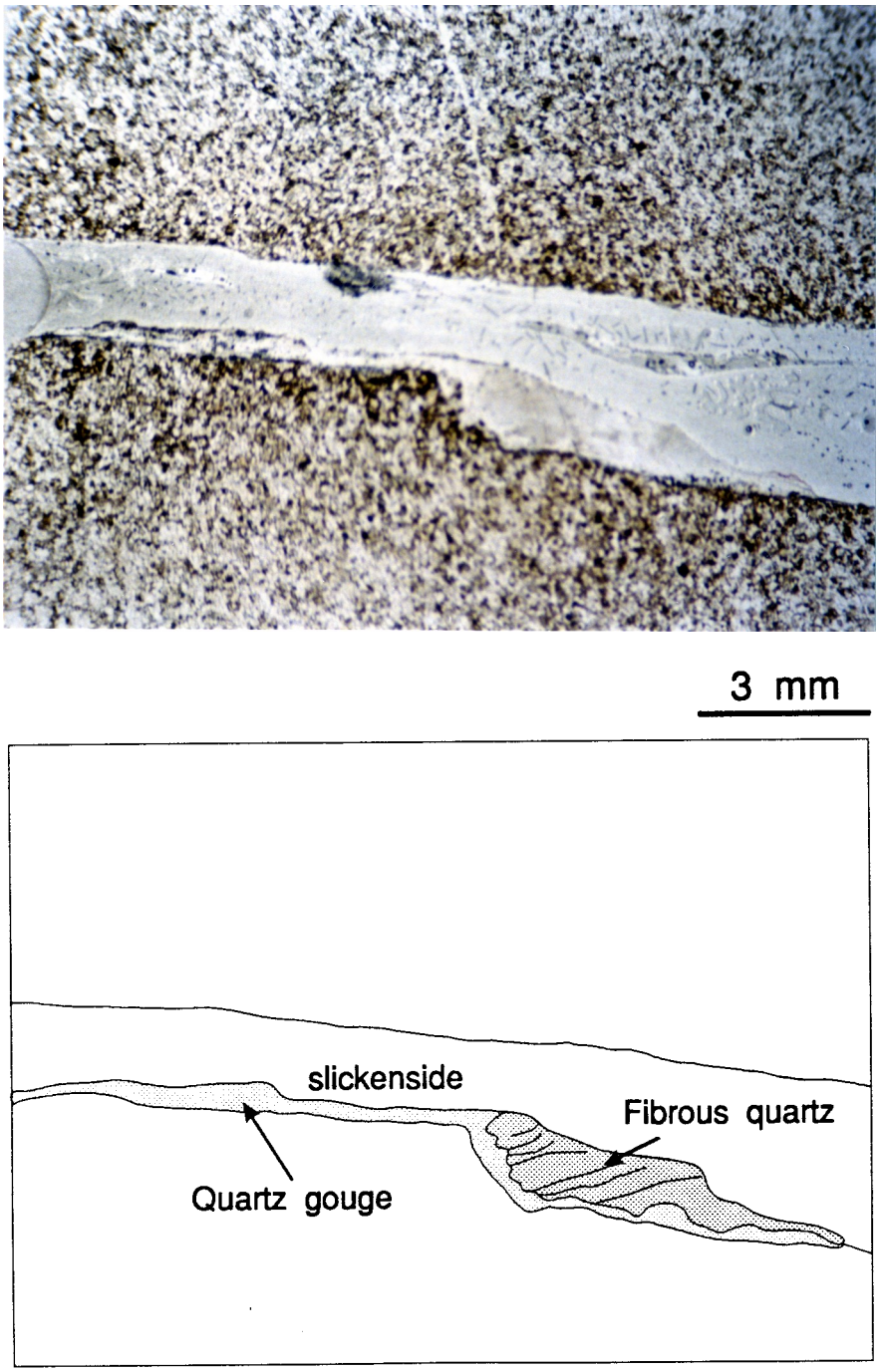

Figure 4.9 Photomicrograph and sketch of slickensided sandstone (No. 70) showing developments of quartz gouges and fibers. Plane-polarized light.

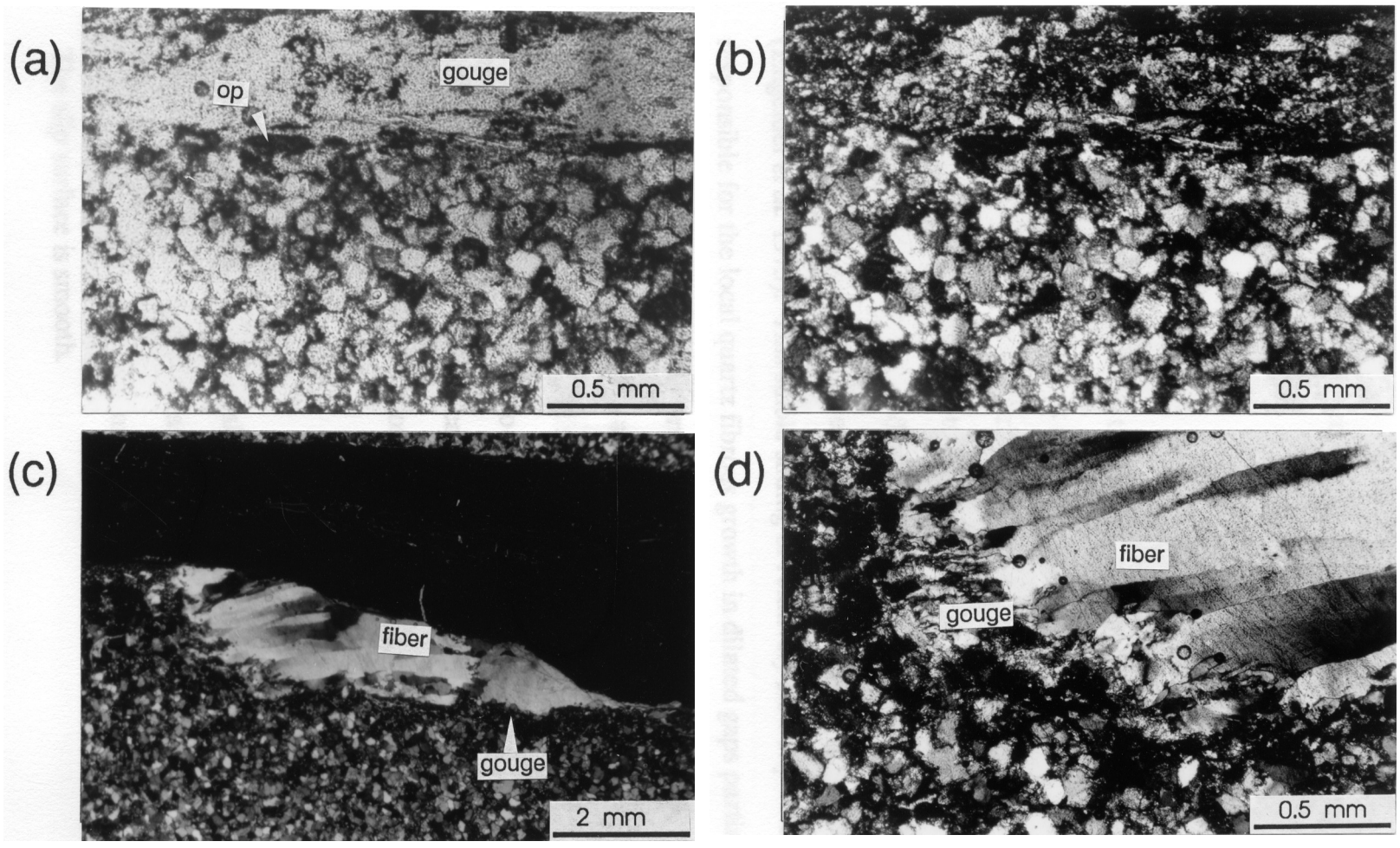

Figure 4.10 Photomicrographs showing textural features of sample 70. (a) and (b) Quartz gouge layer which is partially welded. Opaque minerals are concentrated between the gouge and host rock. (c) Fibrous quartz on the lee of a fault step showing preferred orientation. (d) Enlarged picture of (c). Fibrous quartz developed from the quartz gouges. (a): plane-polarized light. (b), (c) and (d): cross-polarized light. op: opaque.

the step on the slip plane and is rooted in the gouge with irregular boundaries (Fig. 4.10d).

4.5.2 Interpretation

Both the development of the quartz gouge and the absence of deformed host layer in the quartz-rich host rock suggest that the slickenside corresponds to type D slickenside along the path 8 of brittle deformation. Gouge is usually developed at shallow crustal depths where brittle deformation prevails (Sibson 1977). The accumulation of gouge generated between slip surfaces during initial slip may reduce the frictional coefficient of slip and change the slip mode to stable sliding (Engelder *et al.* 1975). This stable sliding of relatively slow slip-rate can be responsible for the local quartz fibrous growth in dilated gaps partially by replacement of pre-existing gouge.

It is difficult to find out the origin of the welded gouge from the simple optical microscopy. It may be produced by frictional melting (Friedman *et. al.* 1974), pressure solution among neighboring grains, cementation or some other process. However the frictional melting seems an unlikely explanation for the welded quartz gouge because no glass is seen under the microscope and the existence of fibrous quartz indicating a relatively slow slip-rate. More detailed work is required to clarify the origin of the welded gouge.

4.5.3 No. 124

Another kind of type D slickenside is a fine-grained mudstone with a massive quartz-opaque vein developed as coating by a secondary process (Fig. 4.11). The opaque minerals occur preferentially on the margins of the vein with the host rock. The slip surface is smooth.

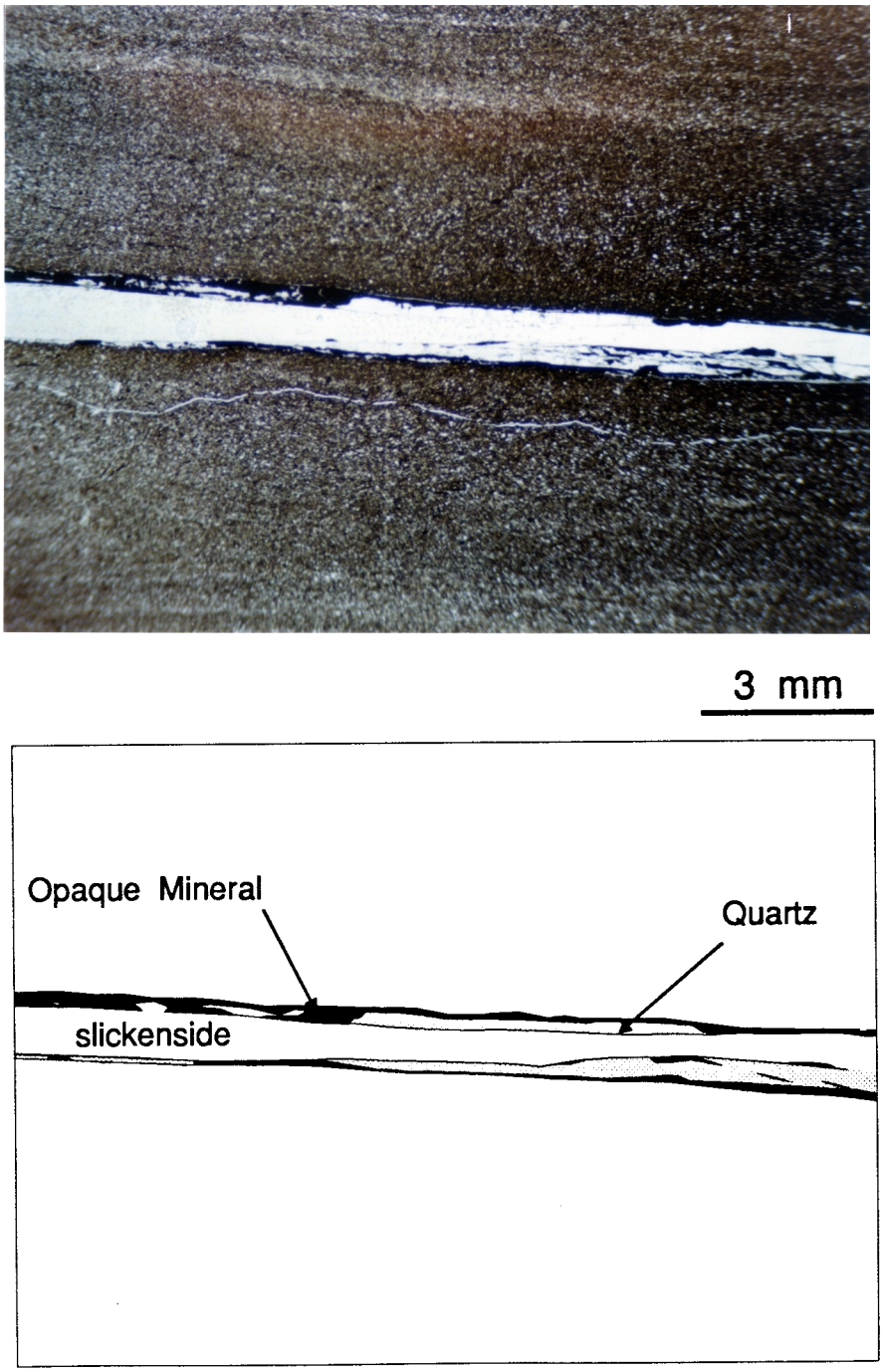

Figure 4.11 Photomicrograph and sketch of slickensided mudstone (No. 124) covered by a quartz-opaque vein. Plane-polarized light.

Host rock: The host rock is composed of fine-grained quartz, substantial mica, clay minerals and minor opaque minerals. No deformation related to slickenside formation is recognized in the host rock.

Quartz-opaque vein: The quartz vein appears as optically continuous grains (Figs. 4.12a & b). Small opaque minerals aligned parallel to the slip plane are included in the quartz vein. Weak plastic deformation is indicated by subgrain boundaries perpendicular to the slip plane (Fig. 4.12d). The trend of c-axes of each domain was determined on a flat stage using a gypsum plate. The majority of c-axes lie subparallel to the slip plane and perpendicular to the subgrain boundaries.

4.5.4 Interpretation

This slickenside corresponds to a secondary type D slickenside following path 11 by an addition of a coating. Before precipitation of the quartz-opaque vein on the host rock, the rock appears to have slipped, which could be inferred from the smooth boundary between the quartz vein and the host rock, This smooth boundary can be produced by the same mechanism as a type C slickenside in mudstone. The fluids that passed through the pre-existing slip plane at shallow depths introduced massive quartz and opaque minerals. At a later stage, plastic deformation may have induced the formation of the subgrain boundaries in quartz vein.

4.6 DISCUSSION

In some examples of the slickenside rocks described, a period of weak ductile deformation is followed by a late stage of brittle or cataclastic faulting (e. g. Nos. 78 and 18). Deformation features in the slickensided rocks indicate two different phases of deformation have occurred. One possible explanation of these changes is that they may be accomplished by alternating behaviors from seismic faulting to

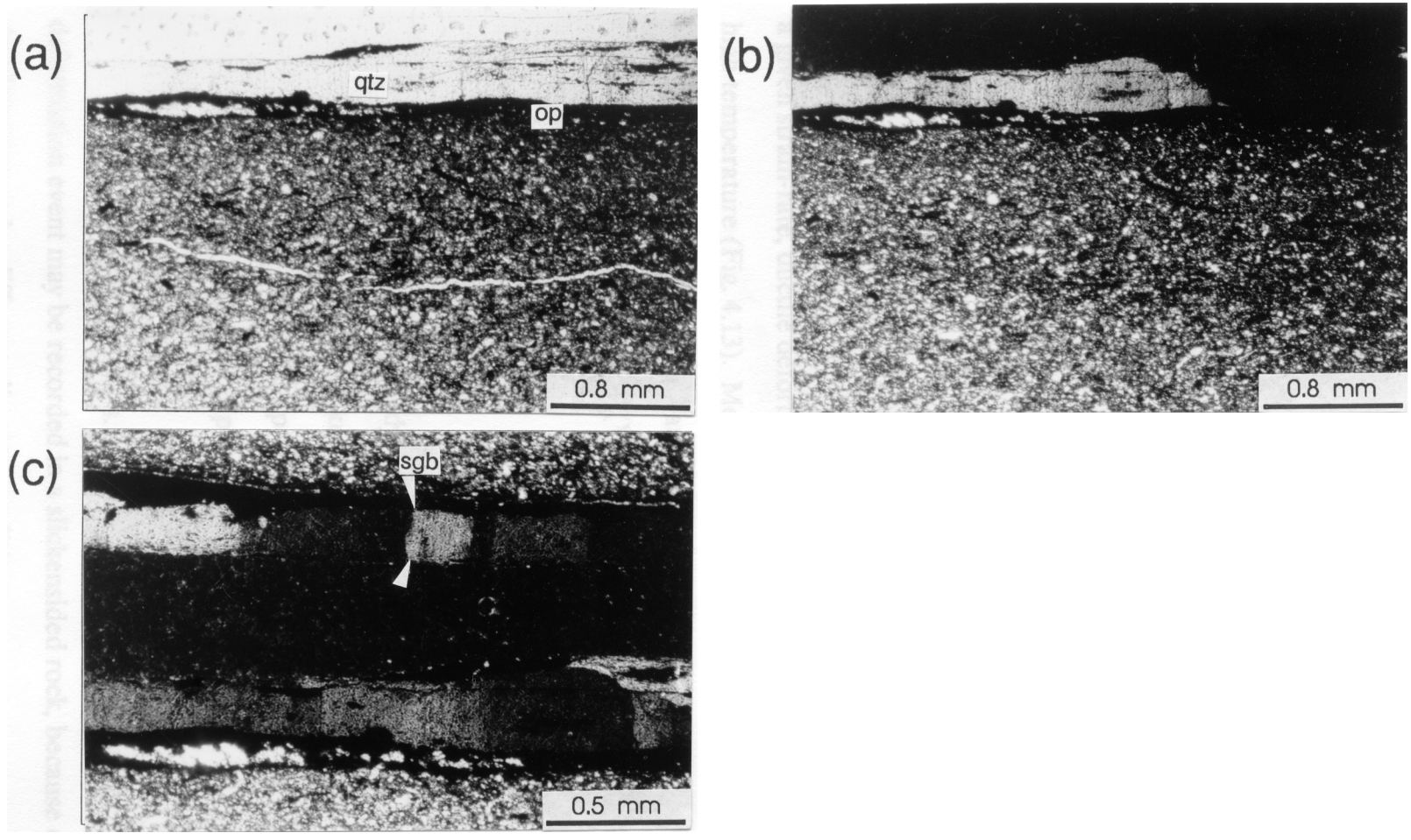

Figure 4.12 Photomicrographs showing textural features of sample 124. (a) and (b) Quartz-opaque vein coating. (c) Subgrain boundaries in the quartz vein perpendicular to the slip plane. (a): plane-polarized light. (b) and (c): cross-polarized light. op: opaque, qtz: quartz, sbg: subgrain boundary.

interseismic faulting (Power and Tullis 1989). Stel (1981) has also suggested that the microstructure of some mylonites and cataclasites can be produced by repeating alternation of brittle and ductile deformation mechanisms. These alternating changes in deformation mode emphasize the cyclical nature of fault rock deformation.

Fluids can play an important role in rock rheology, via influences of fluid pressure or metamorphic (or hydrothermal) reactions. Higher fluid pressure leads to an increase in the permeability of the rock because it facilitates the opening of microcracks by reducing the effective stress. On the other hand, at low fluid pressure rocks may deform as ductile material (Rutter 1974, Sibson *et al.* 1988). For a given strain-rate, ductile deformation may be favored by high effective stress and high temperature (Fig. 4.13). Metamorphic reactions by fluids may play a fundamental role in deformation mode because there is commonly a strong relationship between deformations and metamorphic reactions (Stel 1986). Fluids facilitating fracturing may have caused the alteration and hydrolytic weakening of host rock minerals (e. g. No. 13) (White and Knipe 1978, Mitra 1984).

4.7 SUMMARY

Detailed petrographic study of slickensides provides information not only on mechanical properties of the slickensided rocks but also on fault slip history. Some slickensides described in this chapter show that fluids play important roles in slickenside development by precipitation of coatings (e. g. Nos. 18 and 124) or by alteration of host rocks (No. 13).

Slickenside examples, Nos. 78 and 18 indicate that more than one deformation event may be recorded in a slickensided rock, because of sequential development under different slip-rate conditions.

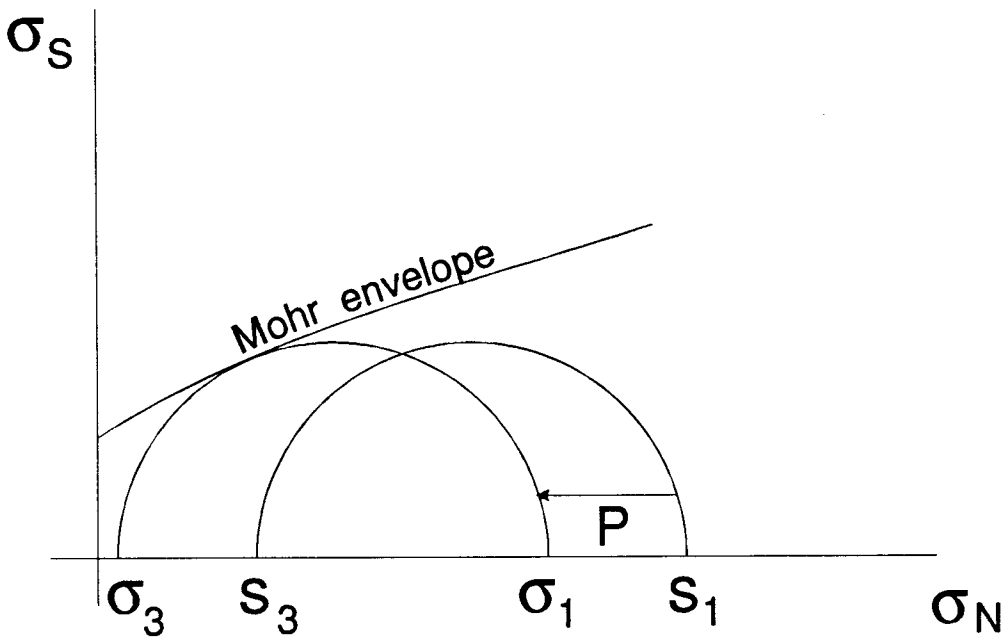

Figure 4.13 Mohr diagram showing the effect of raising the fluid pressure (P), at constant total stress (S). Rocks become unstable and fracture when the circle of the effective stress (σ) intersects the Mohr envelope by an increase in fluid pressure (P). S - P = σ. (combined from Price and Cosgrove 1990, figures in p26 and 29).

This study is limited to petrographic observation. Therefore, the information presented may not be enough for interpretation. Further detailed analytical studies such as chemical analysis, TEM, or fluid inclusion study are required to find out more about faulting conditions at the time of slickenside development.

REFERENCES

Angelier, J. 1979. Determination of the mean principle directions of stresses for given fault population. Tectonophysics, **56**, T17-T26.

Aydin, A. 1978. Small faults formed as deformation bands in sandstone, Pageoph., **116**, 913-930

Aydin, A. and Johnson, A. M. 1978. Development of faults as zones of deformation bands and as slip surfaces in sandstone. Pageoph., **116**, 931-942.

Berthe, D., Choukroune, P and Jegouzo, P. 1979. Orthogneiss mylonite and non coaxial deformation of granite: the example of the South Armorican Shear Zone. J. Struct. Geol., **1**, 31-42.

Billings, M. P. 1954. Structural Geology. New York, Prentice-Hall, 2nd ed.

Boyer, S. and Elliott, D. 1982. Thrust system. Am. Ass. Petro. Geol., **66**, 1196-1230.

Byerlee, J. D. and Brace, W. F. 1968. Stick-slip, stable sliding and earthquakes-effect of rock type, pressure, strain rate, and stiffness. J. Geophys. Res., **73**, 6031-6037.

Conybeare, W. D. and Phillips, W. 1822. Outlines of the Geology of England and Wales. London.

Cox, S. F. 1987. Antitaxial crack-seal vein microstructures and their relationship to displacement paths. J. Struct. Geol., **9**, 779-787.

Dennis, J. G. 1967. International Tectonic Dictionary. Mem. Am. Ass. Petro. Geol., 7.

Durney, D. W. and Ramsay, J. G. 1973. Incremental strains measured by syntectonic crystal growths. In: Gravity and Tectonics (edited by DeJong, K. A. and Scholten, R.). John Wiley and Sons, New York, 67-96

Elliott, D. 1976. The energy balance and deformation mechanisms of thrust sheets. Phil. Trans. R. Soc. London, **A283**, 289-312.

Engelder, J. T. 1974a. Microscopic wear grooves on slickensides: indicators of paleoseismicity. J. Geophys. Res., **79**, 4387-4392.

Engelder, J. T. 1974b. Cataclasis and the generation of fault gouge. Geol. Soc. America Bull., **85**, 1515-1522.

Engelder, J. T., Logan, J. and Handin, J. 1975. The sliding characteristics of sandstone on quartz fault-gouge. Pageoph., **113**, 69-86.

Fleuty, M. J. 1975. Slickensides and slickenlines. Geol. Mag., **112**, 319-321.

Friedman, M., Logan, J. M. and Rigert, J. A. 1974. Glass-indurated quartz gouge in sliding-friction experiments on sandstone. Geol. Soc. America Bull., **85**, 937-942.

Gamond, J. F. 1983. Displacement features associated with fault zones: a comparison between observed examples and experimental models. J. Struct. Geol., **5**, 33-45.

Gamond, J. F. 1987. Bridge structures as sense of displacement criteria on brittle faults. J. Struct. Geol., **9**, 609-620.

Gay, N. C. 1970. The formation of step structures on slickensided shear surfaces. J. Geology, **78**, 523-532

Harper, G. D. 1985. Tectonics of slow spreading mid-ocean ridges and consequences of a variable depth to the brittle/ductile transition. Tectonics, **4**, 395-409.

Hills, E. S. 1940. Outlines of Structural Geology. London.

Hobbs, B. E., Means, W. D. and Williams, P. F. 1976. An Outline of Structural Geology. John Wiley and Sons, Int. ed.

Hull, J. 1988. Thickness-displacement relationships for deformation zones. J. Struct. Geol., **10**, 431-435.

Laurent, P. 1987. Shear-sense ermination on striated faults from e twin lamellae in calcite. J. Struct. Geo **9**, 591-595.

Liou, J G., Maruyama, S. and o, M. 1985. Phase equilibria and mineral

parageneses of metabasites in low-grade metamorphism. Mineralogical Magazine, **49**, 321-333.

Liou, J. G., Kuniyoshi, S. and Ito, K. 1974. Experimental studies of the phase relations between greenschist and amphibolite in a basaltic system. Am. Jour. Sci., **274**, 613-632.

Lister, G. S. and Snoke, A. W. 1984. S-C mylonites. J. Struct. Geol., **6**, 617-638.

Logan, J. M., Friedman, M., Higgs, N., Dengo, C. and Shimamoto, T. 1979. Experimental studies of simulated gouge and their application of studies of natural fault zones, Proc. Conf. VIII Analysis of Actual Fault Zones in Bedrock, U. S. Geol. Surv. Open-File Rep. **79-1239**, 305-343.

McCaig, A. M. 1987. Deformation and fluid-rock interaction in metasomatic dilatant shear bands. Tectonophysics, **135**, 121-132.

Means, W. D. 1987. A newly recognized type of slickenside striation. J. Struct. Geol., **9**, 585-590.

Means, W. D. 1989. Stretching faults. Geology, **17**, 893-896.

Means, W, D. 1990. One-dimensional kinematics of stretching faults. J. Struct. Geol., **12**, 267-272.

Mitra, G. 1984. Brittle to ductile transition due to large strains along the White Rock Trust, Wind River mountains, Wyoming. J. Struct. Geol., **6**, 51-62.

Moore, D. E., Summers, R. and Byerlee, J. D. 1989. Sliding behavior and deformation textures of heated illite gouge. J. Struct. Geol., **11**, 329-342.

Norris, D. K. and Barron, K. 1969. Structural analysis of features on natural and artificial faults. Geol. Survey of Canada Paper **68-52**, 136-157.

Paterson, M. S. 1958. Experimental deformation and faulting in Won-beyan marble. Geol. Soc. America Bull., **69**, 465-476.

Petit, J. P. 1987. Criteria for the sense of movement on fault surfaces in brittle rocks. J. Struct. Geol., **9**, 597-608.

Petit, J. P. and Laville, E. 1987. Morphology and microstructures of "hydroplastic slickensides" in sandstone. In: Deformation Mechanisms in Sediments and Sedimentary Rocks (edited by Jones, M. E. and Preston, R. M. F.) Spec. Publs. Geol. Soc. London, 107-121.

Power, W. L. and Tullis, T. E. 1989. The relationship between slickenside surfaces in fine-grained quartz and the seismic cycle. J. Struct. Geol., **11**, 879-893.

Price, N. J. and Cosgrove, J. W. 1990. Analysis of Geological Structures. Cambridge University Press.

Rutter, E. H. 1974. The influence of temperature, strain rate and interstitial water in the experimental deformation of calcite rocks. Tectonophysics, **22**, 311-334.

Rutter, E. H. 1986. On the nomenclature of mode of failure transitions in rocks. Tectonophysics, **122**, 381-387.

Scholz, C. H. 1987. Wear and gouge formation in brittle faulting. Geology, **15**, 493-495.

Sibson, R. H. 1975. Generation of pseudotachylyte by ancient seismic faulting. Geophys. J. Royal astro. Soc., **43**, 775-794.

Sibson, R. H. 1977. Fault rocks and fault mechanisms. J. Geol. Soc. London, **133**, 191-231.

Sibson, R. H. 1983. Continental fault structure and the shallow earthquake source. J. Geol. Soc. London, **140**, 741-767.

Sibson, R. H., Robert, F. and Poulsen, H. 1988. High angle faults, fluid pressure cycling and mesothermal gold-quartz deposits. Geology, **16**, 551-555.

Simpson, C. and Schmid, S. M. 1983. An evaluation of criteria to deduce the sense of movement in sheared rocks. Bull. Geol. Soc. Am. **94**, 1281-1288.

Spray, J. G. 1989a. Frictional phenomena in rock: an introduction. J. Struct. Geol., **11**, 783-785.

Spray, J. G. 1989b. Slickenside formation by surface melting during the mechanical

excavation of rock. J. Struct. Geol., **11**, 895-905.

Stel, H. 1981. Crystal growth in cataclasites: diagnostic microstructures and implications. Tectonophysics, **78**, 585-600.

Stel, H. 1986. The effect of cyclic operation of brittle and ductile deformation on the metamorphic assemblage in cataclasites and mylonites. Pageoph., **124**, 289-307.

Stesky, R. M., Brace, W. F., Riley, D. K. and Robin, P.-Y. F. 1974. Friction in faulted rock at high temperature and pressure. Tectonophysics, **23**, 177-203.

Suppe, J, 1985. Principles of Structural Geology. Prentice-Hall.

Tjia, H. D. 1964. Slickensides and fault movements. Geol. Soc. America Bull., **75**, 683-685.

Tjia, H. D. 1967. Sense of fault displacements. Geol. en Mijnbou, **46**, 392-396.

Tullis, J. and Yund, R. A. 1977. Experimental deformation of dry Westerly granite. J. Geophys. Res., **82**, 5705-5718.

Tullis, J. and Yund, R. A. 1980. Hydrolytic weakening of experimentally deformed Westerly granite and Hale albite rock. J. Struct. Geol., **2**, 439-451.

Turcotte, D. L. and Schubert, G. 1982. Geodynamics: an applications of continuum physics to geological problems. John Wiley and Sons.

White, S. H. and Knipe, R. H. 1978. Transformation- and reaction-enhanced ductility in rocks. J. Geol. Soc. London, **135**, 513-516.

Will, T. M. and Wilson, C. J. L. 1989. Experimentally produced slickenside lineations in pyrophyllitic clay. J. Struct. Geol., **11**, 657-667.

Winkler, H. G. F. 1979. Petrogenesis of Metamorphic Rocks. Springer-Verlag, 5th ed.